SUSTAINABLE SUPPLY CHAIN NETWORK DESGIN FOR RENEWABLE ENERGY

A Dissertation Presented for the

Doctor of Philosophy

Degree

The University of Tennessee, Knoxville

Rui Zhou

May 2025

Copyright © 2025 by Rui Zhou
All rights reserved.

ACKNOWLEDGEMENTS

First and foremost, I extend my deepest gratitude to my advisor, Dr. Mingzhou Jin, for his unwavering guidance, mentorship, and support throughout my doctoral journey. Your insightful feedback, encouragement, and belief in my potential have been instrumental in shaping this dissertation and my academic growth. Thank you for fostering an environment that challenged me intellectually while supporting me personally.

I would also like to thank my committee members, Dr. Xueping Li, Dr. James Ostrowski, and Dr. Shih-Lung Shaw, for their invaluable time, expertise, and constructive feedback, which have greatly enriched this research. Your diverse perspectives and thought-provoking suggestions have been critical in refining my work.

I am profoundly grateful to my colleagues Dr. Wenquan Dong, Dr. Zefeng Lyu, Dr. Di Bo, Ziwei Liu, Jinwei Chen, Sarita Rattanakunuprakarn, and Xudong Wang for their camaraderie and support. The stimulating discussions, shared challenges, and moments of celebration have made this journey both productive and enjoyable.

To my family, I owe an immeasurable debt of gratitude. To my parents, Chunyun Lei and Shuming Zhou, thank you for instilling in me the values of perseverance and curiosity and for supporting me unconditionally in every endeavor. To my cat, Leo, thank you for your company during the long hours and late nights.

To my friends, both near and far, your words of encouragement and moments of joy have provided balance and perspective, helping me navigate the challenges of this journey.

ABSTRACT

This study designs sustainable supply chain networks for renewable energy systems, focusing on carbon dioxide (CO_2), hydrogen, and biomass. By integrating economic, environmental, and social factors, the research develops optimized networks to maximize efficiency and minimize costs.

For CO_2, the study examines the techno-economic performance of CO_2-to-fuel pathways, specifically the CO_2-CO-FTS-fuel and CO_2-methanol-fuel processes, within the U.S. A life cycle assessment quantifies environmental impacts. Results show that the FTS pathway is preferred at all selected refineries when hydrogen costs $1,000/t and electricity conversion costs are reduced by 95%, generating $8 billion annually while reducing emissions by 88.8 million tons. Sensitivity analysis highlights electricity and hydrogen prices as cost drivers. The CO_2 recycle rate and higher conversion efficiency improve the cost-effectiveness of methanol pathways.

For hydrogen, the study evaluates three delivery pathways—gaseous hydrogen, liquid hydrogen, and ammonia—as carriers, based on costs and greenhouse gas emissions. Hydrogen demand is projected for 1,927 fueling station locations under various fuel cell electric truck (FCET) market penetration scenarios. To enhance computational efficiency, binary variables are replaced with integers. Results reveal the liquid hydrogen pathway as the most cost-effective, with a levelized cost of $4.6/kg at 10% FCET penetration. Improvements in gaseous hydrogen station costs, ammonia pathway energy losses, and station scalability are recommended to enhance feasibility.

For biomass, the study investigates the techno-economic feasibility of biomass-to-biofuel with carbon capture and storage (BECCS), using corn stover, switchgrass, and miscanthus in the southeastern U.S. A two-stage mixed-integer programming model optimizes supply chains using spatial and seasonal biomass data. Results demonstrate that biofuel production is viable across market maturity levels, producing 3.01 million tons annually under high maturity. Switchgrass emerges as the dominant feedstock. Sensitivity analysis identifies operating costs and biofuel prices as profitability drivers, with a minimum selling price of $2.62/gallon. Multi-feedstock biorefineries yield higher

profitability and stable production. Policy recommendations emphasize public awareness and robust biomass supply chains for long-term BECCS viability.

This research provides actionable insights for developing efficient, sustainable renewable energy supply chains.

TABLE OF CONTENTS

Chapter One Introduction and General Information 1
1.1 Challenges to Renewable Energy 2
1.2 Literature Review 3
Chapter Two Techno-economic Analysis and Network Design for CO_2 Conversion to Jet Fuels in the United States 6
2.1 Abstract 7
2.2 Introduction 7
2.2.1 CO_2 Conversion Pathways 8
2.2.2 Techno-economic Analysis for CO_2 Conversion 10
2.2.3 Supply Chain Network Optimization 11
2.3 Network Design 12
2.4 System Boundary and Data Description 13
2.4.1 CO_2-CO-FTS-Fuel and CO_2-Methanol-Fuel routes 13
2.4.2 Techno-economic Performance of FTS and MeOH 16
2.5 Results 23
2.5.1 Resulting network 23
2.5.2 Sensitivity analysis 26
2.6 Discussion 32
2.7 Conclusion 33
Chapter Three Hydrogen Logistics Network Design for Hydrogen Fuel Cell Electric Long-haul Trucks 35
3.1 Abstract 36
3.2 Introduction 36
3.2.1 Hydrogen Logistics Technologies 37
3.2.2 Hydrogen Logistics Models 41
3.3 System Boundary and Data Description 44
3.3.1 Hydrogen Production 44
3.3.2 Hydrogen Delivery Pathways 45
3.3.3 Hydrogen Fueling Station Demand 51

3.4 Hydrogen Logistics Network Design 54
3.4.1 Variable and Parameter Definition 54
3.5 Numerical Experiment 57
3.5.1 Resulting Network 57
3.5.2 Sensitivity Analysis 61
3.6 Discussion 66
3.7 Conclusion 68
Chapter Four The Value of Circular Biomass-bioenergy and Biofuel with Carbon Capture and Storage 70
4.1 Abstract 71
4.2 Introduction 71
4.3 Literature Review 74
4.3.1 Biomass Conversion Pathways 74
4.3.2 BECCS Supply Chain Optimization Overview 76
4.4 Integrated Circular Bioenergy System 77
4.4.1 Network Model 77
4.5 Numerical Experiment 80
4.5.1 System Boundary and Data Description 80
4.5.2 Resulting network 83
4.5.3 Sensitivity and Uncertainty Analysis 94
4.6 Policy and Regulatory Recommendations 99
4.7 Conclusion 104
Chapter Five Conclusions and Recommendations 107
List of References 110
Vita 129

LIST OF TABLES

Table 2-1 Characteristic of FTS and MeOH pathways 17
Table 2-2 Data Values and Sources for All Parameters 22
Table 2-3 Nationwide CO_2-to-Fuels supply chain network results of optimal pathways under the conditions of an 85.8% CO_2 recycle rate for FTS pathways, a $1,000 per ton unit H_2 price, and 5% of the operating cost 27
Table 3-1 Comparison of Major Physical and Chemical Hydrogen Storing and Transporting Methods 38
Table 3-2 Comparison of Hydrogen Delivery Pathways 50
Table 3-3 Daily Costs of the Optimal National Hydrogen Logistics Network Design under 10% FCETs Market Penetration 57
Table 3-4 The Optimal Hydrogen Infrastructure Needed, Total Costs and Total Delivered H_2 under Base, Gas Hydrogen Pathway, and Ammonia Pathway Scenarios 62
Table 4-1 Data Values and Sources of Corn Stover, Switchgrass and Miscanthus 82
Table 4-2 The Capacity, Operating, and Production Capacity of the Existing and New Biorefineries 85
Table 4-3 The Optimal Amount of Biomass, Costs of BECCS, and Revenues of Bioproducts when Biorefinery has Capability of Handling One Type of Biomasses under Different Market Maturity Scenarios 87
Table 4-4 The Timeline of Significant Policy Developments of EBCCU in the United States . 100

LIST OF FIGURES

Figure 2-1 Potential CO_2 Conversion Routes to Produce Fuels..... 9
Figure 2-2 Simplified CO_2-CO-FTS Process..... 15
Figure 2-3 Simplified CO_2-Methanol-Fuel Process 16
Figure 2-4 Distribution of Stationary Sources, Potential Refineries, and Major Airports 21
Figure 2-5 Supply Chain Network Design under Different Electricity Rate..... 24
Figure 2-6 Sensitivity Analysis: Impact of Unit H_2 Price and Unit CO_2 Capture Cost on Profits 28
Figure 2-7 Heatmaps of the CO_2 Capture Cost and H_2 Purchase Cost on Profits of FTS Pathway and MeOH Pathway..... 28
Figure 2-8 Sensitivity Analysis: Impact of H_2 Price and CO_2 Capture Cost on Utilized CO_2 and Produced Jet Fuel 28
Figure 2-9 Sensitivity Analysis: Impact of the CO_2 Recycle Percentage of the FTS Pathway on Costs and Profits, 56%, 66%,76%,86% (base case), and 96% CO_2 Recycled. 31
Figure 2-10 Impact of CO_2 Conversion Rate on Total Profit, Utilized CO_2, and Produced Jet Fuel of the Optimal Pathway..... 31
Figure 3-1 Hydrogen Delivery Pathways from Production to End Use..... 46
Figure 3-2 Hydrogen Refueling Daily Demand for Long-haul Trucks at Potential Locations under 10% FCETs Market Penetration Rate..... 53
Figure 3-3 Hydrogen Logistics Flow Chart..... 55
Figure 4-1 Biomass-Bioenergy and Biofuel Conversion Technologies 75
Figure 4-2 Circular Biomass-Bioenergy and Biofuel with Carbon Capture and Storage Process 78
Figure 4-3 Monthly Production of Corn Stover, Switchgrass, and Miscanthus under Low, Medium, and High Market-Mature Scenarios in Southeast Area of United States..... 84
Figure 4-4 Percentage of the Optimal costs of BECCS, and Revenues of Bioproducts under Mature-Market Medium Scenario 89
Figure 4-6 Biomass Feedstock Feed in and Biofuel and Bio-products Feed out under Market-mature Medium and Biorefinery Handles Multiple Types of Biomass Scenario 92
Figure 4-7 The comparison of distribution map of elevators, selected biorefineries and biomass resources under market-mature medium scenario. Figure 7(a) is biorefinery can only handle one type of biomass. Figure 7(b) is biorefinery can handle multiple types of biomass under low variable operating cost. 93

Figure 4-8 Sensitivity Analysis: The Impact of Unit Costs and Biofuel Price Vary from 20% to 200% on the Total Profit 95
Figure 4-9 Sensitivity Analysis: The Impact of Unit Biorefinery Fixed Operating Cost and Biofuel Price Vary from 20% to 180%. Figure 9(a) is the impact on all other costs, revenues, and total profit. Figure 9(b) is the impact on harvest biomass, produced products, and captured CO_2 97
Figure 4-10 Sensitivity Analysis: The Impact of Biorefinery Production Capacity and Bio-oil to Biofuel Conversion Rate Vary from 80% to 120% on Harvested Biomass, Produced Biofuel, Biochar, Diesel, Steam, Captured CO_2, and Profit. Figure 10(a) is under both low and high production capacities. Figure 10 (b) is under low and high biofuel conversion rates 98
Figure 4-11 The Distribution of Total Profit, Total Cost, Total Revenue, Produced Biofuel, and Captured CO_2 102

CHAPTER ONE
INTRODUCTION AND GENERAL INFORMATION

1.1 Challenges to Renewable Energy

Renewable energy sources, including biomass, hydrogen, and carbon dioxide conversion, present promising alternatives to traditional fossil fuels. However, several significant challenges must be addressed to realize their full potential. These challenges can be broadly categorized into technical, economic, environmental, and social dimensions (K. Alper et al., 2020 Xu et al., 2020; Megia et al., 2021). The technical challenges include reliability, energy density and storage, and technological maturity (Sinsel et al., 2020). Renewable energy sources such as solar and wind are inherently intermittent and unpredictable (Notton et al., 2018). This variability necessitates the development of efficient energy storage systems. The energy density of renewable sources is often lower than fossil fuels (Dijkman & Benders, 2010). Therefore, the storage of renewable energy is more different. For instance, hydrogen storage requires advanced materials and technologies to store it safely and efficiently at high pressures or low temperatures (Bosu & Rajamohan, 2024). Additionally, many renewable energy technologies are still in the developmental or early deployment stages. For example, the large-scale implementation of carbon capture and storage (CCS) technology with bioenergy (BECCS) faces technical uncertainties and scalability issues (Stavrakas et al., 2018). Then, the economic challenges include high initial capital investment, cost competitiveness with conventional energy, market and policy support (Arutyunov & Lisichkin, 2017). The capital expenditure for renewable energy projects can be substantial. This includes costs for technological development, infrastructure, and grid integration. For example, constructing pipelines for hydrogen delivery and refineries for CO_2 conversion to fuels requires significant investment (Wietschel et al., 2006). Because of the high costs, the price of renewable energy could be uncompetitive compared with fossil fuels. Besides, the economic viability of renewable energy often depends on supportive policies and market conditions (Abdmouleh et al., 2015). Inconsistent policy frameworks and lack of long-term incentives can hinder investment and development. Environmental challenges include land and resource use, water usage, and lifecycle emissions (Arent et al., 2014). Large-scale deployment of renewable energy can impact land use and biodiversity. For instance, growing biomass for biofuels can compete with food production and lead to

deforestation and habitat loss (Arent et al., 2014). Some renewable energy processes, particularly bioenergy and hydrogen production, require significant water resources (Holmatov et al., 2019; Mehmeti et al., 2018). This can strain water availability, especially in arid regions. While renewables generally produce lower emissions than fossil fuels, the full lifecycle of production, including manufacturing of renewable energy infrastructures, still has carbon emissions (Singh et al., 2013). Last but not the least, the social challenge is the public acceptance of renewable energy. Concurs about energy price, efficiency and safety can lead to delays in project implementation (Gareiou et al., 2021). In conclusion, while renewable energy holds great promise for sustainable development, addressing these multifaceted challenges is critical for its widespread adoption and success. Efforts must be made to advance technological innovations, create supportive economic and policy environments, mitigate environmental impacts, and ensure social inclusivity in the transition to renewable energy systems.

1.2 Literature Review

Several studies have explored solutions to the various challenges posed by renewable energy. A recent study by Kapelewski et al., (2018) explores novel metal-organic frameworks (MOFs) for hydrogen storage, demonstrating higher storage capacities and improved thermal stability compared to traditional materials. (Haszeldine et al., 2018) evaluate the latest advancements in BECCS technology, focusing on pilot projects that demonstrate the potential for scalable carbon-negative energy production. A study by (Abdmouleh et al., 2015) examines the effectiveness of different policy instruments, such as carbon pricing and renewable energy certificates, in promoting investment and reducing the cost gap between renewables and fossil fuels. Amponsah et al., (2014) demonstrates the variability of existing LCA studies (results) in tracking GHG emissions for electricity and heat generation from renewable energy technologies. These studies mainly focus on specific challenges of renewable energy. To implement these renewable energy sources on a large scale, it is essential to integrate the entire supply chain while addressing the associated challenges. However, the long-term large-scale logistics network design for various renewable energy technologies is still at an early stage. This dissertation aims to fill this gap for three renewable energy technologies: CO_2-jet fuel,

hydrogen fuel, and BECCS. Research on renewable jet fuel primarily focuses on production from biomass (Doliente et al., 2020; Matos-Ríos et al., 2022). However, a large amount of CO_2 emissions from stationary points can also be used to produce jet fuel, which can significantly help with carbon reduction. Hydrogen fuel has significant potential as a renewable energy source due to its high energy density, zero emissions, versatility in applications, and ability to enhance energy storage. (Demir & Dincer, 2018) compares the cost assessment and evaluation of three different hydrogen delivery scenarios. With the development of hydrogen storage technologies, more scenarios need to be explored and compared. Freer et al., (2021a) created a Carbon Navigation System which can search and rout for a precise amount of biomass to a chosen location, route captured CO_2 for offshore geological storage and direct energy output to end-users. However, the seasonality of biomass is ignored in this study.

In summary, a more comprehensive system is needed to effectively integrate and manage various renewable energy sources, ensuring seamless coordination between production, storage, distribution, and consumption while addressing technical, economic, and environmental challenges. Therefore, this dissertation delves into the diverse production and delivery scenarios of the three renewable energies, subsequently evaluating the feasibility of these pathways to determine the optimal solution for varying scenarios through a real-world case study. At the end, this dissertation gives policy suggestions and regulatory for the decision makers in the systems.

Chapter 2 explores the chemical process of two existing CO_2-jet fuel conversion pathways (Fischer-Tropsch synthesis and methanol) and evaluates the economic performance of these two pathways via techno-economic analysis. A mixed-integer programming model is developed to optimize the supply chain network for renewable jet fuel production with the minimum total cost. Incorporating spatial and techno-economic data, the model considers the selection of source plants and conversion pathways, locations of conversion refinery sites, and the amount of captured CO_2 across the United States. The numerical experiments indicate that both pathways are negative net carbon emissions and FTS pathway is more competitive.

Chapter 3 explores the hydrogen storage and delivery technologies' technical performance and costs. A mix-integer programming model is developed to address the critical need for designing effective hydrogen delivery networks for long-haul trucks under different demands. The numerical experiments can indicate the optimal hydrogen delivery pathways (compressed gas, liquid hydrogen, and ammonia for different scenarios.

Chapter 4 considers various seasonal biomass feedstocks to fulfill the demands while recycling the biochar and capture the CO_2 emissions during the conversion process. The numerical experiments can indicate the biomass supply planning for each month.

Finally, Chapter 5 summarized this work and discussed the further research directions.

CHAPTER TWO

TECHNO-ECONOMIC ANALYSIS AND NETWORK DESIGN FOR CO_2 CONVERSION TO JET FUELS IN THE UNITED STATES

2.1 Abstract

The conversion of carbon dioxide (CO_2) into jet fuel holds significant potential for reducing CO_2 emissions, providing an alternative to carbon-based resources, and offering a renewable means of energy storage. This study presents a techno-economic analysis for two CO_2-to-Fuels pathways. This first pathway is based on Fischer-Tropsch synthesis (FTS), a low-temperature CO conversion through reverse water-gas shift reaction and a high-temperature direct CO_2 conversion. The other one is based on the valorization and upgrading of light methanol (MeOH) derived from CO_2 hydrogenation. A mixed-integer linear programming model was developed to optimize the supply chain network for renewable jet fuel production with the minimum total cost. Incorporating spatial and techno-economic data, the model considers the selection of source plants and conversion pathways, locations of conversion refinery sites, and the amount of captured CO_2 across the United States. The results indicate that the FTS pathway is adopted at all selected refineries when the hydrogen price is $1,000/t and the operating cost, mainly electricity used in conversion, is reduced to 5% of its current level. The supply can realize the total annual profit of $8B in the United States and reduce the carbon emissions by 88,783,284 tons. The sensitivity analyses reveal that the prices of electricity and hydrogen significantly contribute to total production costs. Constructing refineries in locations with lower electricity rates could mitigate operational costs associated with conversion. The CO_2 recycle percentage of the FTS pathway influences the choice of applied pathways at refineries. Additionally, a higher conversion rate holds a substantial promise for reducing the total production cost and can make the MeOH pathway a viable choice.

2.2 Introduction

Converting carbon dioxide (CO_2) into fuels and chemicals not only promotes CO_2 reduction in the atmosphere but also provides alternative carbon-based resources and enables the storage of renewable energy (E. Alper & Yuksel Orhan, 2017). However, large-scale CO_2 conversion faces significant technical and economic challenges in industrial applications. The net cost of CO_2 capture and utilization in some conventional conversion pathways might even surpass the value of the final products (Hepburn et al., 2019; X. Li et al., 2016). Capturing and storing CO_2 before conversion involves chemical

transformations that require a substantial amount of energy input, significantly increasing the cost of CO_2 utilization. For example, reducing 810 Gt CO_2 from the atmosphere by 2100 under the current emissions scenario requires 111,320 kWh of energy input, potentially exceeding the energy gained from burning fossil fuels emitting an equivalent quantity of CO_2 (Qin et al., 2020). Research in catalyst selection, unit operation design, process configuration, life cycle assessment, environmental benchmarking, and policy analysis — all crucial aspects of CO_2 utilization — is still in its early stages (Centi et al., 2020; Rafiee et al., 2018). It is imperative to optimally integrate capture, transportation, conversion, and consumption activities to design efficient CO_2 conversion to fuel networks. This study answered the following three questions:

1. Is it economically feasible and environmentally friendly to produce jet fuel via FTS and MeOH pathways in the United States?
2. What does the distribution network in the United States look like to supply jet fuels converted from the CO_2 captured at stationary sources?
3. How do electricity rates, feedstock prices, the CO_2 recycle percentage of the FTS pathway, and conversion rates impact the economic feasibility, environmental impacts, and network configuration for the CO_2 conversion to jet fuels?

2.2.1 CO_2 Conversion Pathways

Current research efforts in CO_2 reduction have primarily concentrated on producing chemical products such as formic acid/formate, CH_4, methanol, ethylene, and ethanol, rather than focusing on fuels (Lee et al., 2020). The ongoing CO_2 reduction projects are still far below the global carbon reduction target. Direct drop-in liquid hydrocarbon fuels, including gasoline, diesel, jet fuels, and marine fuels, are promising candidates for meeting the growing demand for CO_2 reduction due to their large demand and high energy density. Various approaches, such as photosynthetic, non-photosynthetic biological, electrochemical, photo-catalytic, thermochemical, and hybrid methods, can be employed to convert CO_2 to drop-in hydrocarbons (Ahmed et al., 2019; Kumaravel et al., 2020; F. Li et al., 2021). As depicted in **Figure 2-1**, four general steps are required for converting CO_2 to fuel products: 1) capturing CO_2 from stationary sources or directly from the air and then transporting the captured CO_2 to the refineries; 2) converting CO_2

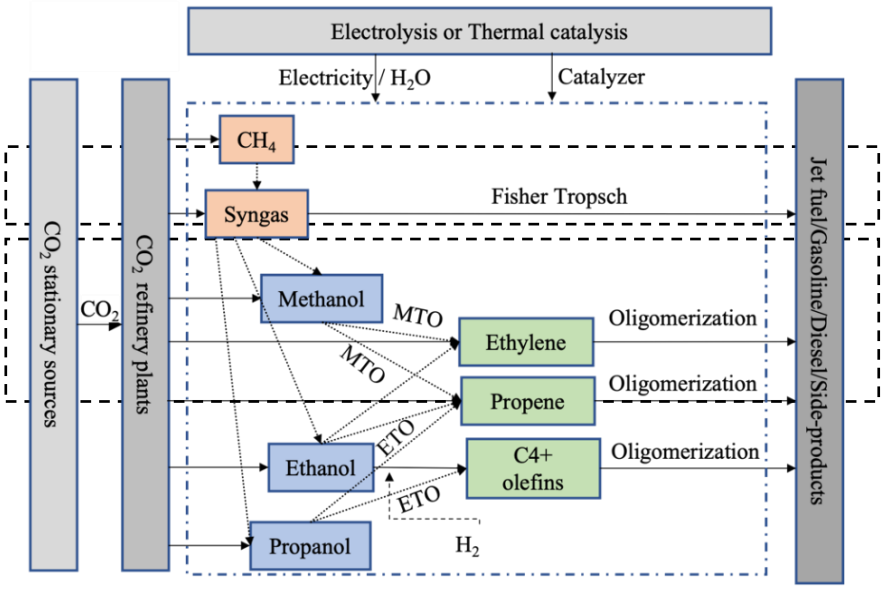


Figure 2-1 Potential CO_2 Conversion Routes to Produce Fuels

to CO or CH_4, syngas, methanol, ethanol, and propanol using electrolysis or thermal catalysis; 3) convert syngas or other intermediate products via the Fisher-Tropsch process or oligomerization of ethylene, propene, C_4+ olefins into hydrocarbons; and 4) fuel separation and finishing to produce fuel products and integrating the overall process and plant. This paper investigates two potential conversion pathways for CO_2 to jet fuels, with one involving the Syngas direct Fisher-Tropsch process. The other one is converting methanol to olefins first and then olefin oligomerization to distillate using methanol as an intermediate.

2.2.2 Techno-economic Analysis for CO_2 Conversion

Several prior studies have explored the techno-economic feasibility of different pathways for converting CO_2 into chemicals and fuels. A Gross-Margin model was developed to assess the techno-economic viability of various C_1-C_2 products produced through the electro-reduction of CO_2 (Verma et al., 2016). This model optimized the performance benchmarks of different electro-reduction products, including carbon monoxide, formic acid, methanol, methane, ethanol, and ethylene (Verma et al., 2016). In another investigation, a process mass and energy balance model in CHEMCAD evaluated the technological and economic feasibility of formic acid synthesis from CO_2 (Qin et al., 2020). Calculations of molar flow rates were employed in a separate study to determine the capital investment, operating costs, and product revenue associated with CO_2 reduction to liquid products. Four potential routes, analyzed under various performance scenarios using a consistent model, assessed their techno-economic viability. The primary expense was the capital cost associated with the purchase and installation of the CO_2 electrolyzer (Spurgeon & Kumar, 2018). Assessing the end-of-life net present value (NPV) of a generalized electrochemical CO_2 reduction (eCO_2R) plant under proposed performance targets revealed the profitability of chemicals and fuels production. NPVs indicated that electrochemical CO_2 reduction could be profitable, but improvements such as lower electricity costs and enhanced catalytic performance were needed to increase profits (Jouny et al., 2018). A techno-economic analysis was conducted by calculating the levelized cost of products from CO_2 reduction reactions to identify the most profitable products and the required performance targets (Kibria et al., 2019). Recently, a more

intelligent, comprehensive, and fully automated process synthesis framework was developed to predict the levelized cost of chemicals derived from CO_2 conversion. This model explored 295 electrochemical coproduction combinations to identify profitable combinations of CO_2RR technology combined with value-added organic oxidation reactions (OORs) (Na et al., 2019).

2.2.3 Supply Chain Network Optimization

Geographically, the locations of CO_2 supply sites (stationary sources) and jet fuel end-use sites (airports) are not contiguous, which presents a challenge for establishing a supply chain network for the CO_2-to-Fuels conversion industry (Netl.Doe. Gov, 2023.). A strategic optimization of the supply chain network of CO_2 conversion is crucial for addressing this challenge by selecting the number, locations, and capacities of facilities at each stage of the supply chain. Numerous studies have focused on supply chain systems optimization for renewable fuel products. Various optimization techniques, such as linear programming (LP), mixed integer linear programming (MILP), and mixed integer nonlinear programming (MINLP), have been extensively utilized to develop technical and economic models for different carbon conversion technologies (Elia et al., 2012, 2014; Leila et al., 2018; Wassermann et al., 2022). These models consider many factors, including the availability of feedstocks, the selection of conversion technologies, the locations of refineries, geographical diversity, infrastructure compatibility, demand distribution, and government incentives. For example, a multi-objective and multi-period MILP model that considered various conversion pathways and technologies was used to address the logistical challenges in a biomass-to-liquid system (You & Wang, 2011; Baliban et al., 2013).

Although considerable attention has been given to supply chain systems for renewable fuel production, there are few quantitative models for optimizing the supply chain network design for CO_2 conversion to valuable jet fuel. This paper bridges this gap by building a MILP model to optimize the supply chain network of CO_2 conversion to jet fuel with minimal total cost. The model determines the overall supply chain costs via different CO_2 conversion pathways, which include CO_2 capture costs, CO_2 and jet fuel transportation-related costs, refinery capital investment, and refinery operating costs. The

originality of the developed optimization work includes 1) defining a large-scale CO_2 utilization process that includes carbon capture, conversion, and consumption (CCCC) scheme, 2) evaluating the techno-economic feasibility of FTS and MeOH conversion pathways and identifying the major cost drivers, and 3) calculating the carbon emissions from the conversion and transportation in the CO_2-to-Fuel process.

2.3 Network Design

This paper considers a three-stage CO_2-to-Fuels supply chain network, including I stationary CO_2 source sites (i as its index), J potential CO_2 conversion refineries (j as its index), and A large airports (a as its index) in the United States as jet fuel demand points. Each stationary source i has up to E_i tons of CO_2 to be captured annually at the cost of c_i^c per ton. CO_2 and H_2 are synthesized into jet fuels at refineries via S conversion pathways (s as its index). Each potential refinery j has an annual capacity to convert C_{sj} tons of CO_2 at the conversion rate of α^s and at the H_2 cost for processing one ton of CO_2 of c_j^h. Building and operating conversion capacity following pathway s at refinery j incurs c_{sj}^f annualized capital investment and c_{sj}^o operating cost per ton of CO_2. This study only considered transporting CO_2 by pipelines at the unit cost of c_{ij}^l (\$/t) from source i to facility j. The transportation cost of jet fuel is performed by trucks and is c_{ja}^v (\$/t) from facility j to airport a. The annual jet fuel demand at airport a is D_a tons. The average jet fuel sale price is p per ton. The model decides x_{ij} tons of captured CO_2 from source i transported to refinery j and y_{ja} tons of produced jet fuel from refinery j to airport a. The binary decision z_j^s represents the selection of conversion pathway s at potential refinery j. If no pathway is selected, it means no capacity is built at potential location j.

The objective of the MILP model (2-7) is to minimize the net supply chain cost, which is the total costs minus the overall revenue. The total costs are comprised of five parts: CO_2 capture cost, H_2 purchase cost, CO_2 and jet fuel transportation cost, refinery capital investment, and refinery operating cost.

$$Min \quad \sum_{i\in I}\sum_{j\in J}\left(c_i^c + c_j^h + c_{ij}^l\right)x_{ij} + \sum_{i\in I}\sum_{j\in J}\sum_{s\in S} c_{sj}^o x_{ij} + \sum_{j\in J}\sum_{s\in S} c_{sj}^f z_j^s + \sum_{j\in J}\sum_{a\in A}\left(c_{ja}^v - p\right)y_{ja} \tag{2-1}$$

s.t. $$\sum_{i\in I}\sum_{s\in S} \alpha^s x_{ij} = \sum_{a\in A} y_{ja} \qquad \forall j \in J \tag{2-2}$$

$$\sum_{i\in I} x_{ij} \le \sum_{s\in S} C_{sj} z_j^s \qquad \forall j \in J \tag{2-3}$$

$$\sum_{j\in J} x_{ij} \le E_i \qquad \forall i \in I \tag{2-4}$$

$$\sum_{j\in J} y_{ja} \le D_a \qquad \forall a \in A \tag{2-5}$$

$$\sum_{s\in S} z_j^s \le 1 \qquad \forall j \in J \tag{2-6}$$

$$x_{ij}, y_{ja} \ge 0;\ z_j^s \in \{0,1\}. \tag{2-7}$$

Objective function (2-2) minimizes the total costs of converting CO_2 to jet fuel of the entire supply chain. Constraint set (2-3) maintains a conversion balance at each facility j. Constraint set (2-4) enforces refineries' conversion capacity. Constraint set (2-5) makes sure that the amount of captured CO_2 does not exceed the available CO_2 emissions at sources. Constraint set (2-6) ensures the airports' demand bounds the produced jet fuel shipped to an airport. Constraint set (2-7) guarantees that each potential conversion facility only uses at most one conversion pathway.

2.4 System Boundary and Data Description

2.4.1 CO_2-CO-FTS-Fuel and CO_2-Methanol-Fuel routes

FTS-based fuel synthesis offers a significant advantage because the resulting fuels are highly suitable for use across different transportation sectors. The electrocatalytic reduction of CO_2 with H_2O to produce CO and the subsequent conversion of CO and H_2 into synthetic fuels using the Fischer-Tropsch process have emerged as a promising technology for synthesizing renewable jet fuel from CO_2. Notably, synthetic jet fuel produced via the FTS process has been approved for commercial aviation use in a blend

of up to 50% with conventional jet fuel (Jürgens et al., 2019). This approval underscores the potential of FTS-based synthetic jet fuel to serve as a viable and sustainable alternative for the aviation industry. The CO_2-CO-FTS system process is depicted in **Figure 2-2** and involves three steps:

1) electrocatalytic reduction of CO_2 to CO. CO_2 is fed to the cathode of an electrolyzer and reacts with water as follows:

$$CO_2 + H_2O + 2e^- \rightarrow CO + 2OH^-; \quad (2\text{-}8)$$

2) combining CO with H_2 to produce hydrocarbons via FTS, 85.8% unreacted CO_2 will be recycled into previous step and electrolyzed into CO; and

3) obtaining jet fuel from the chemical products after industrially recognized treatments, such as distillation or hydro-isomerization (Yao et al., 2020;Han et al., 2020). Methanol is a crucial platform chemical for producing fuels and other chemicals, such as olefins. It is also an intermediate product for various chemical syntheses, including formaldehyde, methyl tert-butyl ether, and acetic acid. Alongside the more widely recognized methanol-to-gasoline (MtG) process currently operational in several commercial plants, ExxonMobil has also exhibited the conversion of methanol into middle distillate fuels such as diesel and kerosene. An intriguing option, particularly in the aviation sector, involves the conversion of methanol into liquid hydrocarbon products that have the potential to serve as synthetic jet fuel. A process diagram of the CO_2-Methanol-Fuel (MeOH) route is illustrated in **Figure 2-3**. Currently, commercial methanol production relies on synthesis gas containing CO and H_2. Several methods can produce methanol from CO_2, including direct thermocatalytic conversion, direct electrocatalytic conversion, direct photocatalytic conversion, and hybrid approaches. Direct CO_2 conversion to methanol follows the following reaction:

$$CO_2 + 3H_2 \rightarrow CH_3OH + H_2O. \quad (2\text{-}9)$$

The conversion of methanol to olefins can be achieved over zeolite catalysts, which yield light olefins, such as ethene and propene. These olefins can be further refined into liquid hydrocarbon fuels via oligomerization and hydrotreating.

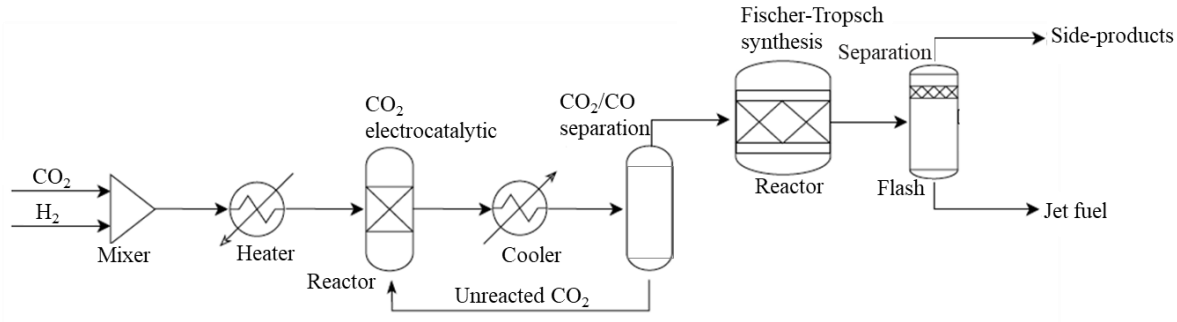


Figure 2-2 Simplified CO_2-CO-FTS Process

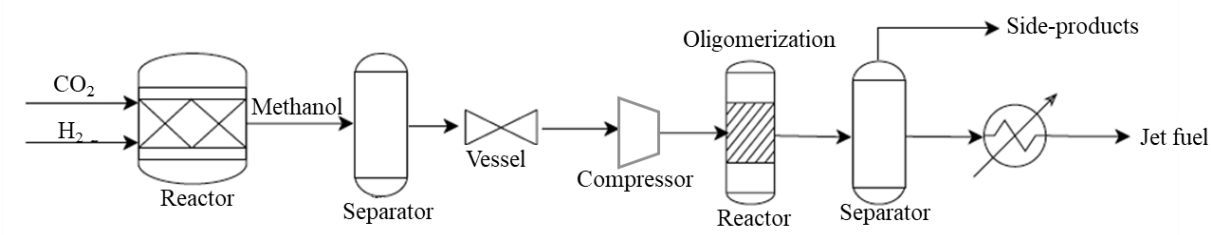


Figure 2-3 Simplified CO_2-Methanol-Fuel Process

2.4.2 Techno-economic Performance of FTS and MeOH

(Wassermann et al., 2020).

Table 2-1 shows the annualized capital investment, unit operating cost, and conversion rate of the FTS and MeOH pathways and the CO_2 recycling rate at the FTS pathway. The reaction equations (7) and (8) of the two pathways show that H_2 is an important feedstock to produce hydrocarbon fuels via reacting with CO_2. A recent review discussed the status of water electrolysis technologies for H_2 production (Buttler & Spliethoff, 2018). The leading technologies are alkaline electrolysis (AEL), proton exchange membrane electrolysis (PEMEL), and solid oxide electrolyzer cells (SOEC). AEL is the most mature technology and currently has

the lowest investment and maintenance costs among these three technologies, which have been commercially available for over a century. From the existing studies, the H_2 consuming is 0.27 and 0.44 kgH_2 per kg_{fuel} in the FTS and MeOH route, respectively (Gonzalez-Garay et al., 2022). Recently, the H_2 price fluctuated from $0.8/kg to $5.0/kg (U.S. Department of Energy, 2023).

In general, CO_2 used in synthesis can be obtained from stationary sources with high CO_2 partial pressure, such as power plants, or directly from the air using direct air capture (DAC) technologies. DAC requires significantly higher energy inputs and involves processing larger gas volumes compared with capturing CO_2 from stationary sources. Therefore, this study only considered capturing CO_2 from power plants. The primary CO_2 capture technologies from stationary sources are absorption and adsorption. From an existing techno-economic analysis, one ton of CO_2 can be converted to 0.46 tons of FT fuel (the summation of 26% naphtha, 47% jet fuel, and 27% diesel) (Zang et al., 2021). Considering the recycling of unreacted CO_2 in the FTS pathway, the utilized CO_2 fraction is calculated by dividing the converted CO_2 by the product of one minus the unused CO_2 fraction and the recycled CO_2. Generally, it is estimated that the production of 1 MJ (50 g) of methanol requires 83 g of CO. In an ideal process, 2,260g of methanol would be needed to produce 1000g of jet fuel. Consequently, 1 kg of CO_2 can yield 0.265 kg of jet fuel via the MeOH pathway. The co-products in the MeOH pathway include 0.212 kg of diesel, 0.053 kg of gasoline, and 0.053 kg of liquefied petroleum gas (Wassermann et al., 2020).

Table 2-1 Characteristic of FTS and MeOH pathways

	FTS	MeOH
Annualized capital investment, $/yr	9,125,625.0	9,653,250.0
Unit operating cost, $/t*		
Synthesis and conditioning	2400.0	2500.0
Electricity	16.7-50.3	49.0-99.4
Conversion rate of pathways, %	21.6%	26.5%
CO_2 recycling rate of FTS pathway, %	85.8%	-

* $/t means US Dollars per ton of produced jet fuel

The estimated cost of capturing CO_2 from different types of power plants ranges from $35 to $112 per ton (David & Herzog, 2011).

We assumed the potential refineries can produce 100 kt of jet fuel per year requires 600 MW_e of installed electrolyzer production capacity, with a 30-year lifetime and 365-day operating time per year for both FTS and MeOH pathways. Electricity stands as the primary contributor to the annual operational costs for electrolyzers and other equipment in the entire process. The FTS and MeOH pathways require 279 to 838 kWh and 828 to 1,656 kWh of electricity, respectively, to produce one ton of jet fuel (Schmidt et al., 2018). The U.S. grid price of $0.06 per kWh was first applied to both pathways in this study, with a subsequent analysis considering varying electricity prices across states. In addition, the other operating cost for synthesis and conditioning are $2,400 and $2,500 for the FTS and MeOH pathways, respectively, to produce one ton of jet fuel (Wang et al., 2022). As the unreacted CO_2 will be recycled for the FTS pathway, the production time for this pathway is calculated as one divided by one minus the unused CO_2 fraction times the recycled CO_2 fraction as shown in equation (9). The unit refinery operations costs for the FTS pathway are the unit refinery operations cost ($/t/yr) without considering recycling, multiplied by the production time. The total one-time capital investment, yearly operating costs, and the discounted cash flow of the FTS and MeOH pathways were evaluated. Four levels of capital investment have been considered: Bare Erected Cost (BEC), Engineering, Procurement and Construction Cost (EPCC), Total Plant Cost (TPC), and Total Overnight Capital (TOC). The one-time annualized capital investments are $9,125,625 for the FTS pathway and $9,653,250 million for the MeOH pathway, with an annual interest rate of 10% for each (Wang et al., 2022).

$$Production_time_{FTS} = 1/(1 - CO_{2_{unsued}} \times CO_{2_{recycled}}) \quad (2\text{-}10)$$

This study conducts a techno-economic analysis for the United States, dividing the contiguous 48 states into 407 grids based on the U.S. 4-Digit Maidenhead Grid Squares system (Ham Radio - US Detail Grid, 2023). Each 2° by 1° grid approximately represents an area of 100 by 70 miles. The assumption is made that each grid could potentially host a refinery. Additionally, each stationary CO_2 emission source is considered a potential refinery location. Consequently, the study considers 1,337 stationary sources, 1,746

potential refinery locations, and the 47 most heavily trafficked airports, as depicted in **Figure 2-4**. The dot size at a source or airport is proportional to the available CO_2 or jet fuel demand, respectively. Two CO_2 conversion pathways for potential refineries are examined in the analysis, resulting in a total of 219,433,788 scenarios related to CO_2-to-Fuels conversion within the framework of supply chain network topologies. To enhance solver runtime efficiency, the United States is divided into five regions: Southeast, Northeast, Midwest, West, and Southwest. The MILP model (2-7) was solved for each region to obtain the optimal supply chain network. The resulting solution includes: 1) the selection of stationary sources and refineries, along with their respective annual volumes; 2) the choice of the conversion pathway for each selected refinery; 3) the amount of CO_2 captured at each source and converted at each selected refinery; and 4) the distribution of jet fuel from refineries to airports.

The total network cost is the summation of CO_2 capture cost, H_2 purchase cost, CO_2 and fuels transportation cost, annualized refinery capital investment, and refinery operating cost, subtracted by the total revenue from selling jet fuel and co-products. **Table 2-2** provides data sources for all required parameters in the model and analysis. A stepwise optimization approach was employed to calculate the minimum levelized cost of CO_2 transport by pipeline over a designed lifetime of 25 years. This calculation considered different pipeline nominal diameters, wall thicknesses, operational pressures, and the number of boosting pump stations. The levelized cost encompasses both capital investment and operating costs, resulting in a range of 8.26 \$/tCO_2 – 8.72 \$/tCO_2. This cost estimate corresponds to a temperature range from -20℃ to 17 ℃ for a pipeline with diameters ranging from 0.4064 m to 0.4572 m, designed for a length of 150 km and a CO_2 mass flow rate of 252 kg/s (Zhao et al., 2016). The total transportation cost for jet fuel by trucks is determined by the unit variable transportation cost, the quantity of jet fuel being transported, and the transportation distance (Huang et al., 2019). This study assumes a variable transportation cost of 0.9\$/t/mile and a fixed transportation cost of \$24.0/t, which remains independent of distance. The distance between two points is approximated by the straight-line distance derived from their latitude and longitude coordinates. Assuming a truck with a 120-gallon fuel tank can travel approximately 600

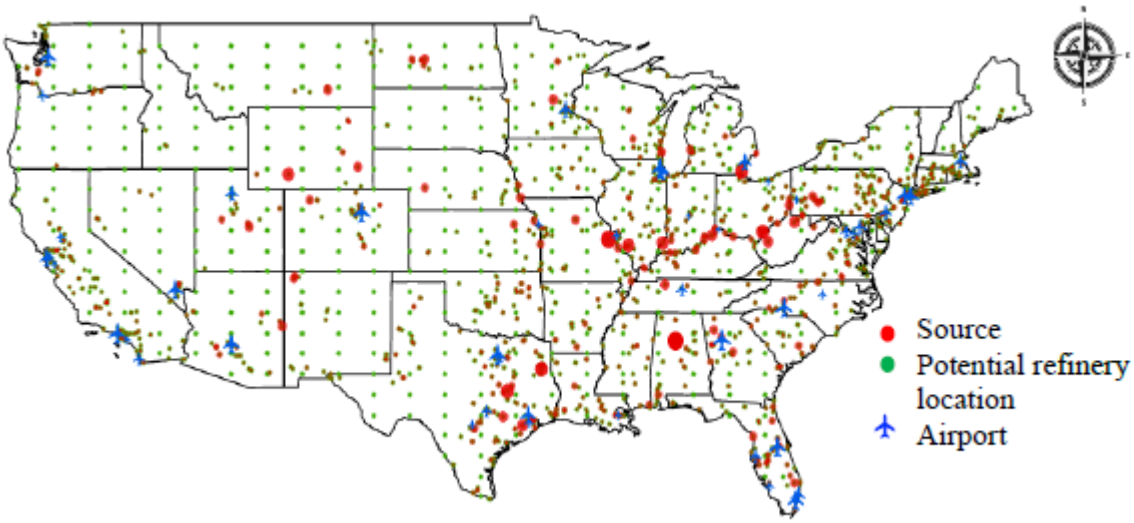


Figure 2-4 Distribution of Stationary Sources, Potential Refineries, and Major Airports

Table 2-2 Data Values and Sources for All Parameters

Parameters	Values	Sources
Costs		
Unit pipeline cost, $/t/mile	8.26-8.72	(Zhao et al., 2016)
Unit variable truck cost, $/t/mile	0.9	(Huang et al., 2019)
Unit fixed truck cost, $/t	24	(Huang et al., 2019)
Jet fuel sale price per ton, $/t	732.5	(Bureau of Transportation Statistics, 2023)
Unit CO_2 capture cost, $/t	35 - 112	(David & Herzog, 2023)
Annualized refinery capital cost, $	(Wassermann et al., 2020). Table 2-1	(Wang et al., 2022)
Unit refinery operational cost, $/t	(Wassermann et al., 2020). Table 2-1	(Schmidt et al., 2018)
Unit H_2 price, $/t	800-5000	(Wang et al., 2022)
Others		
U.S. stationary CO_2 source locations	GitHub	(Netl.Doe.Gov, 2022.)
U.S. stationary CO_2 source emissions, t/yr	GitHub	(Netl.Doe.Gov, 2022.)
Potential refinery locations	GitHub	(Ham Radio - US Detail Grid,2011)
Top 47 busiest airport locations in the U.S.	GitHub	(The Busiest & Biggest Airports in the US, 2024)
Annul jet fuel demands, Mt/yr	GitHub	(Wang et al., 2022)
Electricity price by states, $/kWh	GitHub	(US Electricity Profile 2021 - U.S. Energy Information Administration (EIA), 2021)
Conversion rate of pathways	(Wassermann et al., 2020). Table 2-1	(Zang et al., 2021)(Wassermann et al., 2020)
CO_2 recycling rate of FTS pathway	(Wassermann et al., 2020). Table 2-1	(Zang et al., 2021)

miles at a fuel consumption rate of 6 mpg and considering government regulations limiting a truck driver's maximum travel distance, we restrict that potential refineries should be located within 300 miles of airports. Refinery costs encompass one-time capital investment and operating costs, including expenses for feedstock purchase, equipment installation, electricity usage, management, and maintenance. Revenue is generated by selling jet fuel and side products to airports and other customers. The market price of jet fuel in the U.S. stood at $732.5/t in 2023 (Bureau of Transportation Statistics, 2023.).

2.5 Results

2.5.1 Resulting network

Under the current cost structure, both paths cannot realize profitability. To be futuristic, we assumed the hydrogen price at $1,000/t and reduced the operating cost to 5%. The map in **Figure 2-5(a)** demonstrates the resulting distribution network map under varying electricity rates across states. The FTS pathway is implemented at all refineries. All 14 selected refineries are strategically situated in states characterized by lower electricity rates and proximate to the 108 selected stationary sources, obviating the necessity for new pipelines to transport the captured CO_2. The distances between refineries and airports are meticulously maintained within a 300-mile radius.

In addition, we explored the network configuration under the assumption of uniform electricity prices ($0.06/kWh) across all states. **Figure 2-5(b)** and **Figure 2-5(c)** provide a comparative analysis of the network maps for four airports: Harry Reid International Airport (LAS), Los Angeles International Airport (LAX), John Wayne Airport (SNA), San Diego International Airport (SAN), and Phoenix Sky Harbor International Airport (PHX). The depicted maps reveal that under different electricity rates for all states, the cost-optimal supply chain analysis advocates to build refinery in lower electricity

location. Given the same electricity rate for the whole nation, the refineries will be strategically located in proximity to areas exhibiting higher demand for jet fuel.

To facilitate a comparative assessment of both the CO_2 conversion efficiency and economic viability of the FTS and MeOH pathways, we conducted separate executions of the optimization model for each pathway alone, considering different electricity prices by state. The outcomes reveal that on the condition of \$1,000/t H_2 price and 5% of the

(a) Nationwide CO_2-to-jet fuel supply chain network



(b) Under different electricity prices by states

(c) Under the same electricity price in the nation

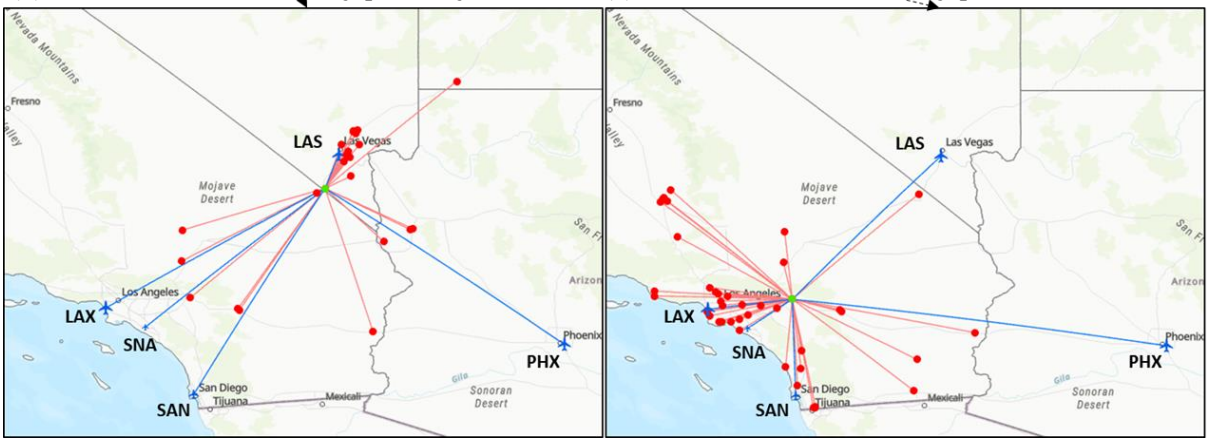


Figure 2-5 Supply Chain Network Design under Different Electricity Rate

(a) is the nationwide CO_2-to-jet fuel supply chain network in the U.S. based on the electricity prices by state in 2022, 1,000\$/t H_2 price and 5% of the operating cost. (b) and (c) are regional CO_2-to-jet fuel supply chain network map for LAX, SNA, SAN, LAS and PHX airports under average electricity rates by state and same electricity rate across the states in 2022, \$1,000/t H_2 price and 5% operating cost.

operating cost, the MeOH pathway is still not economically feasible. However, the overall annual profit of the FTS pathway is $8 billion with a cost of $73 billion and the revenue generated from selling jet fuel and side-products at $81 billion. The profit of the FTS pathway is. The FTS pathway could potentially convert 116,724,796 tons of CO_2 into 46,938,776 tons of jet fuels per year, which 100% meet the jet fuel demand in the selected airports. Notably, the pipeline length is 1,809 miles, and the one-way truck transportation distance spans 4,493 miles. The comparison indicates that the costs associated with CO_2 capture, H_2 purchase, refinery capital, and refinery operations are lower for the FTS pathway than the MeOH pathway. In addition, the difference is caused by the recycling of CO_2 within the FTS pathway, with the expense of H_2 purchase and the operating of the refinery being the predominant contributor to the total cost. Although the overall MeOH pathway is not economically feasible under the assumed cost structure, the profit of selling side-products in the MeOH pathway is higher than the FTS pathway. If its conversion rate could be improved, the production of jet fuel through MeOH would be profitable. Subsection 4.2 provides the sensitivity analysis of the conversion rate of the MeOH pathway.

The life cycle assessment was modeled in OpenLCA using NETL CO_2U LCA (Netl.Doe.Gov, 2022) and exiobase 2.2 (OpenLCA Nexus: The Source for LCA Data Sets, 2022) open-source databases to assess the environmental impact of the integrated CO_2 conversion to jet fuel transportation and production process. A comparison of the global warming potential of jet fuel produced from the optimal, FTS-only, and MeOH-only pathway was conducted. The system boundaries are defined according to the cradle-to-gate approach. One kg of produced jet fuel is considered a functional unit, and TRACI 2.1 was used to calculate an impact assessment method (OpenLCA Nexus: The Source for LCA Data Sets, 2022). The life cycle inventory data were created based on the generated mass balance.

Without considering economic feasibility, both FTS and MeOH pathways exhibit net negative CO_2 emissions. Specifically, the FTS pathway results in 11,249,866 tons of CO_2 emissions during production and transportation on the condition of 1,000$/t H_2 price and 5% of the operating cost, while to produce the same amount of jet fuel, the MeOH

pathway scenario emits 3,510,806 tons of CO_2 per year. The total CO_2 capture amounts per year are 116,724,796 tons for the FTS pathway scenario and 95,229,814 tons for the MeOH pathway scenario. Net carbon emissions per year are computed as used CO_2 minus the emissions during production and transportation, which are -88,783,284 tons for the FTS pathway scenario, and -6,497,200 tons for the MeOH pathway scenario. The optimal nationwide CO_2-to-Fuels supply chain network is presented in **Table 2-3**.

2.5.2 Sensitivity analysis

The major cost contributors of CO_2-to-Fuels come from hydrogen usage and operating expense. We conducted a sensitivity analysis, exploring the impact of the unit H_2 price and the unit refinery operating cost on total profit, utilized CO_2, and produced jet fuel. The findings are depicted in **Figure 2-6, Figure 2-7**, and **Figure 2-8**. **Figure 2-6** is the optimal total profits when the H_2 price ranges from $600/t to $1,300/t and the unit operating costs are between 4% and 8% of the current cost, which is possible when the conversion happens during the off-peak time when the penetration rate of renewable energy further increases. **Figure 2-6** shows that when the H_2 price is $600/t, the optimal solution can make profit under all the range of unit operating costs from 4% to 8% of the current level. When the H_2 price increases to $1300/t, only under the lowest unit operating cost scenario can be economically feasible. The utilized CO_2 and the produced jet fuel in the optimal solution also decrease as the H_2 price and unit operating cost increase as shown in **Figure 2-8** .

Figure 2-7 is the heatmap of the profits under different H_2 prices and unit operating costs of both pathways. The result shows that the MeOH pathway requires much lower H_2 price and unit operating cost to be economically feasible than the FTS pathway. Currently, the U.S. Department of Energy targets to reduce the hydrogen cost to $1,000/t by 2031 (U.S. Department of Energy, 2023.). To make production profitable, the unit operating cost should be reduced to 6% of the current rate via the FTS pathway. For the MeOH pathway, the H_2 price should be further reduced to $700/t to realize profit. The utilized CO_2, and produced jet fuel The CO_2 recycle percentage of the FTS pathway

Table 2-3 Nationwide CO_2-to-Fuels supply chain network results of optimal pathways under the conditions of an 85.8% CO_2 recycle rate for FTS pathways, a $1,000 per ton unit H_2 price, and 5% of the operating cost

Costs	Unit, $/t	Total, $/yr
CO_2 capture	183	8,579,272,478
H_2 purchase	709	33,266,566,750
Refinery capital	3	127,758,750
Refinery operations	569	26,689,190,364
Pipeline	4	182,057,768
Truck transportation	75	3,537,900,995
Total cost	1,542	72,382,747,105
Revenue, $/yr	-	
Jet fuel	-	34,382,653,061
Naphtha	-	16,213,252,280
Diesel	-	29,939,049,066
Gasoline	-	0
Liquefied petroleum gas	-	0
Total revenue	-	80,534,954,407
Profit, $/yr	-	8,152,207,302
Transportation, mile	-	
Pipeline length	-	1,809
Truck travel distance	-	4,493
CO_2, ton	-	
Captured CO_2	-	116,724,796
Used CO_2	-	100,033,150
Unused CO_2	-	16,691,646
Emissions during production and transportation	-	11,249,866
Net CO_2 emissions	-	-88,783,284
Jet fuel, ton/yr	-	46,938,776
Jet fuel demand meet, %	-	100%

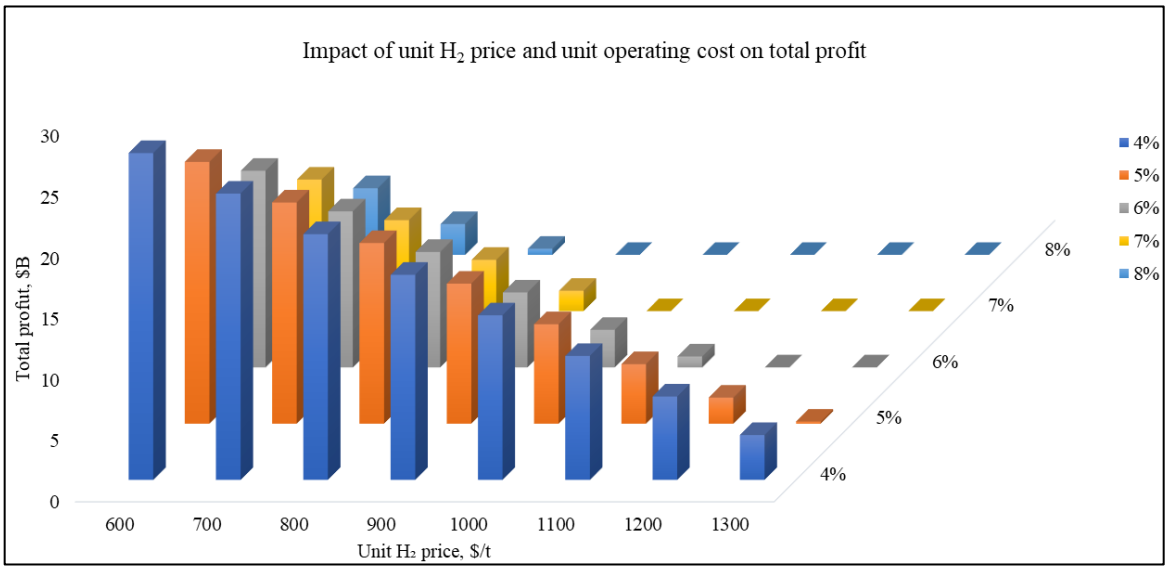


Figure 2-6 Sensitivity Analysis: Impact of Unit H_2 Price and Unit CO_2 Capture Cost on Profits

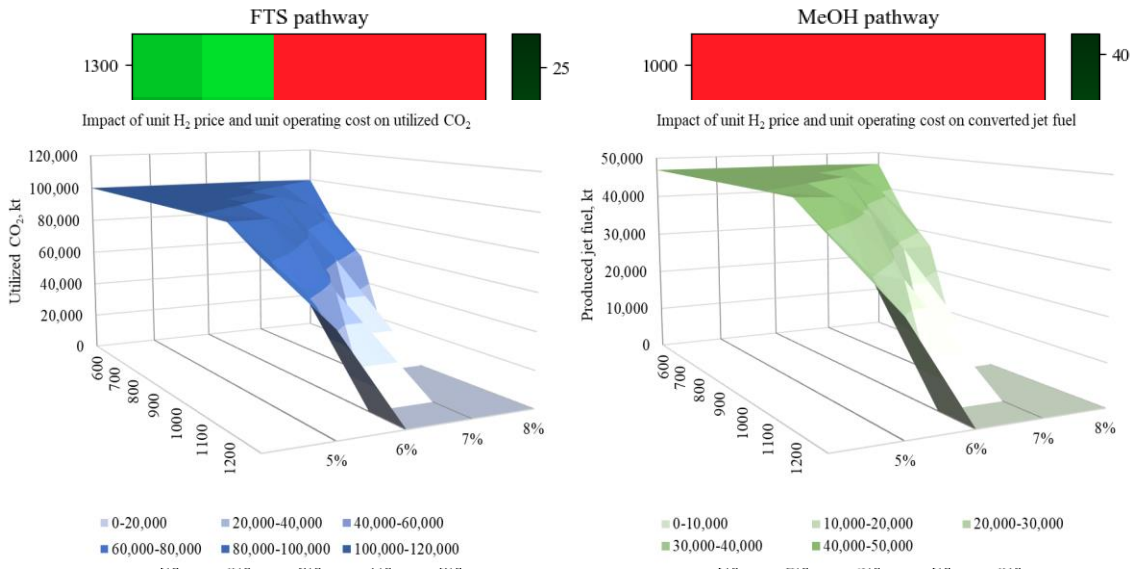


Figure 2-7 Heatmaps of the CO_2 Capture Cost and H_2 Purchase Cost on Profits of FTS Pathway and MeOH Pathway

Figure 2-8 Sensitivity Analysis: Impact of H_2 Price and CO_2 Capture Cost on Utilized CO_2 and Produced Jet Fuel

influences the costs of CO_2 capture, H_2 purchase, refinery capital and operations, utilized CO_2 and produced jet fuel. **Figure 2-9** depicts the outcomes of a sensitivity analysis examining the CO_2 recycling percentage ranging from 56% to 96%, with 86% serving as the baseline. The result reveals a clear relationship between the CO_2 recycle percentage and total costs. Beyond the 86% threshold, all the costs and utilized CO_2 will decrease while the system can fulfill the total jet fuel demand at the selected airports. The refinery capital costs remain constant across all observed variations in CO_2 recycling percentages. The CO_2 conversion rate significantly impacts captured CO_2, utilized CO_2 and produced jet fuel. As illustrated in **Figure 2-10**, the optimal levels of captured CO_2, utilized CO_2, and produced jet fuel, under both relatively low and high H_2 prices and operating costs, are contingent upon varying CO_2 conversion rates ranging from 30% to 90**%. Figure 2-10(a)** shows the optimal total profit and captured CO_2 under the lower cost scenario ($100/t for the H_2 price and 3% of the operating cost). In this scenario, all demands are

met, and the utilized CO_2 and produced jet fuel amount to 99,870 kt and 46,939 kt, respectively. Of course, the captured CO_2 decreases with increasing conversion rates. Within the range of 30% to 70% conversion rates, the FTS pathway dominates the MeOH pathway at all selected refineries, whereas beyond an 80% conversion rate, the MeOH pathway prevails. This can be attributed to the inherent CO_2 recycling mechanism within the FTS pathway, resulting in a higher final CO_2 conversion rate compared to the MeOH pathway. When the conversion rate is very high, the recycling advantage diminishes. However,

despite the FTS pathway's advantage in profit generation in most cases, the MeOH pathway demonstrates higher revenue due to its capacity to produce additional side-products. Consequently, while the MeOH pathway may initially appear economically unfeasible at lower CO_2 conversion rates, an increase in the conversion rate renders this pathway financially viable. Conversely, as depicted in **Figure 2-10(b)**, under higher costs, the FTS pathway emerges as the preferred choice for all refineries regardless of fluctuations in the CO_2 conversion rate. It is noteworthy that under a 30% CO_2 conversion rate, the demand for jet fuel cannot be fully met.

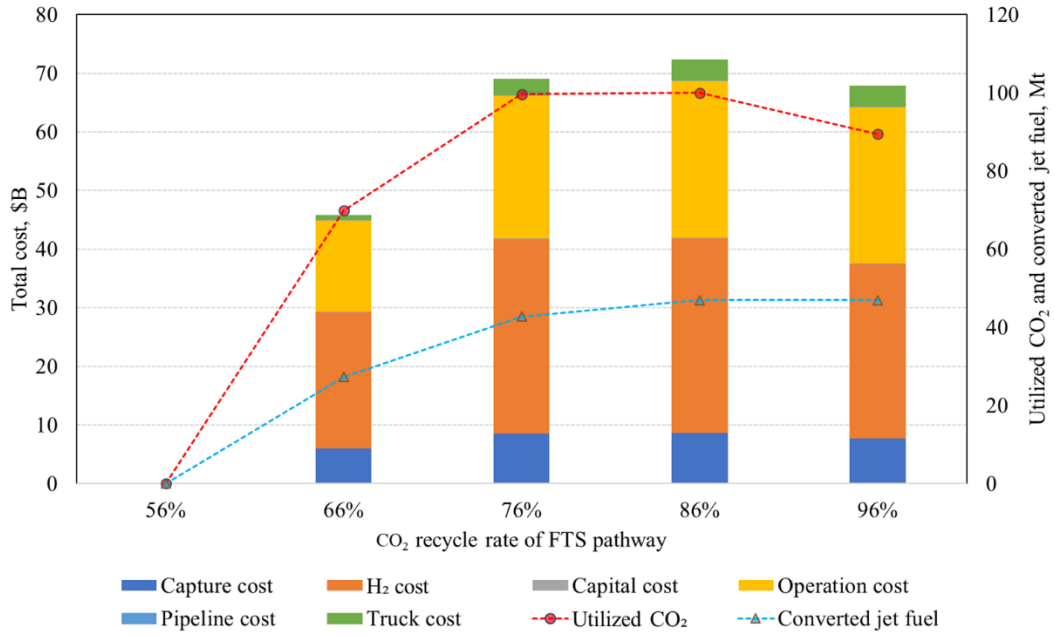


Figure 2-9 Sensitivity Analysis: Impact of the CO_2 Recycle Percentage of the FTS Pathway on Costs and Profits, 56%, 66%,76%,86% (base case), and 96% CO_2 Recycled.

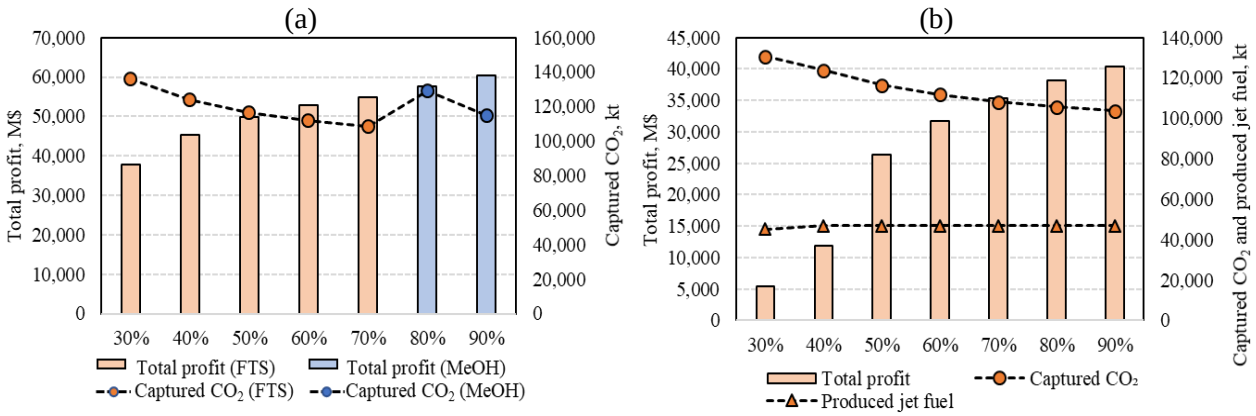


Figure 2-10 Impact of CO_2 Conversion Rate on Total Profit, Utilized CO_2, and Produced Jet Fuel of the Optimal Pathway

Figure 2-10 (a) is the optimal total profit and captured CO_2 under \$100/t of H_2 price and 3% of operating cost. Figure 2-10 (b) is the optimal total profit, captured CO_2 and produced jet fuel under \$500/t of H_2 price and 5% of the unit operating cost.

2.6 Discussion

Our study underscores the optimal network design for CO_2 conversion to jet fuel considering both cost-effectiveness and environmental concerns. Notably, the H_2 price and refinery operating cost are substantial contributors to total expenses, emphasizing the need for further exploration of cost-effective H_2 production and distribution, CO_2 conversion technologies, and possible usage of renewable energy during conversion. The recycling percentage within the FTS pathway plays a pivotal role in determining the applied conversion pathway at refineries. Since CO_2 will be recycled from the FTS pathway, the final conversion rate of this pathway is higher than the MeOH pathway. Therefore, the FTS pathway dominates all the refineries at the base scenarios. Our analysis reveals an inverse relationship between the CO_2-to-Fuels conversion rate and costs associated with CO_2 capture, H_2 purchase, annualized refinery capital investment, refinery operations, and fuel transportation. Thus, increasing the conversion rate is deemed crucial for enhancing the economic viability of the CO_2-to-Fuels technologies, especially for MeOH pathway. Pipeline construction costs significantly influence refinery location decisions due to substantial initial investments in land use and labor. In our study, the proximity of selected sources to the refineries results in significant cost savings. The electricity rate constitutes a substantial component of the operational expenses incurred by refineries, which implies the importance of using renewable energy during the conversion, especially during the energy surplus period. Consequently, optimal refinery sitting tends to favor locations characterized by lower electricity rates, thereby mitigating overall operational costs associated with refinery activities. As the transition to renewable electricity progresses, an anticipated decrease in electricity rates from \$0.060/kWh to \$0.029 kWh is expected to result in a significant reduction in refinery operations costs (U.S. EPA, 2023.). This shift will enable the establishment of refineries closer to airports, enhance transportation efficiency, and potentially reduce overall transportation expenses and emissions.

The CO_2-to-Fuels through the FTS and MeOH pathways holds significant environmental potential by effectively reducing carbon emissions from stationary power plants and contributing to climate change mitigation. Both the FTS and MeOH pathways exhibit a

noteworthy characteristic of being CO_2 emission negative. This unique feature allows for the continued utilization of high-value jet fuel without contributing excess energy and emissions from transportation-related activities. In summary, the combined application of techno-economic analysis and network design for CO_2 conversion to fuels represents tools for a comprehensive evaluation of feasibility and viability. The life cycle assessment provides valuable insights into the potential environmental impacts of the process. This ensures that investments in CO_2 conversion to fuels align with sustainability goals, making them a strategic and environmentally conscious choice.

2.7 Conclusion

This study proposed a mixed-integer linear programming model for the optimal design and operation of the CO_2 conversion to jet fuel supply chain to minimize the total cost. In the evaluation of CO_2 conversion technologies, the FTS pathway emerges as the more economical option under the current conversion rates but a lower H_2 price and operating costs. MeOH could also be viable when the conversion rate is increased, even for both pathways. When economically feasible, both pathways can yield high impacts on carbon emissions. The contributions of H_2 price, electricity price, and conversion rates are pivotal for their economic feasibility, which highlights the necessity of the current hydrogen initiatives led by the U.S. Department of Energy and a higher penetration rate of renewable energy in electricity generation. Moreover, fostering collaboration between power plants, refineries, airports, and governments is imperative for the development of sustainable CO_2 conversion technologies. Such collaboration enables a comprehensive approach to technology development, identifying optimal locations for plants, supply chains, and transportation infrastructure.

While this study provides an extensive overview of the technical, economic, and environmental aspects of CO_2 conversion to fuels, there is a need to explore other CO_2 utilization technologies. To promote sustainable CO_2 conversion technologies, prioritizing research, and development efforts, investing in infrastructure, and fostering collaboration among stakeholders are essential. A deeper understanding of the potential of alternative CO_2 conversion to fuels technologies, combined with strategic planning and

investment, can contribute to reducing greenhouse gas emissions and creating a more sustainable future.

CHAPTER THREE

HYDROGEN LOGISTICS NETWORK DESIGN FOR HYDROGEN FUEL CELL ELECTRIC LONG-HAUL TRUCKS

3.1 Abstract

With the growing emphasis on reducing carbon emissions and transitioning towards sustainable transportation solutions, hydrogen fuel cell electric long-haul trucks (FCETs) have emerged as a promising alternative to conventional diesel-powered vehicles. This study seeks to determine the optimal hydrogen delivery infrastructure that balances cost efficiency with environmental sustainability, thereby supporting the transition to cleaner transportation systems. We conduct a comprehensive comparative analysis of three key hydrogen delivery pathways, which including gaseous hydrogen, liquid hydrogen, and ammonia carrier, for hydrogen FCETs in the United States. A mixed-integer programming model has been developed to assess all associated costs throughout the hydrogen supply chain, encompassing hydrogen pre-processing and delivery, terminal and refueling stations operating and distribution. The findings reveal that the liquid hydrogen pathway is the most cost-effective option under the current cost structure, with a levelized cost of hydrogen of $4.6/kg in the baseline scenario for a 10% FCET market penetration rate. However, significant improvements are needed in other pathways to enhance their feasibility. Specifically, the operating costs of gaseous hydrogen fueling stations must be reduced, while the energy losses and cracking costs associated with the ammonia pathway require substantial optimization. Additionally, the refueling capacity of hydrogen fueling stations must be increased to accommodate the growing hydrogen demand and ensure the scalability of the network.

3.2 Introduction

The transition to a low-carbon economy has placed significant emphasis on decarbonizing the transportation sector, which remains one of the largest contributors to global greenhouse gas emissions. Hydrogen fuel cell electric vehicles (FCEVs), particularly long-haul trucks, have emerged as a promising solution for achieving deep decarbonization in heavy-duty transport. FCEVs offer several advantages, including zero tailpipe emissions and high energy density, making them well-suited for long-distance freight transport. Furthermore, hydrogen-powered vehicles are nearly three times more efficient than traditional internal combustion engines and require less frequent refueling on long journeys, enhancing their operational efficiency (Hydrogen’s Role in

Transportation, 2022). Hydrogen for FCEVs is primarily produced through water electrolysis, a process that does not generate carbon emissions, contributing further to the sustainability of this technology (P.A. Le et al., 2023). However, the adoption of hydrogen-powered vehicles, particularly in long-haul applications, is contingent upon the availability of a robust hydrogen logistics network. Current infrastructure in the United States is inadequate, with only 50 hydrogen refueling stations, all located in California, supporting approximately 12,000 hydrogen fuel cell-powered vehicles and nearly 70 buses (Hydrogen's Role in Transportation, 2022). This lack of infrastructure poses a significant barrier to the widespread deployment of hydrogen-powered long-haul trucks. Meanwhile, the global demand for hydrogen is expected to increase substantially in the coming decades. Currently, the total demand for hydrogen, which includes that which is not separated from other compounds or materials is projected to exceed 120 Mt (Corbeau, 2022). By 2040, hydrogen demand is expected to rise to 130 Mt, and by 2050, it is anticipated to approach nearly 300 Mt (Global Hydrogen Demand by Sector in the Sustainable Development Scenario, 2019-2070, 2020). This surge in demand underscores the urgent need for the development of hydrogen supply chains, particularly in the transport sector, where significant investment in refueling infrastructure is required to meet the needs of hydrogen-powered long-haul trucks. Addressing these challenges will be crucial for enabling the widespread adoption of hydrogen as a clean energy source for heavy-duty transport.

3.2.1 Hydrogen Logistics Technologies

Hydrogen logistics encompasses the complex processes of producing, on-site storage, transporting, and distributing hydrogen for various applications (Villalba-Herreros et al., 2023a). Given hydrogen's low-density, high-energy content per mass, high flammability, small molecular size, low boiling point, high diffusivity, reactivity with certain materials, its logistics present distinct challenges that necessitate advanced technologies and infrastructure (Mulky et al., 2024). There are two primary approaches to hydrogen storage and transportation: physical methods and chemical methods as shown in **Table 3-1.** These approaches differ significantly in terms of energy efficiency, scalability, and infrastructure requirements. First, physical methods involve the direct storage and

Table 3-1 Comparison of Major Physical and Chemical Hydrogen Storing and Transporting Methods

Hydrogen Transport Technologies		Benefits	Drawbacks	Sources
Physical Methods	Compressed Gas	Minimal equipment, only compressor and storage vessel required. Practical for smaller scale projects.	Low storage density of 7.8 kg/m^3. Gas unused at end of discharge. Heat loss during compression process.	(Lahnaoui et al., 2019)
	Liquid Hydrogen	High storage density of 70 kg/m^3. Practical for large-scale projects.	Cryogenic temperatures of -253℃ required. High energy cost required for hydrogen liquefication (15 kWh), 45% of hydrogen's heating value.	(Andersson & Grönkvist, 2019)
Chemical Methods	Ammonia	High storage density of 17% hydrogen by weight. High return on investment. Electrolysis compression ROI 63-84% Hauber Process ROI 42-52%.	13-34% loss of energy when converting ammonia to hydrogen. High temperatures of 400-450℃	(Blanco, 2022)(The Haber Process, 2023)
	Metal hydrides	Compression not required Relatively high storage density (up to 19.6% hydrogen by weight depending on the compound). Extremely safe and durable.	High temperatures required to extract hydrogen (sodium alanate requires temperatures of up to 225℃). Heavyweight adds to transport costs.	(L. Li et al., 2013)
	Carbon-based Materials	High gravimetric energy density of 10%. No wasteful byproduct formation.	Cryogenic temperatures (-197 ℃).	(Z. Li et al., 2022)

Table 3-1 Continued

LOHCs	Transported via ship or truck at ambient temperatures. Minimal losses of 0.1% per cycle.	Hydrogenation and dehydrogenation require temperatures of 20-50 bars and up to 420℃.	(Preuster et al., 2017)

transportation of hydrogen in either its compressed gaseous form or as a cryogenic liquid. For the compressed gaseous, hydrogen can be stored and transported as compressed gas, typically at pressures of 20-30 bars. It is predominantly transported using tube-trailers or pipelines. The key challenge with this method lies in the low storage density of hydrogen in its gaseous form. As a result, compressed hydrogen is more suited for smaller-scale transport operations, such as those relying on trucks, where the distance and volume are limited (Amos, 2011). While pipelines provide a potential large-scale solution, they require specialized materials to handle high-pressure hydrogen safely (Tian & Pei, 2023). Another physical method of storing and transporting hydrogen is by compressing hydrogen into a liquid. In this method, hydrogen can be stored as a liquid by cooling it to extremely low temperatures (78 K), before the hydrogen is propelled through a valve. Liquid hydrogen has the highest energy density of any transportation method (Amos, 2011). However, liquefaction is highly energy-intensive, requiring up to 15 kWh for every kilogram of hydrogen, which equates to about 45% of hydrogen's lower heating value (Zhang et al., 2023). As a result, liquid hydrogen is generally more suitable for large-scale projects, particularly when transportation over long distances or bulk storage is required (Al Ghafri et al., 2022).

In addition to physical methods of storing and transporting hydrogen, several chemical methods exist. By chemically bonding hydrogen with another compound, supply chain distributors can avoid some of the difficulties of transporting large volumes of hydrogen liquid or compressed has. However, chemical methods also involve removing hydrogen from a chemical compound, which can be energy intensive. The most common chemical method is ammonia. Hydrogen is combined with diatomic hydrogen in a process called the Haber Process, a reversible and exothermic process. The combined nitrogen is heated to 450℃ and compressed to 200 atm (Chemistry LibreTexts, 2023). This high pressure allows liquid ammonia to be collected and any gas to be returned to the storage cycle for the process to begin again (The Haber Process, 2023). Ammonia has a high energy storage density, but significant energy is consumed when chemically forming ammonia and chemically removing hydrogen (International Renewable Energy Agency, 2022). Another chemical method of storing and transporting hydrogen is by forcing a chemical

bond between hydrogen and another molecule to form a metal hydride. Because hydrogen is chemically bonded, high pressures and temperatures are not needed such as they are in physical methods of storing and transporting hydrogen (L. Li et al., 2013). Furthermore, another advantage of metal hydride is their relatively high storage density, with compounds such as $NaBH_4$ and NH_3BH_3 having weight storage densities of 7.3% and 19.6% respectively (L. Li et al., 2013). With a high storage density and relatively simple transportation logistics compared to physical methods, metal hydrides are very attractive to suppliers. However, the main drawback is that high temperatures are required for hydrogen from the compound. With sodium alanate specifically, hydrogen is extracted via a two-step reaction at temperatures as high as 225℃ (L. Li et al., 2013). Another method of storing hydrogen is by adsorbing hydrogen into carbon-based materials like nanotubes. While carbon-based materials have a high energy (gravimetric) density of 10%, the necessary temperatures for storing said hydrogen are near -197℃ causing the method to be impractical (Critical Review on Carbon Based Materials, 2023). Specific temperatures and energy densities vary based on the specific material, but low temperatures do tend to outweigh the high energy density in nearly all compounds. The final chemical method being analyzed by this literature review is liquid organic hydrogen compounds or LOHCs. When hydrogen is added to LOHCs, the volumetric and gravimetric storage capacity of the LOHC increases (Niermann et al., 2021). LOHCs can be hydrogenated through electrolysis and unloaded using a catalyst; both processes require high temperatures and pressures of up to 50 bar and 420℃ (Niermann et al., 2021). However, once hydrogenated, LOHCs can be transported via truck or ship like crude oil (Niermann et al., 2021).

3.2.2 Hydrogen Logistics Models

Hydrogen logistics models generally consist of three types of models: optimization models often using linear programming or mixed-integer linear programming, spatial models often using GIS, and transition models using specific data and scenarios to better understand how hydrogen energy could be used in specific areas or contexts (Riera et al., 2023). It is also important to note that these categories are not mutually exclusive, models can and do incorporate different elements of these three categories depending on the

research question and model's goals. Optimization models, commonly formulated using linear programming (LP) or mixed-integer linear programming (MILP), are widely employed to focus on the production, transportation, and distribution of hydrogen across an entire network. In contrast, spatial models often rely on Geographic Information Systems (GIS) to analyze regional or local hydrogen logistics, while transition models use scenario-based approaches to explore how hydrogen infrastructure and technologies may evolve over time.

The choice of modeling technique often depends on the research objective. For instance, mathematical optimization models, such as those using linear or mixed-integer programming, are instrumental in solving large-scale problems related to hydrogen production, transportation, and dispensing. These models balance cost, operational efficiency, and environmental impacts. Linear programming is often favored for its simplicity and computational efficiency, while non-linear programming can offer higher accuracy, albeit at the cost of increased complexity. For example, a South Korean study utilized mixed-integer linear programming to optimize hydrogen logistics by integrating both imported and domestic hydrogen data, along with energy prices and usage patterns. The model provided valuable insights into the future use of blue and green hydrogen, recommending optimal import sources and estimating hydrogen unit costs under various scenarios (Seo et al., 2020). Spatial models, on the other hand, emphasize the geographic distribution of hydrogen infrastructure. These models integrate hydrogen demand, production data, and the location of filling stations, pipelines, and transportation networks to assess regional logistics. For example, a UK-based spatial model incorporated data on hydrogen demand and infrastructure to forecast the spread of hydrogen demand and the development of refueling infrastructure across the country. Such models are crucial for determining how hydrogen logistics will evolve at a localized level, especially when considering refueling stations and delivery routes (Balta-Ozkan & Baldwin, 2013).

Finally, transition models play a pivotal role in examining the broader implications of hydrogen adoption. These models go beyond mathematical optimization, aiming to capture the evolving dynamics of hydrogen technology and infrastructure. They often incorporate environmental and societal factors, such as emissions reduction, fuel

efficiency, and the logistics of integrating emission-free vehicles into existing transportation systems. By analyzing different scenarios, transition models provide insights into the long-term sustainability and scalability of hydrogen logistics networks. For instance, previous studies have examined the environmental impact of hydrogen pathways, evaluating emissions and fuel efficiency to ensure that hydrogen technologies align with broader sustainability goals (Sayer et al., 2024).

The successful development of a hydrogen logistics network requires comprehensive consideration of various interrelated factors, regardless of the specific modeling approach employed. Key factors include hydrogen production methods, transportation modes, storage technologies, and the infrastructure required for refueling, along with the spatial and temporal dynamics of hydrogen demand. Additionally, optimizing infrastructure investments, operational logistics—such as delivery pathways—and refueling schedules is essential to minimize costs and emissions while ensuring a reliable hydrogen supply. These challenges become particularly pronounced in the context of long-haul freight transport, where maintaining sufficient hydrogen availability requires the strategic placement of refueling stations along critical transportation corridors. Given the complexity and interdependence of these factors, the development of hydrogen logistics networks necessitates a holistic and integrated strategy.

This paper seeks to address these complexities by investigating three central research questions:

1. What is the levelized cost of hydrogen, including preprocessing, delivery, and terminal and fueling station operations, for fuel cell electric long-haul trucks in the United States?

2. What are the trade-offs and impacts of various hydrogen delivery options on the associated costs of hydrogen delivery under different market penetration rates of fuel cell electric trucks (FCETs)?

3. What are the optimal locations and quantities of hydrogen terminal facilities and refueling stations, as well as the allocation of transportation units (tube trailers, liquid trucks, and carrier trucks) and the anticipated hydrogen flow patterns between them?

Following the research questions, this study is structured into key sections. First, it reviews hydrogen production methods, storage technologies, and transportation pathways, focusing on their operational and economic implications. Next, a mixed-integer programming model is presented to optimize hydrogen logistics, including terminal and refueling station locations and transportation unit allocation. The model results are analyzed to address economic feasibility, hydrogen flow patterns, and infrastructure needs. A sensitivity analysis explores the impact of varying key parameters, followed by a discussion on delivery pathway trade-offs and future research directions.

3.3 System Boundary and Data Description

3.3.1 Hydrogen Production

Hydrogen is produced through a variety of thermal, biomass, and electrolysis-type processes. On medium and large scales, green hydrogen methods are the most common. Green hydrogen includes using electrolysis or biomass to extract hydrogen (Yu et al., 2021a). Electrolysis involves the use of electricity to split water into hydrogen and oxygen within an electrochemical cell. In this process, electricity passes through two compartments, the anode and cathode, where hydrogen ions migrate from the anode to the cathode, where hydrogen gas is subsequently extracted (U.S. Department of Energy, 2023). Various types of electrolysis cells are used, each with distinct materials and ion exchange mechanisms. Alkaline electrolysis, for example, generates hydrogen from hydroxide ions and employs sodium or potassium solutions in the anode and cathode (U.S. Department of Energy, 2023). Solid oxide electrolysis cells (SOEC) differ in that they extract hydrogen from steam, with oxygen ions moving between electrodes, offering potential benefits at higher temperatures. Another commonly discussed technology is proton exchange membrane (PEM) electrolysis, which is known for its higher efficiency, though it is still in the early stages of commercialization (Yu et al., 2021a).

The other common category of green hydrogen production methods involves extracting hydrogen from biomass. For example, hydrogen can be extracted from methane using steam methane reforming (SMR). In this process, methane is heated up to 1,000℃ in the presence of a catalyst. Hydrogen can then be extracted with other by-products, such as

carbon monoxide and carbon dioxide. Another method, called partial oxidation reformation, utilizes natural gas reacting with oxygen. This method is typically less efficient than steam reformation but can also be used on larger scales. Other methods use similar processes involving high temperatures and catalysts to remove hydrogen from hydrocarbons in liquid form. Because liquids have a higher energy density, they can be advantageous, though the cost tends to be higher (U.S. Department of Energy, 2023).

In terms of cost and energy usage, electrolysis, particularly green hydrogen production, is energy intensive. The efficiency of electrolysis processes is often evaluated by their electrical energy consumption, with current systems consuming between 50–55 kWh per kilogram of hydrogen produced. The levelized cost of hydrogen (LCOH) from electrolysis varies depending on the source of electricity and the scale of the production facility, typically ranging from $2 to $6 per kilogram, with lower costs achievable when renewable energy sources are used (Parks et al., 2014). From an environmental perspective, electrolysis can result in near-zero carbon emissions if powered by renewable energy sources, offering a significant advantage over fossil-based hydrogen production pathways (Yu et al., 2021b). However, biomass-based hydrogen production, unless coupled with carbon capture, leads to significant CO_2 emissions, though it remains a key option in transitioning to a greener hydrogen economy (P. A. Le et al., 2023).

3.3.2 Hydrogen Delivery Pathways

Thera are three major pathways of hydrogen production, storage, transportation, and dispensing, which are gaseous hydrogen, liquid hydrogen and via ammonia as carrier as shown in **Figure 3.1**. Each pathway is organized into three primary stages: hydrogen production, terminal & transportation, and fueling station (end use). Currently, more than 9 million metric tons of gaseous hydrogen are produced annually in the United States, with much of this hydrogen stored and transported in high-pressure systems (USDrive, 2013). In the gaseous hydrogen pathway, hydrogen is compressed, stored, and transported via pipelines and tube trailers or combine both. In the numerical experiment, we will only consider tube trailers as the transportation mode to compare with others due to high capital investment of constructing new pipelines. At the compressed gas hydrogen refueling stations, high-pressure cascade systems will be used to deliver hydrogen to

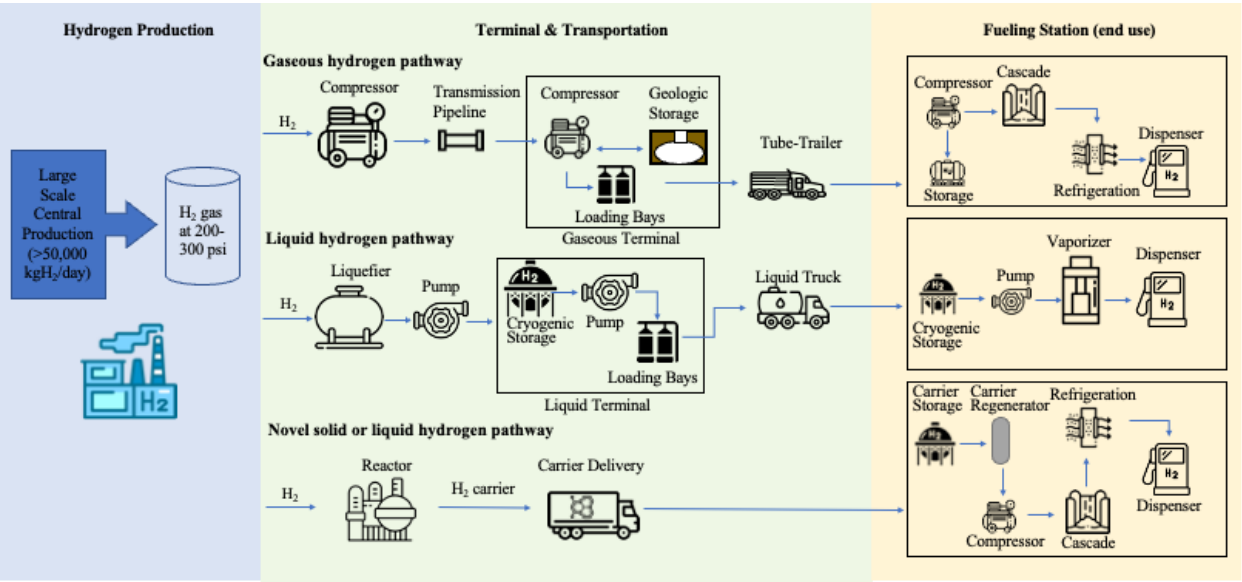


Figure 3-1 Hydrogen Delivery Pathways from Production to End Use

vehicles, with current compressors capable of delivering up to 35 kg/h at pressure ratios of 20-900 bar (Genovese & Fragiacomo, 2023). In the liquid hydrogen pathway, hydrogen gas undergoes liquefaction. The liquefied hydrogen is then stored in cryogenic storage facilities at the terminals and pumped into liquid trucks via loading bays for delivery to end-use locations. The liquefaction process involves cooling gaseous hydrogen to below -253°C (-423°F) using liquid nitrogen and a series of compression and expansion steps. At the liquid hydrogen fueling station, unused hydrogen will be stored at cryogenic storage sites. For fuel cell applications such as hydrogen vehicles, the pressure of hydrogen molecules needs to be increased using a pump and then vaporized at the desired pressure before dispensing into the onboard storage vessel. In addition to directly storing and delivering Figureydrogen in compressed or liquid form, there are some other alternative options including the production of chemicals, such as ammonia. Ammonia is easy to liquefy and becomes liquid when cooled to -33.34 °C (239.75 K) under normal pressure or pressurized to 7-8 bar under average temperature (Shi et al., 2022). Hydrogen can be combined with nitrogen to generate ammonia. Green ammonia is produced using renewable energy sources, such as wind, solar, or hydroelectric power, to generate the hydrogen required for the ammonia synthesis process. Then ammonia will be delivered via standard transportation trucks to the fueling stations, where further processing enables its usage. At the hydrogen fueling stations, ammonia will be cracked back into molecular hydrogen. Then the hydrogen produced from the ammonia cracking process exits at relatively low pressure, necessitating compression to meet the fueling standards required for vehicle applications and follow the same steps as the compressed gas hydrogen fueling stations.

The costs associated with the initial processing of hydrogen vary among the pathways. Gaseous hydrogen compression costs $1.45 per kg of hydrogen (Parks et al., 2020), while liquefaction for liquid hydrogen is slightly lower at $1.35 per kg of liquid hydrogen (Yilmaz & Kaska, 2018). According to IRENA, the current production cost for new green ammonia is in the range of $0.72 to $1.4 per kg (Blanco et al., 2022). Form the Hydrogen Delivery Scenario Analysis Model (HDSAM) V4.5 (U.S. Department of Energy, 2022), both gaseous and liquid hydrogen experience minor throughput losses of 0.5%, whereas

ammonia shows negligible or no losses during this pre-process stage. Gaseous hydrogen pre-processing emits 0.5 $kgCO_2e$ per kg of hydrogen, while liquid hydrogen has significantly higher emissions at 9 $kgCO_2e$ per kg of hydrogen due to the energy-intensive liquefaction process. Ammonia production exhibits lower GHG emissions, at 0.00264 $kgCO_2e$ per kg of hydrogen equivalent, making it a potentially lower-emission option for hydrogen transport (The Royal Society, 2023). Ammonia does not require additional storage costs at this stage. Gaseous hydrogen incurs a 0.5% loss, while liquid hydrogen sees a slightly lower loss rate of 0.25% during storage (Houchins & James, 2020). Ammonia, again, shows no noted loss. Daily capital investment requirements vary significantly across pathways. Both terminals have a 30-year plant lifetime and a 10% discount rate. Gaseous hydrogen terminals require $34,276 per day, while liquid hydrogen terminals need $14,167 per day, reflecting the higher infrastructure costs for gaseous hydrogen storage (U.S. Department of Energy, 2022). Ammonia storage (for synthesis plants) has a daily capital investment of $25,584.

Gaseous hydrogen incurs a higher terminal unit operating cost of $0.51 per kg compared to $0.11 per kg for liquid hydrogen, reflecting the operational demands of maintaining gaseous hydrogen in compressed storage (U.S. Department of Energy, 2022). Tube trailers for gaseous hydrogen operate at 250, 350 or 500 bars. Gaseous hydrogen delivery vehicles carry between 700 to 1,100 kg, liquid hydrogen trucks have a capacity of 4,372 kg, and ammonia trucks can transport up to 29,715 kg, indicating the much higher transport efficiency of ammonia as a hydrogen carrier (International PtX Hub, 2023; U.S. Department of Energy, 2022). All pathways experience a hydrogen leakage rate of approximately 5% during delivery, with ammonia showing a slightly higher leakage at 5.5%, impacting the overall delivery efficiency. The unit transportation cost per 62 miles for gaseous hydrogen is $0.23 per kg, with liquid hydrogen costing $0.22 per kg and ammonia ranging between $0.2 and $0.5 per kg, depending on distance and handling requirements (U.S. Department of Energy, 2022). GHG emissions (CO_2, CH_4, N_2O, and GHGs) during the delivery for gaseous hydrogen pathway amount to are 64.5, 48.7, and 32.8 g/MJ H_2 out for tube tailer under 250, 350, and 500 bar pressure, while for liquid hydrogen pathway is 13.7 g/MJ H_2 out (U.S. Department of Energy, 2022). Ammonia has

the lowest emissions at 0.84 g CO_2e per MJ, reflecting its lower energy requirements during transportation. All three pathways aim to meet a standardized service pressure of 700 bar for end-use applications. Gaseous hydrogen loses 0.5% during compression, liquid hydrogen 0.3%, and ammonia reformation back to hydrogen incurs a 0.5% loss. Gaseous and ammonia-based hydrogen each require 0.089 kWh per kg of hydrogen for refrigeration. Liquid hydrogen, however, requires a substantially higher energy input of 0.295 kWh per kg due to the added refrigeration demands for cryogenic hydrogen. Liquid hydrogen refueling stations have the highest capacity, handling up to 1,400 kg per day. Gaseous hydrogen and ammonia refueling stations have a daily maximum of 770 kg (International PtX Hub, 2023). Both hydrogen fueling stations have 30-year plant lifetime and a 10% discount rate. Liquid hydrogen stations have a higher daily capital investment ($552 per day) compared to gaseous hydrogen ($407 per day). Operating and maintenance costs are highest for gaseous hydrogen at $2.51 per kg, while liquid hydrogen costs $2.15 per kg (U.S. Department of Energy, 2022). Ammonia refueling incurs an additional cracking cost ranging from $0.61 to $2.2 per kg of hydrogen. Ammonia experiences a notable 25-30% energy loss during the conversion and re-conversion processes, which impacts the total efficiency of using ammonia as a hydrogen carrier.

This detailed analysis reveals the complexities of hydrogen storage and transportation. Gaseous hydrogen requires higher infrastructure costs and operational expenditures but avoids the high GHG emissions associated with liquid hydrogen liquefaction. Liquid hydrogen offers larger transport capacities and lower storage costs, though it has high refrigeration energy needs. Ammonia, while introducing conversion inefficiencies, provides substantial transport capacity and has lower GHG emissions, making it a promising alternative for large-scale hydrogen transport. This table underscores the trade-offs in choosing the most suitable hydrogen carrier pathway based on costs, energy demands, and emissions at each stage of the supply chain. **Table 3-2** lists all these data of these three hydrogen delivery pathways.

Table 3-2 Comparison of Hydrogen Delivery Pathways

	Gaseous Hydrogen			Liquid Hydrogen	Ammonia
Pre-process					
Hydrogen compression, liquification or ammonia production cost, $/kg	1.45/kg GH_2			1.35/kg LH_2	0.72-1.4/kg NH_3
Throughput losses, %	0.5			0.5	-
Terminal					
Hydrogen losses at terminal, %	0.5			0.25	-
Terminal daily capital investment, $/day	34,276			14,167	-
Ammonia plant daily capital investment, $/day	-			-	25,584
Terminal unit operating, $/kg	0.51			0.11	-
Delivery					
Tube trailer or truck pressure, bar	250	350	500	1	1
Tube trailer or truck capacity, kg	700	900	1,100	4,372	29,715
Hydrogen leakage rate during delivery, %	5	5	5	5.5	0
Tube trailer or truck unit transportation cost, $/kg/62 miles	0.23	0.22	0.30	0.16	0.2-0.5
GHG emissions during delivery, g/ MJ H_2 out	64.5	48.7	32.8	13.8	79.8
Fueling Station					
Vehicle service pressure, bar	700			700	700
Hydrogen lost during compression, %	0.5			0.3	0.5
Refrigeration energy use, kWh/kg of H_2 out	0.089			0.295	0.089
Gaseous or liquid hydrogen refueling station maximum daily refueling capacity, kg/day	770			1,400	770
Gaseous or liquid hydrogen refueling station daily capital investment, $/day	407			552	407
Gaseous or liquid hydrogen refueling station unit operating and maintenance cost, $/kg of H_2	2.51			2.15	2.51
NH_3 cracking cost, $/kg$H_2$	-			-	0.61-2.2
Energy losses during conversion and reconversion, %	-			-	25-30
GHG emissions during refueling, g/ MJ H_2 out	0.000013			3.28	0.000013

3.3.3 Hydrogen Fueling Station Demand

We assume FCETs have similar annual freight shipping distance and operating range with diesel trucks. This study adopts freight shipment demand data from the Freight Analysis Framework (FAF) model, which provides detailed U.S. O-D freight data by zone (Department of Transportation. Bureau of Transportation Statistics., 2017). Truck shipments for 2025 are used as the baseline demand. Fuel Cell Electric Trucks (FCETs) market penetration rate σ of 10% is considered as the baseline in this study. Shipment demand for each origin-destination pair is adjusted based on this penetration level. The shortest paths between origin and destination zones along major interstate highways were identified using Dijkstra's algorithm. This study identifies locations of existing alternative fueling stations for heavy-duty vehicles as potential sites for new hydrogen refueling infrastructure (Alternative Fuels Data Center, 2024). Specifically, 1,927 candidate locations l are selected, that are systematically deployed along all interstate highway segments with a maximum spacing of 30 miles, which is normally lower bound of vehicle ranges when the empty fuel light is on. A candidate location is selected only if it is positioned along paths of at least one O-D pair. For each O-D pair (o, d), let R_{od} be the set of all stations along the shortest path between o and d. This spacing criterion was selected to minimize drivers' inconvenience in locating stations. For each origin-destination pair, hydrogen fuel demand is allocated equally to refueling locations along the shortest path.

The annual total hydrogen fuel demand H_l at each candidate location $l \in L$ could be determined by summing all allocated fuel demand from all O-D pairs as equation (3-1) based on Liu's research (Liu et al., 2020).

$$H_l = \sum_{o \in O} \sum_{d \in D} \Delta_{od}^{l} \times \frac{F_{od}}{|R_{od}|} \qquad \forall s \in S \qquad (3\text{-}1)$$

where

$$\Delta_{od}^{l} = \begin{cases} 1 \; l \in R_{od} \\ 0 \; l \notin R_{od} \end{cases} \text{ and} \qquad (3\text{-}2)$$

$$F_{od} = \frac{\sigma f_{od} d_{od}}{\rho \beta (1 - \theta)} \qquad (3\text{-}3)$$

Δ_{od}^{l} in equation (3-2) is a binary indicator of whether location l is located on the shortest path for each O-D pair (o, d). Equation (3-3) estimates the annual total hydrogen fuel demand F_{od} based on the annual shipment f_{od} using hydrogen fuel and the shipment distance d_{od} (miles) for each O-D pair (o, d). In addition to the flow demand and distance, F_{od} is also a function of average FCET fuel economy ρ (mile/kg), average truckload capacity β (tons/truckload), and average empty rate of truck θ (%) per truck. We also assume that all stations along path O-D will have the same probability or demand of serving F_{od}. In this study, the fuel economy of FCET ρ is estimated at 8.72 miles/kg. This is estimated that diesel truck fuel economy is 5.59 miles/gallon (Moghadasi et al., 2024) and FCET fuel economy measured by miles/kg is 1.56 times diesel truck fuel economy measured by miles/gallon (Kast et al., 2018). The average truckload capacity β is assumed at 46,040 pounds (Reinhart, 2015). The average empty rate of truck θ is estimated at 20%, an average value based on a recent truck survey conducted by the American Transportation Research Institute (ATRI) (Leslie, 2023). Note that the empty rate considers both non-revenue/dead-head miles (trips to pick 5 up a load) of truck operations.

The spatial distribution of hydrogen refueling demand for long-haul trucks across potential refueling locations in the United States under a 10% market penetration rate for fuel cell electric trucks (FCETs) is shown in **Figure 3.2**. The demand is measured in kilograms per day (kg/day) and is represented by various sizes of circles. The circles indicate daily hydrogen demand at specific locations, with demand values segmented into ranges, such as 23–3000 kg/day, 3000–5000 kg/day, 5000–7000 kg/day, 7000–9000 kg/day, and 9000–11000 kg/day. The distribution shows that higher hydrogen demand clusters predominantly along major interstate highways and key logistic corridors. Regions in the central and eastern United States display particularly high demand concentrations, with several locations exceeding 7000 kg/day. Notably, demand is comparatively lower in the western states, though some high-demand nodes exist along primary transit routes. In addition, the refueling capacity of gas and liquid hydrogen fueling stations are 770kg/day and 1,400kg/day, which are less than most of the hydrogen refueling demand for long-haul trucks under 10% FCETs market penetration rate.

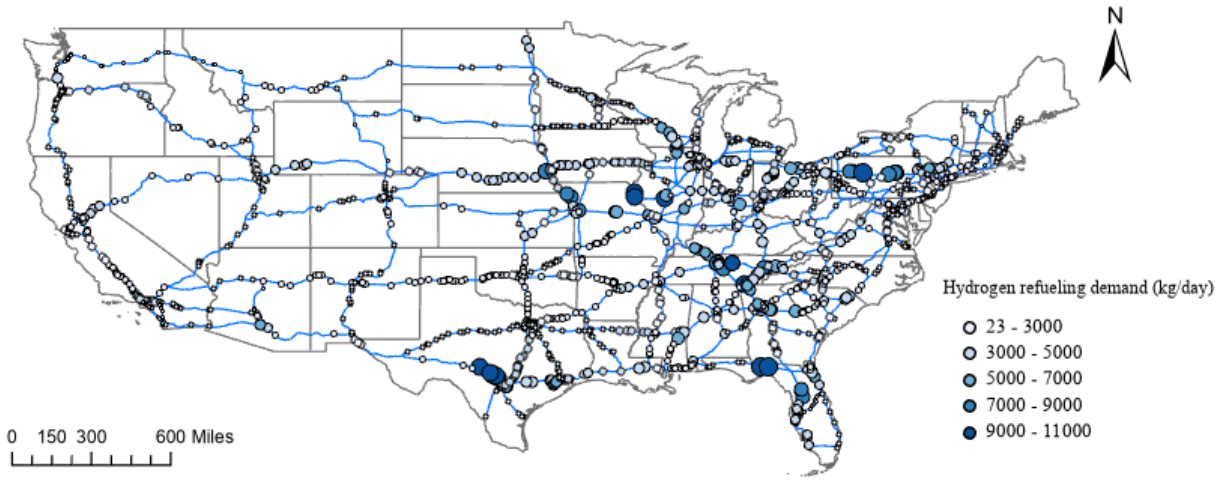


Figure 3-2 Hydrogen Refueling Daily Demand for Long-haul Trucks at Potential Locations under 10% FCETs Market Penetration Rate

Therefore, for exceeding demand, we can build more hydrogen fueling stations at the same locations. In section 3, we will take the refueling capacity into consideration.

3.4 Hydrogen Logistics Network Design

3.4.1 Variable and Parameter Definition

For the strategical long-term decision of hydrogen delivery network design, this paper considers a fix-cost hydrogen logistics network, including a set of J storage terminals (j as its index), a set of L potential locations (l as its index) to build hydrogen stations in the United States as shown in **Figure 3-3**. S_l is the set of fueling stations associated with each location $l \in L$. S ($S = \bigcup_{\forall l \in L} S_l$) is the union of all unique stations (s as its index) across the locations in L. The storage terminals are utilized for the preprocessing and loading of produced hydrogen, and they are constructed near the hydrogen production plants. The hydrogen available at the terminal j is K_j (kg) a day. The processed hydrogen then will be transported via different transportation modes. P (p as its index) is the set of all considered hydrogen delivery pathways, including those delivered by compressed gas tube trailers (GH_2), liquid tank trucks (LH_2), and ammonia carrier trucks (AMO). The capacity of refueling station p is k_p^f (kg) a day. The dialyzed capital cost of the storage terminal j using the pathway p is f_{jp}^t. The delivered hydrogen will be processed for the fuel cell electric long-haul trucks refueling at the fueling stations. The dialyzed capital cost of the fueling station s using hydrogen delivery pathway p is f_{sp}^f. The daily hydrogen demand is D_l (kg) at the potential location l. The unit delivery cost of shipment from storage terminal j using the hydrogen delivery pathway p to fueling station s is c_{jsp} per ton. This cost includes pre-processing, transportation, storing, and cracking hydrogen from terminals to fueling stations, as well as the unit operating costs of terminals and fueling stations. Decision variable x_{jsp} is the daily tonnage flow of hydrogen delivered from terminal j to fueling station s using hydrogen delivery pathway p. Binary variable z_{jp}^t indicating whether the potential storage terminal j is selected to have capability of handling delivery pathway p. Binary variable z_{sp}^f indicating whether fueling station s is served by hydrogen delivery pathway p. The objective function is to minimize the overall cost, including the daily capital costs for fueling terminals and stations and all other

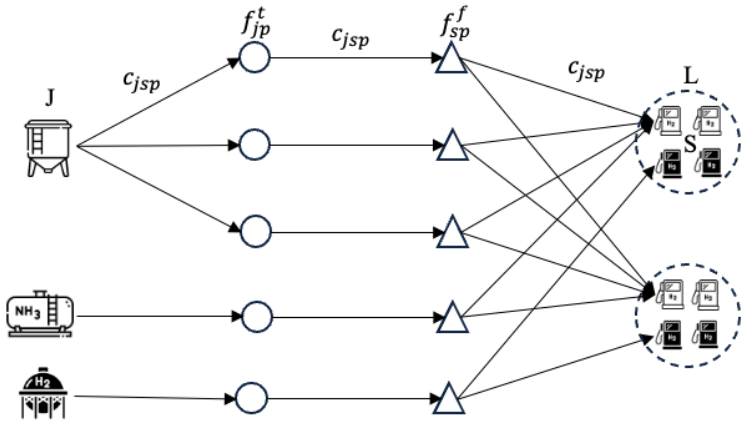


Figure 3-3 Hydrogen Logistics Flow Chart

variable costs. The objective of the mixed integer linear programming model can be formulated as Equation (3-4):

$$Min \quad \sum_{j\in J}\sum_{s\in S}\sum_{p\in P} c_{jsp}x_{jsp} + \sum_{j\in J}\sum_{p\in P} f_{jp}^{t} z_{jp}^{t} + \sum_{s\in S}\sum_{p\in P} f_{sp}^{f} z_{sp}^{f} \qquad (3\text{-}4)$$

$$s.t. \quad \sum_{s\in S_l}\sum_{j\in J}\sum_{p\in P} x_{jsp} \geq D_l \qquad \forall l \in L \quad (3\text{-}5)$$

$$\sum_{s\in S}\sum_{p\in P} x_{jsp} \leq K_j \qquad \forall j \in J \quad (3\text{-}6)$$

$$\sum_{j\in J} x_{jsp} \leq k_p^f z_{sp}^f \qquad \forall s \in S, \forall p \in P \quad (3\text{-}7)$$

$$\sum_{s\in S} x_{jsp} \leq K_j z_{jp}^t \qquad \forall j \in J, \forall p \in P \quad (3\text{-}8)$$

$$\sum_{p\in P} z_{jp}^t \geq 1 \qquad \forall j \in J \quad (3\text{-}9)$$

$$\sum_{p\in P} z_{sp}^f \leq 1 \qquad \forall s \in S \quad (3\text{-}10)$$

$$x_{jsp} \geq 0, z_{jp}^t, z_{sp}^f \in \{0,1\}$$

Constraint (5) enforces every fueling station's demand is satisfied. Constraint set (6) ensures the delivered hydrogen does not exceed the available amount at the terminal. Constraint set (7) ensures the daily flow of hydrogen to the hydrogen fueling stations doesn't exceed the refueling capacity, and the delivery can only occur when the fueling station is selected. Constraint set (8) ensures delivery can only occur when the terminal is selected. Constraint set (7) and (8) make sure that only delivery can only occur when both the same delivery pathway is selected. Constraint set (9) enforces each fueling station is served by only one delivery pathway at most. The traditional fixed-cost network flow problem is NP-hard and only considers one binary variable, which is a special case of our model (D. S. Hochbaum & A. Segev, 1989).

The original model becomes intractable and cannot be solved when applied to large-scale networks due to the increased computational complexity and resource requirements. Therefore, we relax z_{sp}^f to integer decision variable z_{lp}^f to fast the computational running

time, and $z_{lp}^{f} \in Z^{+}$, which represents how many hydrogen stations are served by hydrogen delivery pathway p at location l. At each potential location, the fueling stations are modeled as duplicate points sharing the same coordinates. Equations (5) – (9) are still maintain the same for the larger scale cases. This approach effectively mitigates the symmetrical inherent in the original model, ensuring that the solutions remain unaffected while maintaining the computational integrity of the optimization process.

3.5 Numerical Experiment

3.5.1 Resulting Network

The results presented in **than other** categories, suggesting that the logistics network has been optimized to

Table 3-3 provide a comprehensive breakdown of the daily costs associated with an optimized national hydrogen logistics network design under 10%, 50%, and 100% market penetration rate scenarios for fuel cell electric trucks (FCETs), enabling delivery of 4,426,796 kg of hydrogen per day. The levelized cost of hydrogen is 4.6$/kg. The preprocess cost, amounting to $5,989,542 per day, constitutes a significant proportion of the total daily expenses. This cost typically includes activities such as hydrogen purification, compression, or liquefaction, which are essential to prepare hydrogen for storage, transport, and subsequent utilization. The high preprocess cost emphasizes the technical complexity and energy intensity of preparing hydrogen for distribution, particularly at the national scale required for substantial FCET adoption. The terminal operating cost and capital cost are $488,037 and $2,011,714 per day, respectively. These costs represent the ongoing expenses to operate and maintain terminals (operating costs) and the daily amortization of the investment needed to establish the terminal infrastructure (capital costs). The operating cost is relatively modest in comparison to other categories. However, the terminal capital cost, which accounts for approximately 10% of the total daily costs, underscores the significant initial infrastructure investment required to support a distributed network of terminals for hydrogen refueling. The transportation cost is $901,712 per day across the national logistics network. This cost includes the expenses associated with the physical movement of hydrogen from production sites to fueling stations. While substantial, it is relatively lower than other categories, suggesting that the logistics network has been optimized to

Table 3-3 Daily Costs of the Optimal National Hydrogen Logistics Network Design under different FCETs Market Penetration Rates

Costs, $/day	FCETs market penetration rate		
	10%	50%	100%
Preprocess cost	5,989,542	29,947,711	59,895,423
Terminal operating cost	488,037	2,440,183	4,880,368
Terminal capital cost	2,011,714	2,011,714	2,011,714
Transportation cost	901,712	3,635,347	8,867,547
Cracking cost	0	0	0
Fueling station operating cost	8,537,316	42,686,580	85,373,162
Fueling station capital cost	2,299,632	9,276,360	18,006,240
Total cost, $	20,227,953	89,997,895	179,034,453
Total delivered hydrogen, kg/day	4,426,796	22,183,490	44,366,980
Levelized cost of hydrogen, $/kg	4.6	4.0	4.0

minimize transport distances and improve distribution efficiency, thus reducing lower transport expenses. Notably, the cracking cost is reported as zero, suggesting that within the optimized network design, cracking technology is unnecessary due to the exclusion of ammonia as a carrier pathway. This decision reflects the high energy losses associated with ammonia cracking, which significantly reduces the pathway's efficiency. To enhance the competitiveness of ammonia as a viable hydrogen carrier, substantial improvements in cracking efficiency would be essential, thereby reducing energy losses and potentially making this pathway more attractive for future network configurations. Fueling station operating costs and capital costs are $8,537,316 and $2,299,632 per day, respectively, representing the largest expenses in the hydrogen logistics network. The substantial operating costs are indicative of the intensive resource requirements for maintaining and operating fueling stations, likely due to high throughput requirements associated with FCETs. The capital cost reflects the large-scale investment required to establish a national network of fueling stations, which are critical to providing widespread refueling access and supporting FCET market penetration. In summary, with high preprocess and fueling station-related costs, this cost breakdown informs stakeholders of critical areas to target for cost reductions, potentially through advancements in hydrogen production efficiency, streamlined station operations, and strategic infrastructure investments. These insights are essential for developing scalable hydrogen logistics networks capable of supporting broader decarbonization goals in the transportation sector.

The hydrogen infrastructure spatial distribution and logistics network logistics network generated by the optimized model, including the strategic placement of hydrogen terminals and refueling stations across the network under 10% FCETs market penetration is illustrated in **Figure 3-**. The model identifies optimal locations for hydrogen terminals, strategically positioned to minimize transportation costs and meet the refueling demands of fuel cell electric long-haul trucks. The liquid gaseous hydrogen pathway is selected for the entire network. Represented by circles of varying bule color, each circle indicates a station's daily demand in kilograms, categorized into five ranges: 0–260 kg, 260–530 kg, 530–810 kg, 810–1,100 kg, and 1,100–1,400 kg. Higher demand stations, indicated by darker bule circles, are concentrated in regions with dense transportation

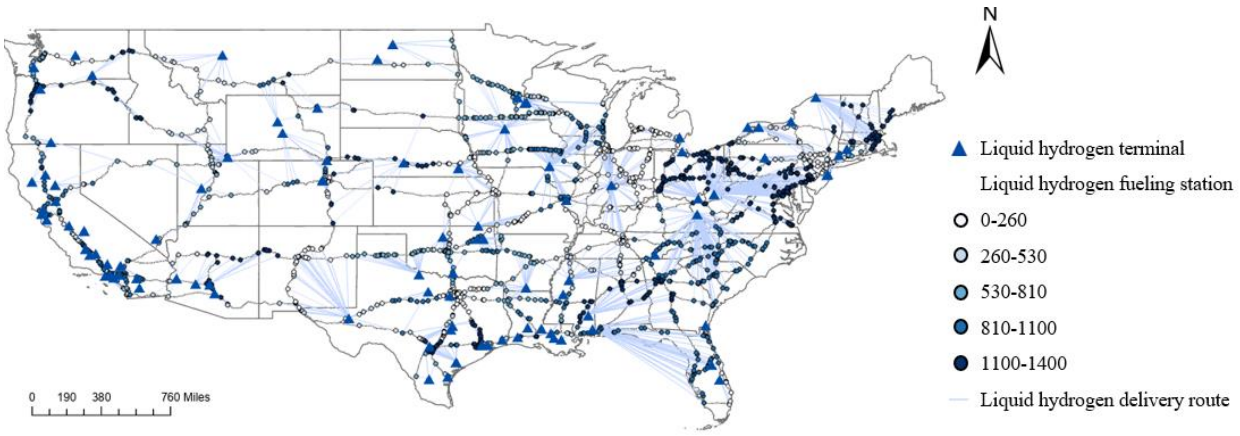


Figure 3-4 Hydrogen Logistics Network under 10% FCETs Market Penetration

networks and significant freight traffic, particularly along the eastern and central United States. A total
of 4,175 liquid hydrogen refueling stations are required to satisfy the hydrogen demand at a 10% market penetration level for the FCETs. These stations are strategically served by proximate liquid hydrogen terminals, ensuring an efficient and continuous supply to meet the logistical needs of long-haul transportation networks.

To explore conditions under which the gas hydrogen pathway becomes viable, we adjusted the primary cost driver, the unit operating cost of gas fueling stations, to 50% of its current level. This adjustment yields the optimized hydrogen logistics network across the United States under a 10% market penetration scenario for fuel cell electric trucks (FCETs), as shown in Error! Reference source not found.. The red scheme is the gas hydrogen pathway and the bule scheme is liquid hydrogen pathway. There are 8 terminals that only implement gas hydrogen, 116 terminals that only implement liquid hydrogen, and 18 terminals that implement both gas and liquid hydrogen. In cases where the hydrogen demand at a potential location is less than 770 kg per day, a single gaseous hydrogen fueling station is sufficient to meet the demand at minimal cost. When the demand falls between 770 kg and 1400 kg per day, a single liquid hydrogen fueling station becomes more appropriate. For demands ranging from 1400 kg to 2800 kg per day, a combination of one liquid hydrogen and one gaseous hydrogen fueling station is required to adequately fulfill the need. For locations where hydrogen demand exceeds 2800 kg per day, liquid hydrogen fueling stations are prioritized, with an additional gaseous hydrogen fueling station used to cover any remaining unmet demand. The network layout highlights the strategic placement of hydrogen terminals, fueling stations, and delivery routes for both gas and liquid hydrogen, reflecting adjustments in infrastructure to optimize for cost-effectiveness and accessibility across varying regions.

3.5.2 Sensitivity Analysis

The results in

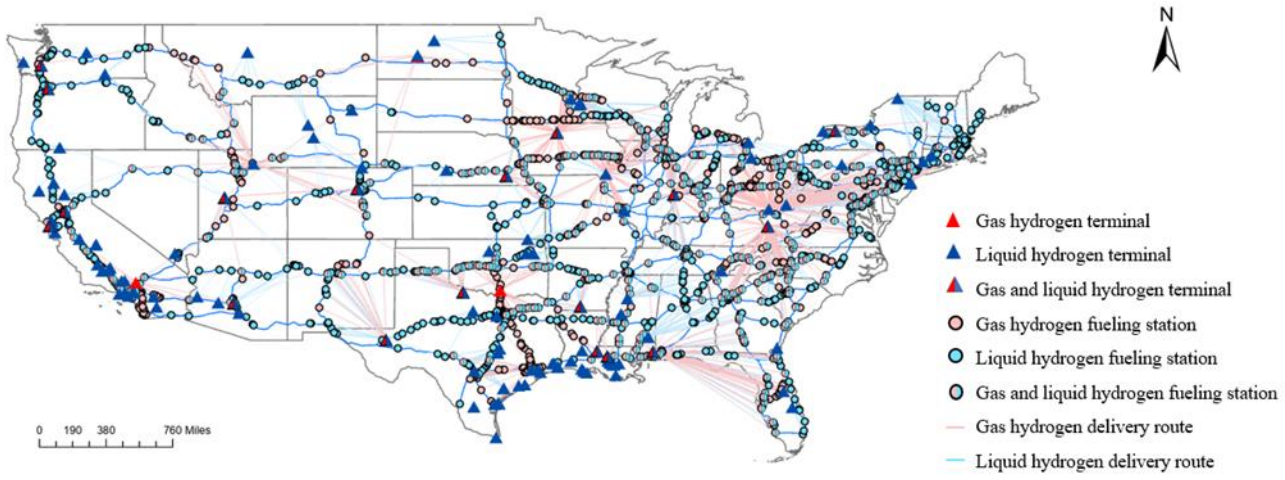


Figure 3-5 Hydrogen Logistics Network When Adjust the Unit Operating Cost of Gas Fueling Station to 50% of Current Level under 10% FCETs Market Penetration

Table 3-4 outline the optimal hydrogen infrastructure required, total costs, and total hydrogen delivered across different scenarios: the base, gas hydrogen (GH_2) pathway, and ammonia (AM) pathway scenarios. The base scenarios reflect the current cost structure of each hydrogen delivery pathway. The GH_2 scenarios assume a reduction

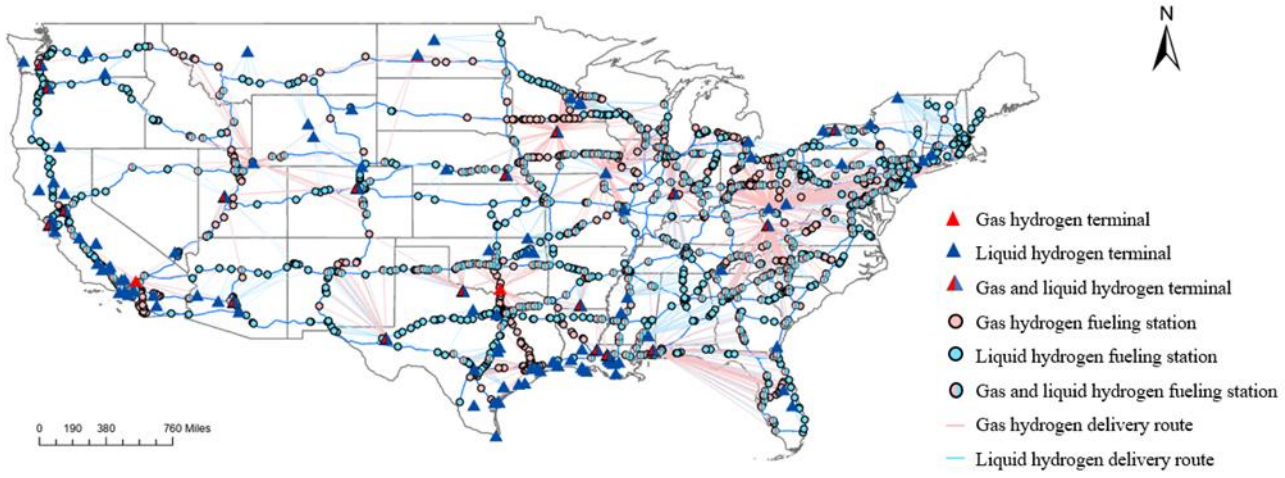


Figure 3-5 Hydrogen Logistics Network When Adjust the Unit Operating Cost of Gas Fueling Station to 50% of Current Level under 10% FCETs Market Penetration

Table 3-4 The Optimal Hydrogen Infrastructure Needed, Total Costs and Total Delivered H_2 and total GHG emissions under Base, Gas Hydrogen Pathway, and Ammonia Pathway Scenarios

	FCETs market penetration rate	# of GH_2 terminal	# of LH_2 terminal	# of AM terminal	# of GH_2 fueling station	# of LH_2 fueling station	# of AM fueling station	Total costs, M$	Total delivered H_2, kg	Total GHG emissions, kg
Base	1%	0	142	0	0	1928	0	4.6	443,670	1,073,681
	10%	0	142	0	0	4173	0	20.2	4,426,796	10,712,846
	100%	0	142	0	0	32,620	0	179.0	44,366,980	107,368,092
GH_2	1%	5	137	0	1769	162	0	4.5	441,631	2,881,268
	10%	26	134	0	2556	2305	0	20.7	4,426,796	21,140,888
	100%	66	119	0	47,180	6,233	0	177.0	44,167,582	281,665,898
AM	1%	0	113	30	0	61	1886	4.6	441,364	4,864,620
	10%	96	121	102	765	2,746	1406	33.6	5,079,151	28,728,781
	100%	0	93	78	0	3,024	52,924	170.3	44,143,377	477,632,854

in the unit operating cost of gas hydrogen fueling stations to 50% of the present cost structure. In the AM scenarios, both the unit operating cost of gas hydrogen fueling stations and the unit cracking cost are reduced to 50% of the current levels, with an additional increase in energy loss during the cracking process to 10%. Each scenario considers three levels of fuel cell electric truck (FCET) market penetration, at 1% 10%, and 100%. As the penetration level reaches 100%, the existing hydrogen capacity at the terminals becomes insufficient to meet the demand. To address this, the terminal capacity is scaled up by a factor of 10 to ensure the feasibility of the model. Additionally, infrastructure elements, such as the number of terminals and fueling stations by type (gaseous hydrogen, liquid hydrogen, and ammonia) and total costs and hydrogen delivery volumes are assessed.

In the Base scenario, where gaseous hydrogen (GH_2) and ammonia (AM) options are not considered, the number of liquid hydrogen (LH_2) terminals remain constant at 142 across all penetration levels (1%, 10%, and 100%). The required number of LH_2 fueling stations increases significantly with market penetration. At 100% penetration, 32,620 fueling stations are needed, with a total cost of $179 million, delivering approximately 44,366,980 kg of hydrogen. This highlights the scalability of the infrastructure as penetration levels rise. In the GH_2 scenario, GH_2 terminals and fueling stations are introduced, reducing reliance on LH_2 infrastructure. At 10% penetration, 26 GH_2 terminals and 2,556 GH_2 fueling stations are required, complemented by 134 LH_2 terminals and 2,305 LH_2 fueling stations. The total cost amounts to approximately $20.68 million, delivering 4,426,796 kg of hydrogen. At 100% penetration, the GH_2 infrastructure expands considerably, with 66 GH_2 terminals and 47,180 fueling stations. LH_2 terminals and fueling stations are correspondingly reduced to 119 and 6,233, respectively. The total cost increases to $177 million, with a slightly lower total hydrogen delivery of 44,167,582 kg compared to the Base scenario. The AM scenario integrates ammonia (AM) terminals and fueling stations, further diversifying the hydrogen delivery infrastructure. At 1% penetration, 113 LH_2 terminals, 30 AM terminals, and 61 LH_2 fueling stations are required alongside 1,886 AM fueling stations. The total cost is $4.6 million, delivering 441,364 kg of hydrogen. At 10% penetration, AM infrastructure

expands substantially, requiring 96 GH_2 terminals, 121 LH_2 terminals, and 102 AM terminals. The fueling infrastructure includes 765 GH_2 fueling stations, 2,746 LH_2 fueling stations, and 1,406 AM fueling stations. The total cost rises to $33.63 million, with a hydrogen delivery of 5,079,151 kg. At 100% penetration, the AM infrastructure dominates, with 93 LH_2 terminals, 78 AM terminals, and 52,924 AM fueling stations, completely replacing GH_2 fueling stations. The total cost is $170 million, with a hydrogen delivery of 44,143,377 kg.

The total greenhouse gas (GHG) emissions associated with the optimal hydrogen infrastructure required under different pathways and FCETs market penetration rates are also listed in

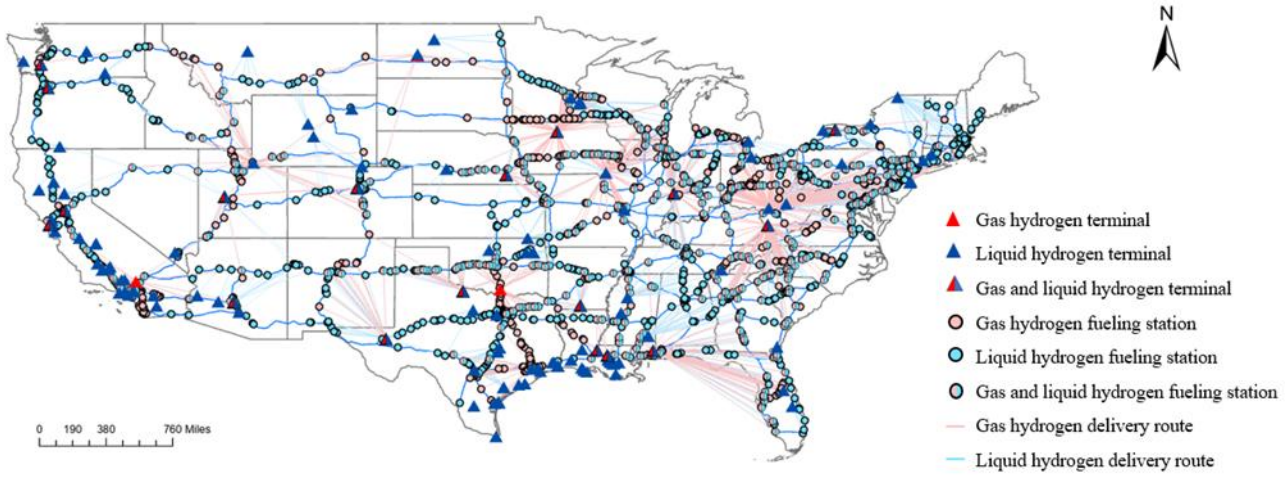


Figure 3-5 Hydrogen Logistics Network When Adjust the Unit Operating Cost of Gas Fueling Station to 50% of Current Level under 10% FCETs Market Penetration

Table 3-4. The results highlight the significant variation in GHG emissions based on the pathway selection and the scale of hydrogen delivery. In the baseline scenario (1% FCET market penetration), total GHG emissions are approximately 1,073,681 kg, with no reliance on gaseous hydrogen or ammonia pathways. While LH_2 transport has the lowest GHG emissions rate per unit energy, the emissions increase with the volume of hydrogen delivered, resulting in considerable GHG emissions at higher market penetration rates. At 100% market penetration, the GHG emissions reach 107,368,092 kg due to the significant increase in delivered hydrogen. Incorporating gaseous hydrogen infrastructure results in higher total GHG emissions in GH_2 scenario. This is attributed to the smaller number of GH_2 terminals and fueling stations required compared to the exclusive use of LH_2 pathways. The ammonia pathway shows the highest GHG emissions among the pathways, particularly at higher penetration rates. At 1% penetration, total GHG emissions are 4,864,620 kg, which is slightly higher than the baseline scenario. However, at 100% penetration, GHG emissions reach 477,632,854 kg, far exceeding those of the LH_2 and GH_2 pathways. This increase is due to the additional emissions generated during ammonia shipping, which is more energy-intensive compared to LH_2 and GH_2 pathways. Ammonia-based hydrogen delivery becomes less favorable in terms of emissions at large scales due to the energy requirements for its decomposition and the inefficiency of utilizing ammonia as a hydrogen carrier. However, its advantages in terms of storage and

ease of transportation may still make it a practical option in regions with limited infrastructure for LH_2 or GH_2.

In summary, the results indicate that the infrastructure requirements, costs, and hydrogen delivery volumes vary notably depending on the selected pathway and market penetration rate. Under the assumption of the technology improved gas hydrogen and ammonia carrier pathway at the fueling station. The base scenario demonstrates a stable but costly expansion as market penetration grows, while the GH_2 pathway offers a comparable cost structure with lower reliance on LH_2 infrastructure. Conversely, the AM pathway introduces higher infrastructure diversity and significant cost increases, correlating with a marked rise in hydrogen delivery capacity at higher market penetration levels. The GHG emissions associated with hydrogen delivery pathways vary significantly based on the infrastructure type and scale. The liquid hydrogen pathway is the most efficient in terms of emissions at all market penetration rates, followed by the gaseous hydrogen pathway. The ammonia pathway, despite its advantages in storage and transport, exhibits the highest emissions, particularly at high market penetration rates, due to the energy-intensive ammonia shipping. These findings emphasize the importance of considering both infrastructure scalability and environmental impacts when selecting hydrogen delivery pathways to support the transition to a hydrogen-based economy.

3.6 Discussion

This study presents the optimal hydrogen transportation modes as well as the strategic placement and technology implement of hydrogen terminals and refueling stations with minimize variable operating costs and fixed capital investment. The findings of this study align with and expand upon existing research in the field of hydrogen logistics networks, providing new insights into cost optimization, infrastructure scalability, and environmental impacts across different hydrogen delivery pathways. Previous studies identified liquid hydrogen as a scalable and efficient delivery pathway for long-haul hydrogen logistics due to its high energy density and transport efficiency (Villalba-Herreros et al., 2023b). This study corroborates those findings, showing that LH_2 remains the most cost-effective and environmentally sustainable pathway under baseline conditions, with the levelized cost of hydrogen at $4.6/kg and GHG emissions at 13.7

g/MJ during delivery. Compared to the gaseous hydrogen pathway, which exhibits higher emissions (up to 64.5 g/MJ), LH_2 offers significant advantages in reducing environmental impacts at scale. Ammonia has been proposed in prior studies as a promising hydrogen carrier due to its high storage density and lower emissions during transport (IRENA and AEA, 2022). However, this study reveals that the energy losses and GHG emissions associated with ammonia cracking and transportation significantly reduce their overall efficiency. These findings align with earlier research but provide a more detailed quantification of the trade-offs involved, emphasizing the need for technological advancements to improve ammonia cracking efficiency. Amos (2023) previously estimated hydrogen logistics GHG emissions for different pathways, emphasizing the critical role of reducing emissions during preprocessing and delivery stages (Amos, 2023). This study extends those analyses by evaluating end-to-end emissions, showing that LH_2 offers the most environmentally friendly solution at high market penetration rates, with total GHG emissions of 107,368,092 kg for a 100% FCET adoption scenario. The GH_2 pathway, while cost-competitive at smaller scales, results in significantly higher emissions (281,665,898 kg) due to increased reliance on high-pressure compression and the extensive infrastructure required.

Compared to earlier studies that focused on regional hydrogen logistics, this study employs a national-scale optimization model, offering a broader perspective on infrastructure requirements. The model identifies the need for 32,620 liquid hydrogen (LH_2) refueling stations under a 100% market penetration scenario, consistent with previous research emphasizing the scalability of LH_2 infrastructure. However, it also highlights critical limitations in refueling capacity. At 100% market penetration, a significant expansion in the number of hydrogen refueling stations is necessary to meet the substantial increase in hydrogen demand. A single hydrogen fueling station can serve a maximum of approximately 30 trucks per day, significantly lower than a diesel fueling station, which can accommodate around 386 trucks per day (*Alternative Fuels Data Center*, 2024; *U.S. Department of Energy*, 2022). This disparity stems from differences in daily fuel consumption, heavy-duty truck tank capacities, and the number of diesel fueling stations available across the United States. Moreover, under high market

penetration scenarios, the current hydrogen terminal capacity would prove inadequate, necessitating significant infrastructure upgrades to accommodate elevated demand. These findings underscore the importance of substantial investments in hydrogen refueling and terminal infrastructure to support widespread adoption of fuel cell electric trucks (FCETs) and ensure sufficient hydrogen availability and accessibility.

In summary, while consistent with prior studies in recognizing the scalability and environmental advantages of liquid hydrogen, this study advances the field by quantifying the trade-offs among cost, emissions, and infrastructure requirements across different pathways at varying market penetration levels. It also incorporates ammonia as a potential pathway, offering a detailed analysis of its operational inefficiencies and emissions impacts. Furthermore, the study highlights the limitations of the current hydrogen refueling infrastructure and underscores the need for substantial upgrades to meet future demand effectively.

3.7 Conclusion

This study presents a comprehensive evaluation of hydrogen logistics network design to support the adoption of fuel cell electric trucks (FCETs) under 10%, 10%, and 100% market penetration rate in the United States. By integrating techno-economic modeling and optimization techniques, the research identifies optimal strategies for hydrogen production, storage, transportation, and refueling infrastructure to minimize costs while meeting projected demand. The findings emphasize the strategic advantages of liquid hydrogen as the primary delivery pathway under current cost structure and technological capabilities, highlighting its scalability, cost-effectiveness, and environmental sustainability. The flexibility of the proposed network to adapt to varying market and technological conditions is further demonstrated, such as reductions in operating costs for gaseous hydrogen fueling stations or advancements in ammonia-based hydrogen delivery, including lower cracking costs and reduced energy losses. Under these assumptions, the results indicate that the GH_2 pathway is preferable for meeting small hydrogen demand, while the AM pathway is better suited for addressing large hydrogen demand. Despite the promising potential of hydrogen logistics networks, this study identifies critical challenges, including high fueling station operating costs, energy-intensive cracking

processes, and limited refueling capacities, which must be addressed to achieve widespread adoption. Furthermore, the results underscore the need for significant investments in infrastructure, particularly at higher FCET market penetration levels, to ensure sufficient hydrogen availability and accessibility.

The current model incorporates several simplifying assumptions that may limit its applicability in dynamic real-world contexts. For example, demand levels and cost structures are assumed to remain static, overlooking potential regional variations and market dynamics. Furthermore, data limitations restricted the inclusion of behavioral and policy-driven factors, which could have significant implications for network performance. The scalability of the proposed infrastructure under higher market penetration rates also requires further investigation. Future research should prioritize the integration of real-time data and advanced demand forecasting techniques to enhance model robustness and accuracy. Investigating the potential of emerging hydrogen production and storage technologies, such as solid-state storage systems and high-efficiency electrolysis, could significantly improve network efficiency.

CHAPTER FOUR

VALUE OF CIRCULAR BIOMASS-BIOENERGY AND BIOFUEL WITH CARBON CAPTURE AND STORAGE

4.1 Abstract

The circular bioenergy and biofuel production with carbon capture and storage (BECCS) system presents a promising pathway for renewable energy generation and carbon mitigation. This study investigates the techno-economic feasibility of BECCS incorporating biochar recycling of corn stover, switchgrass, and miscanthus in the southeastern United States. We developed a two-stage mix-integer programming model with incorporates spatial and seasonal biomass supply data to optimize the BECCS supply chain network with minimal total cost. Our results indicate that biofuel production remains economically viable across varying levels of market maturity. Under high market maturity conditions, biofuel output reaches 3.01 million tons annually, accompanied by substantial biochar, steam and diesel from converting captured CO_2. The model also highlights the geographic distribution of biorefineries, optimizing facility placement based on biomass availability and transportation cost-efficiency. Switchgrass will be the major feedstock for production. Sensitivity analyses reveal that fixed operating costs and biofuel prices significantly impact profitability, emphasizing the importance of cost management and market conditions for sustained success. The minimal selling price of biofuel is $2.62/gallon. A biorefinery capable of handling multiple types of biomass have significant potential for higher profitability and more stable production. Policy recommendations derived from this study focus on enhancing public awareness and ensuring reliable biomass supply chains to support the BECCS system's long-term viability.

4.2 Introduction

The utilization of biomass to produce biofuels and bioenergy represents a pivotal intersection of sustainability and energy generation. Biomass offers a renewable resource that can be harnessed to address both energy demands and environmental concerns. Currently, biomass provides approximately 10% of the global energy supply amounting to 50 EJ of energy. The potential of energy generation from biomass is expected to be 140-270 EJ (Liew et al., 2021). Through advanced processes, terrestrial (corn grain, oil seed, and agricultural residues, etc.) and aquatic (algae, cyanobacteria, and seaweeds, etc.) biomass can be transformed into biofuels and bioenergy (SNG, biochar, syngas,

ethanol, and electricity, etc.), providing an alternative to fossil fuels while contributing to efforts aimed at mitigating climate change (Naqvi et al., 2018; Yue et al., 2014). Bioenergy with carbon capture and storage (BECCS) involves not only converting biomass into energy but also capturing the carbon dioxide (CO_2) produced during this process and securely storing it within geological formations. BECCS stands as a further crucial negative emission technology essential for attaining the global warming objectives outlined in COP 21. BECCS entails the conversion of biomass into energy while securely storing the resultant CO_2 within the geological structure (Talei, 2020). Several Integrated Assessment Models (IAM) studied in literature have also proposed BECCS technology as an essential component necessary to achieve emission targets with the potential to eliminate 2-10 $GtCO_2$/yr (Pour, 2019).

Nowadays, the deployment of BECCS remains in its nascent stages and is confronted with a myriad of challenges. These challenges encompass multifaceted dimensions such as concerns about food security, land utilization, water resource allocation, public perception, and societal acceptance. Additionally, the viability of BECCS faces uncertainties related to biomass supply, the potential for large-scale implementation, and its overall energy efficiency compared with conventional fuels (Babin et al., 2021). The use of monoculture crops for biofuel production in the bioenergy sector can negatively impact biodiversity by destroying natural vegetation and habitats, as well as altering species richness, abundance, composition, and distribution (Immerzeel et al., 2014; Popp et al., 2014). Carbon capture and storage increases water consumption in power plants by 20-60% (Magneschi et al., 2017). Collateral CO_2 emissions and other factors may hinder the negative emission potential. Notably, the sustainability, scalability, and seasonal variability of biomass resources are imbued with ambiguity, contingent upon factors like land usage, water accessibility, and competition with agricultural production. It is pertinent to highlight that presently, the Illinois Industrial CCS facility stands as the sole large-scale BECCS installation, capable of capturing up to 1 million metric tons per annum of carbon dioxide. The remaining establishments primarily consist of smaller-scale ethanol production facilities (Christopher consoli, 2019). Large-scale employment of BECCS will lead to an increase in average crop yield by 2-4 times. Because of

bioenergy expansion, the cropland area will increase as well. Three multi-model approaches were proposed to compare the results of different models to assess the impact of large-scale bioenergy crop deployment on land use dynamics. Furthermore, it is essential to acknowledge that biofuels generally exhibit a relatively lower energy return on investment (EROI) when juxtaposed with conventional fossil fuels. For instance, EROI assessments have yielded values ranging from 1.25 to 1.61 for corn ethanol, 4.32 to 5 for sugar cane ethanol, 1.5 to 3.0 for biodiesel, and potentially up to 6 for cellulosic ethanol (Moriarty & Honnery, 2017). This stands in stark contrast to the significantly higher EROI values of 46 for coal and 20 for oil and gas Fields(Hall et al., 2014). Besides, the transportation of CO_2 is also a challenge. Transportation through trucks and motor carriers is considered unfavorable in terms of capacity and costs, leaving pipelines as the only viable option for large-scale onshore transportation over long distances (Svensson et al., 2004).

Above all, policy support remains a major barrier to the implementation of BECCS. Concerns over the uncertainties of the potential of BECCS were raised. Regulation of BECCS shapes decision-making and policy support. An international regulatory framework is needed to help bridge the gap between contradictory concerns at national and international levels. Public awareness or support for BECCS remains relatively low (Donnison et al., 2020). Another obstacle to public support of BECCS is the polarization among citizenries and groups of policymakers over negative emission technologies. This polarization can result in unproductive debates that focus on defending entrenched positions rather than finding solutions, leading to poor policy choices (Searchinger & Heimlich, 2015). Hence, the aim of this paper is to methodically structure and enhance the complete supply chains for bioenergy and biofuel. This encompasses every stage, starting from the production and selection of biomass feedstock to the ultimate utilization of bioenergy and biofuel, ensuring both cost-effectiveness and sustainability, particularly with the incorporation of carbon capture and storage. This paper answers the following questions:

1. Is it economically feasible to produce circular bioenergy and biofuel with carbon capture and storage in the U.S.?

2. What is the geographic distribution network in the U.S. for supplying biofuel converted from biomass under conditions of biomass supply uncertainty? Which biomass will be chosen as the resources for bioenergy and biofuel production during different seasons?

3. What policy recommendations can be proposed to enhance the social acceptance of circular biomass-bioenergy and biofuel with carbon capture and storage?

4.3 Literature Review

4.3.1 Biomass Conversion Pathways

Biomass is a renewable resource that can be easily stored until needed and provides liquid fuel alternative, heat, and electricity for use, especially in transportation systems. There are two main types of biomass feedstocks: terrestrial and aquatic biomass. The United States possesses the potential to consistently generate more than 1.6 billion dry tons of terrestrial biomass each year in a sustainable manner to produce bioenergy and various bioproducts, all while ensuring that the ongoing requirements for food, animal feed, and fiber production are met. This substantial biomass resource can yield approximately 85 billion gallons of biofuels on an annual basis, a quantity sufficient to substitute roughly 30% of the nation's present petroleum consumption (DOE/EERE, 2023). The terrestrial biomass feedstock can be generally categorized into two groups. The first group includes corn grain, sugarcane, oil seed, and so on, which are rich in sugar or lipids, and have high yields after converted into bioethanol or biodiesel. The second group is cellulosic biomass, such as agriculture residues, forest residues, and energy crops. Aquatic biomass includes a diverse group of primarily aquatic, algae, and cyanobacteria, which can have faster growth rates than terrestrial crops and minimize the competition on arable land with the cultivation of food crops. More importantly, algae biomass can contain high levels of oil (lipids or triacyl glycerides), making it a promising feedstock to produce renewable gasoline, diesel, and jet fuel (Hasan, 2009). Thermochemical and biochemical conversion technologies are the two major biomass to bioenergy and biofuel processes as shown in **Figure 4-1**. The thermochemical conversion pathways comprise dry processes (i.e., torrefaction, combustion, gasification, and pyrolysis), and wet processes (i.e., liquefaction, supercritical water gasification, and

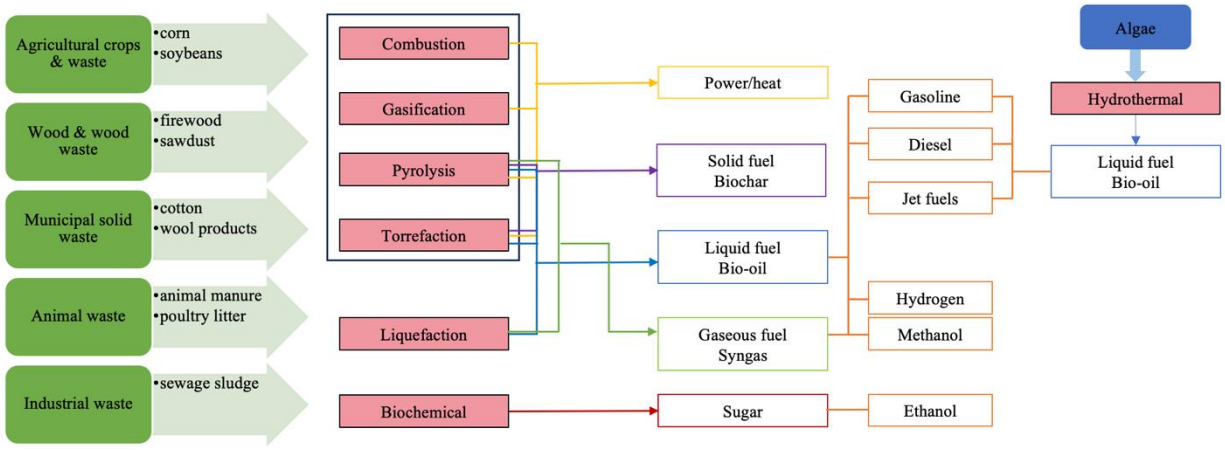


Figure 4-1 Biomass-Bioenergy and Biofuel Conversion Technologies

hydrothermal carbonization) (Danso-Boateng & Achaw, 2022). The biochemical conversion pathways include anaerobic digestion, fermentation, microbial fuel cells, and algae cultivation. These conversion technologies can convert diverse biomass feedstocks to produce bioenergy sources such as direct heat energy, as well as solid, liquid, and gaseous biofuels for instance biochar, bio-oil, and syngas.

4.3.2 BECCS Supply Chain Optimization Overview

The advancement of the United States' advanced bioenergy sector is poised to pave the way for the creation of numerous manufacturing supply chains for hydrocarbon biofuels. These supply chains serve as the critical conduits that interconnect sustainable biomass feedstock sources with the eventual production of biomass-derived gasoline, diesel, and aviation fuels. These supply chains are underpinned by five key components: the biomass production system, biomass logistics system, biofuel production system, biofuel distribution system, and biofuel end-use infrastructure (Gold & Seuring, 2011; Iakovou et al., 2010). A multi-modal model called Carbon Navigation System was used to search and route for a precise amount of biomass to a chosen location, route captured CO_2 for offshore geological storage, and direct energy output to end-users for an illustrative sugar beet-derived bioethanol in the UK (Freer et al., 2021b). Another paper also used the Carbon Navigation System model to explore the implications of siting facilities for wheat straw-derived BECCS-power, a municipal solid waste derived BECCS-waste-to-energy and a sawmill residue-derived BECCS-hydrogen (Freer et al., 2022a). An integrated model that combines biomass inventory management and carbon capture and storage (CCS) construction was built to analyze the operation management of BECCS plants to maximize the total profit for straw-derived biomass power plants under intertemporal conditions (Freer et al., 2022b). The Bioenergy and Land Optimization Spatially Explicit Model (BLOEM) was applied to the Brazilian context by coupling it with the Brazilian Land Use and Energy Systems (BLUES) model. This allowed investigation of the most cost-effective ways of attending to future bioenergy supply projections and studying the role of recovered degraded pasture lands in improving land availability sustainably and competitively (Tagomori et al., 2023).

However, even though those studies explored the optimization of the BECCS supply chain from different economic and environmental aspects. There are still some challenges in the BECCS supply chain system that need to be paid attention. The seasonality, variability, land-use change, and the effects of climate change on biomass supply are big issues for biomass production systems. Therefore, the direct storage and pretreatment processes on raw biomass are important fields (Yoder et al., 2013). Biomass logistics is critical in the bioenergy supply chain as it involves collecting, storing, and delivering feedstock efficiently. Unlike fossil fuels, biomass resources are widely dispersed and require significant efforts in equipment selection, shift arrangement, vehicle routing, and fleet scheduling (Malladi & Sowlati, 2018). The location of independent pretreatment depots that provide uniform-format feedstocks must be carefully considered. Additionally, the challenge in the modeling and optimization of supply chains for these infrastructure-compatible biofuels is to address the full-scale integration with the existing petroleum refinery processes and distribution supply chains (Kwon et al., 2013).

4.4 Integrated Circular Bioenergy System

4.4.1 Network Model

The system initiates at the farm level, where biomass is cultivated. The biomass feedstock is then harvested and transported to an intermediate storage facility, referred to as the "Elevator," which serves as a staging area for further transport. From the elevator, the biomass feedstock is delivered to biorefineries, where it undergoes processing to produce bioenergy and multiple bioproducts. Primary products include biofuel, which is used as a renewable energy source, and secondary outputs such as diesel, generated through a reaction involving captured CO_2 from the production and hydrogen (H_2). Additionally, the biorefinery produces steam, which can be utilized for industrial applications, and biochar, a carbon-rich byproduct that is recycled back to the soil as a fertilizer. This recycling step enhances soil health, further contributing to carbon sequestration and promoting sustainable agricultural practices. The illustrated diagram represents the flow and transformation of biomass within a circular biomass-bioenergy and biofuel system integrated with carbon capture and storage (BECCS) is shown in Error! Reference source not found.. This paper considers a two-stage circular biomass-

bioenergy and biofuel with

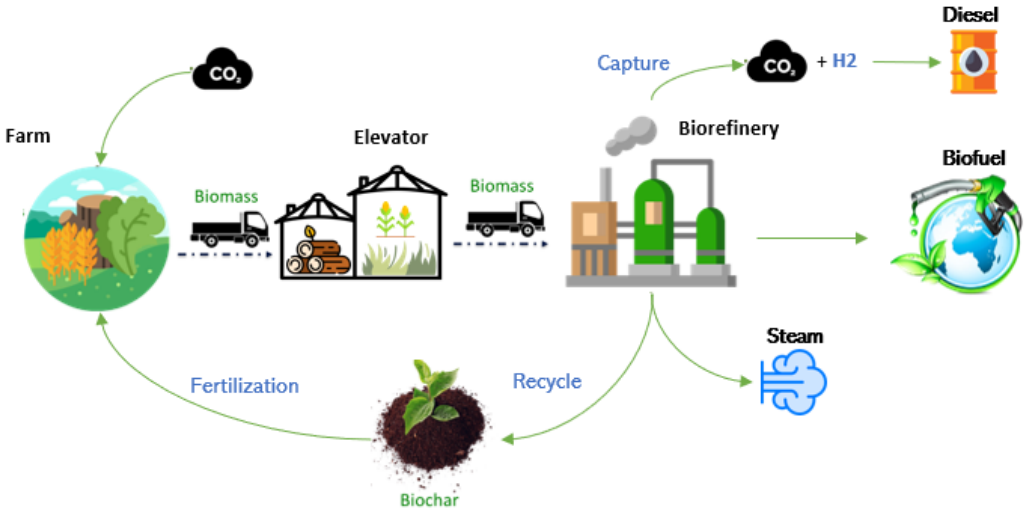


Figure 4-2 Circular Biomass-Bioenergy and Biofuel with Carbon Capture and Storage Process

carbon capture and storage supply chain network, including I biomass elevators (i as its index) and J potential biorefineries (j as its index). Each region has L biomass farms (l as its index). There are M types of biomasses (m as its index). The planning period is T (t as its index). During the harvest seasons, u_{lit}^{m} tons of biomass *m* will be collected from farm l and shipped to elevator *i* in period *t*. The available biomass *m* at farm *l* in period *t* (ton) is V_{lt}^{m}. The unit purchasing cost of biomass *m* from farm *l* in period *t* is pc_{lt}^{m} ($/ton). Due to the seasonality of the biomass, s_{it}^{m} tons of biomass *m* should be stored at elevator *i* in period *t* to reduce the resources shortage. The storage capacity of biomass elevator *i* is SC_i tons. The monthly degradation rate of biomass *m* in the period *t* is d_t^m during storage. Then, x_{ijt}^{m} (ton/month) amount of biomass *m* will be transported from elevator *i* to biorefinery *j* in period *t*. α_m is the conversion rate of biomass *m* to biofuel (%). The binary decision z_j represents whether biorefinery *j* will be built. r_{ijt}^{m} is the profit rate for converting one ton of biomass m from elevator *i* at plant *j* into bioproducts in period *t*. Production capacity of biorefinery *j* (ton) is PC_j. The binary decision y_j^m represents whether biorefinery *j* has the capability of handling biomass *m*. CO_2 emissions from the biorefineries will be captured and converted to fuels. Hydrogen is the feedstock to produce fuel. The unit hydrogen purchase cost is *h* ($/ton). The fixed annual cost of biorefinery *j* is cc_j ($). The additional fixed annual cost of biorefinery *j* for having capability of handling biomass *m* is cm_j^m ($).

The target of the model is to determine the cost-efficient system design and to ensure efficient use and distribution of available biomass resources. Therefore, the objective function (4-1) minimizes the total cost minus the profit of the circular biomass to bioenergy and biofuel with carbon capture and storage supply chain. The total costs are comprised of four parts: biomass purchase cost, production plants capital investment, biomass storage cost, and hydrogen purchase cost. The profit is converting one ton of biomass into bioproducts after considering the operating cost, transportation cost, hydrogen cost and revenues from all three bioproducts.

$$Min \quad \sum_{t\in T}\Big(\sum_{l\in L}\sum_{i\in I}\sum_{m\in M} pc_{lt}^{m}u_{lit}^{m} + \sum_{i\in I}\sum_{m\in M} sc_{i}^{m}s_{it}^{m} + \sum_{j\in J} cc_j\, z_j + \sum_{j\epsilon J}\sum_{m\in M} cm_j^m y_j^m - \sum_{i\in I}\sum_{j\in J}\sum_{m\in M} r_{ijt}^{m}x_{ijt}^{m}\Big) \tag{4-1}$$

$$s.t. \quad s_{it}^{m} = \sum_{l\in L} u_{lit}^{m} - \sum_{j\in J} x_{ijt}^{m} + s_{i,t-1}^{m} \cdot (1 - de_t^m) \qquad \forall i \in I, \forall m \in M, \forall t \in T \tag{4-2}$$

$$\sum_{i\in I} u_{lit}^{m} \le V_{lt}^{m} \qquad \forall l \in L, \forall m \in M, \forall t \in T \tag{4-3}$$

$$\sum_{i\in I}\sum_{m\in M} x_{ijt}^{m}\,\alpha_m \le PC_j z_j \qquad \forall j \in J, \forall t \in T \tag{4-4}$$

$$\sum_{i\in I}\sum_{m\in M} x_{ijt}^{m}\,\alpha_m \le PC_j y_j^m \qquad \forall j \in J, \forall t \in T \tag{4-5}$$

$$\sum_{m\in M} y_j^m \le |M| z_j \qquad \forall j \in J \tag{4-6}$$

$$u_{lit}^{m},\ s_{it}^{m},\ x_{ijt}^{m} \ge 0; \quad z_j, y_j^m \in \{0,1\}$$

Constraint set (4-2) enforces that the biomass *m* stored at elevator *i* in period *t* is balanced by the biomass received from farms, biomass sent to biorefineries, and the remaining biomass from the previous period accounting for degradation. Constraint set (4-3) limits the amount of harvested biomass does not exceed the available biomass. Constraints (4-4) and (4-5) limit the amount of biomass transported from elevator to biorefinery does not exceed the production capacity of the biorefinery if it is selected. Constraint set (4-6) limits the number of biomasses types a biorefinery can handle. The biorefinery can only process several biomasses up to its maximum capacity. And all biomass variables are non-negative.

4.5 Numerical Experiment

4.5.1 System Boundary and Data Description

The Billion-Ton Update analyzed whether farm and forest resources in the United States could sustainably supply about 1 billion tons of biomass annually and broke down its analysis into two categories: forest-based and agricultural. The numerical experiment

focuses on three agricultural biomass resources with the highest production levels in the southeastern United States (Alabama, Georgia, Mississippi, Florida, and South Caronia): corn stover, switchgrass, and miscanthus. The related data of these three feedstocks is shown in **Table 4-1**. The available seasons for corn stover, switchgrass, and miscanthus are October, October through mid-February, and February and March (Connor McDonald, 2013; Kevin Gould, 2015; Mike Jacobson, 2012). The Biofuels Techno-Economic Analyses Database from the U.S. Department of Energy Bioenergy Technologies Office summarized the economic and technical parameters associated with the modeled biorefinery processes to produce biofuels and bioproducts for these three biomasses (BioEnergy KDF, 2023). The bio-oil yields for corn stover, switchgrass, and miscanthus averaged 61.7 wt%, 37 wt%, and 24.17 wt%, while corresponding biochar production rates were measured at 17 wt%, 25 wt%, and 30.27 wt%, respectively. Additionally, the steam generated per dry ton of biomass processed was 0.30, 0.26, and 0.26 tons for corn stover, switchgrass, and miscanthus, respectively (Happs et al., 2024b; Ma et al., 2024b; Mullen et al., 2010). The monthly degradation rate of these feedstocks is around 1%-2% (Nolan et al., 2009; Smith et al., 2020). Then, every ton of bio-oil can be upgraded to 0.65 tons of biofuel. The average unit purchase price from elevator of these three biomasses are $50/dry ton, $65/dry ton, and $70/dry ton. This unit purchase price already includes the transportation cost from farms to the elevators. The unit transportation cost per dry ton per mile of biomass from elevators to biorefineries is DFC + DVC × distance × DM, DFC ($3.318/dry) is the distance fixed cost, DVC is the distance variable cost, distance is the straight-line distance calculated from the latitude and longitude coordinates of two points, and DM (1.1) is the distance multiplier (Elia et al., 2013).

The net carbon benefits of biofuels refer to the overall reduction in greenhouse gas (GHG) emissions when compared to fossil fuels, considering the entire lifecycle of biofuel production and use. From the existing literature reviews, the average carbon emission for producing per ton of biofuel generated biomass are 0.148, 0.311, and 0.133 tons for these three feedstocks (Happs et al., 2024a; Kim et al., 2020; Ma et al., 2024a). While biofuel releases roughly the same amount of carbon dioxide into the atmosphere as

Table 4-1 Data Values and Sources of Corn Stover, Switchgrass and Miscanthus

	Corn stover	Switchgrass	Miscanthus
Available seasons	October	October through February	February and March
Process	Pyrolysis	Fermentation	Pyrolysis and catalytic hydrotreatment
Average bio-oil yield (wt%)	61.7%	37%	24.17%
Average biochar yield (wt%)	17%	25%	30.27%
Average steam yield (ton)	0.3	0.26	0.26
Unit purchase cost from elevator ($/dry ton)	50	65	70
Monthly unit storage cost ($/dry ton)	10	8	7
Biomass distance variable transportation cost from elevator to biorefinery ($/ton-mile)	0.2	0.18	0.22
Monthly degradation rate (%)	2%	1%	1%
CO_2 emissions during production (ton CO_2/ton biofuel generated)	0.148	0.311	0.133

was absorbed by the plants used to produce it during their growth. The monthly production of these three feedstocks for different market maturity levels is shown in Error! Reference source not found.. Mature-market low scenario assumes low market demand and low supply advancements, with business-as-usual (BAU) projections for agriculture, forestry, and waste sectors. There are no yield improvements for purpose-grown energy crops, and biomass use remains limited to current uses. The mature-market medium scenario anticipates moderate market demand and moderate supply-side innovations. In this case, BAU projections are coupled with moderate yield improvements (1%) for purpose-grown energy crops. Biomass production continues alongside current uses. The mature-market high scenario envisions high market demand and significant supply-side advancements. Here, purpose-grown energy crop yields improve by 3%, while conventional crop yields increase by 1.5 times the USDA trend. Waste projections follow BAU, but higher demand for waste drives increased waste prices, complementing existing uses (Department of Energy & Langholtz, 2023). Though April to September, there are no biomass feedstock available. In the Market-mature high scenario, both switchgrass and miscanthus exhibit substantial increases in production, especially in the summer months, indicating their growing contribution in a more developed biomass market. In the next subsection, we used Gourbi to solve the BECCS numerical experiment.

There are 14 different scales existing biorefineries in the southeast of the U.S. We assumed the new biorefineries were all large-scale facilities. The life span of biorefineries is 20 years with 10% interest rate. The unit annualized capacity cost of per dry ton of biomass is $10-100 million. The average unit fixed operating cost of per dry ton of biomass is $152.5. The unit variable operating cost of per dry ton of biomass is $2-20. The monthly biofuel production capacity is 36,950-369,500 tons. The breakdown and sources of the capital and operating costs and production capacity of the biorefinery are shown in **Table 4-2.**

4.5.2 Resulting network

The results of the numerical experiments demonstrate the viability of biomass conversion to biofuel, biochar, steam, and diesel converted from the carbon emissions during

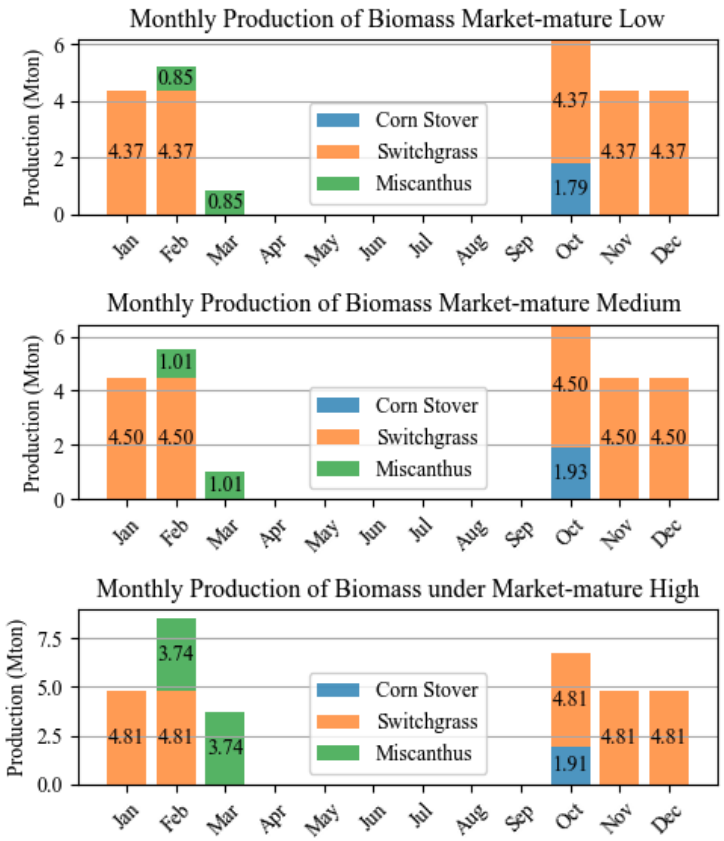


Figure 4-3 Monthly Production of Corn Stover, Switchgrass, and Miscanthus under Low, Medium, and High Market-Mature Scenarios in Southeast Area of United States

Table 4-2 The Capacity, Operating, and Production Capacity of the Existing and New Biorefineries

	Existing biorefineries	New biorefineries	Sources
Biorefinery unit annualized capacity cost (M$/dry ton)	4-40	80	(Tsagkari et al., 2016)
Biorefinery unit fixed operating cost ($/dry ton)	50	50	(Renewable Energy Agency, 2012)
Biorefinery unit variable operating cost ($/dry ton)	2-20	2-20	(Renewable Energy Agency, 2012)
Biorefinery monthly production capacity (ton/month)	36,950-369,500	369,500	(Forsberg et al., 2021)

production under different market scenarios: low, medium, and high market maturity levels. **Table 4-3** indicates the optimal biomass collected and transported to biorefineries, CO_2 emissions during production, biofuel and other bio-products yields, and the associated costs, revenues and profits under these conditions. The result shows that the total amount of biomass transported from farms to biorefineries increases with market maturity. Consequently, biofuel and other bio-products production also increase proportionally. The biofuel output rises from 2.71 million tons in the low scenario to 3.01 million tons in the high scenario. The biochar output is substantial, reaching 2.63 million tons in the high scenario, while steam production increases from 1.30 million tons (low) to 1.44 million tons (high). Capital costs are rising from $296 million to $376 million in the high scenario, which indicates that one more new biorefinery needs to be constructed when the market maturity rises to one more level. However, at the medium market maturity level, a greater number of new biorefineries is required compared to other market maturity levels, as biomass feedstock distribution is more dispersed under medium market conditions, which also results in higher additional operating costs at this level. The fixed operating costs for biorefineries increased from $1.52 billion in the low scenario to $1.69 billion in the high scenario. Transportation, storage, and hydrogen costs rise with higher market demand, reflecting the need for more resources and more complex logistics. As expected, market maturity significantly influences biomass flows, costs, and revenues. In the high market maturity scenario, more biomasses are available, leading to increased biofuel, biochar, and steam production. This growth in production corresponds with higher purchase costs and biorefinery operation expenses, but it also brings in significantly higher revenues. One notable trend is that the profit margins remain robust across all scenarios, demonstrating that biofuel production remains profitable even in less mature markets. However, with higher demand and technological advancements (as assumed in the high market maturity scenario), profitability grows further, reaching nearly $1.2 billion. This underlines the potential of biofuel markets to grow with the right investments in technology, infrastructure, and policies to support biomass supply chains.

Table 4-3 The Optimal Amount of Biomass, Costs of BECCS, and Revenues of Bioproducts when Biorefinery has Capability of Handling One Type of Biomasses under Different Market Maturity Scenarios

	Low	Medium	High
Amount (Ton)			
Amount of biomass from farms	10,333,500	11,079,300	11,428,400
Amount of biomass to biorefineries	9,999,950	10,803,500	11,071,700
Amount of biofuel	2,713,860	2,974,240	3,013,350
Amount of biochar	2,375,350	2,549,150	2,626,430
Amount of diesel	366,294	394,676	405,336
Amount of steam	1,299,990	1,404,450	1,439,320
Amount of CO_2	732,589	789,352	810,672
Costs ($)			
Biomass purchase cost	647,824,000	691,143,000	715,770,000
Biorefinery annualized capital cost	296,000,000	456,000,000	376,000,000
Biorefinery annual fixed operating cost	1,524,990,000	1,647,530,000	1,688,430,000
Biorefinery annual variable operating cost	148,000,000	188,000,000	168,000,000
Biomass transportation cost	58,585,700	56,967,500	61,275,700
Biomass storage cost	257,201,000	209,401,000	274,447,000
Hydrogen purchase cost	219,777,000	236,806,000	243,202,000
Revenue ($)			
Annual biofuel revenue	3,319,050,000	3,637,500,000	3,685,330,000
Annual biochar revenue	311,171,000	333,938,000	344,063,000
Annual diesel revenue	418,308,000	450,720,000	462,894,000
Steam revenue	214,499,000	231,735,000	237,487,000
Total cost ($)	3,152,377,700	3,485,847,500	3,527,124,700
Total revenue ($)	4,263,028,000	4,653,893,000	4,729,774,000
Total profit ($)	1,110,650,300	1,168,045,500	1,202,649,300

Biorefinery annual operating cost is the largest portion of the costs, representing 47%. This suggests that the ongoing operational expenses of the biorefinery, such as labor, utilities, and maintenance, dominate the overall cost structure of the BECCS system. Biomass purchase cost accounts for 20% of the total, indicating that acquiring raw biomass is a significant but not the largest expense. The Biorefinery's fixed annual cost is 13%, this includes fixed costs such as depreciation, equipment maintenance, and other non-variable expenses associated with running the biorefinery. Biorefinery additional fixed annual cost is 5% of the total costs, indicating supplementary costs linked to the biorefinery's capability to handle different types of biomasses. Hydrogen purchase cost represents 7%, hydrogen is critical for upgrading bio-oil to biofuel, and this cost reflects its significance in the biofuel production process. Biomass storage cost is 6%, this reflects the expenses associated with storing biomass before it is processed, although this is a smaller contributor compared to operational or purchase costs. Biomass transportation cost is minimal, likely indicating that the distances between biomass sources and the biorefinery are short or transportation is efficiently managed. Biofuel accounts for 78% of the total revenue, while other bio-products also contribute additional value. **Figure 4-4** Percentage of the Optimal costs of BECCS, and Revenues of Bioproducts under Mature-Market Medium Scenario highlights the economic structure of the BECCS system, where biorefinery operating costs dominate expenses and biofuel revenue drives profitability.

In analyzing the monthly distribution of biomass flows within the BECCS supply chain under medium market maturity, notable patterns emerge that emphasize the operational complexities of balancing supply and demand across different biomass types as shown in Error! Reference source not found.. Each biorefinery is configured to process a single biomass type, aligning with regional resource availability and logistical considerations. Error! Reference source not found. **(a)** reveals that biomass supply and transport volumes to biorefineries follow distinct seasonal trends, with peak volumes aligning closely with harvest cycles. These seasonal peaks necessitate strategic storage solutions, particularly in months of high supply, to sustain a steady feedstock flow to biorefineries during periods of limited availability. Storage volumes are therefore highest in these peak

months, reflecting the need to manage

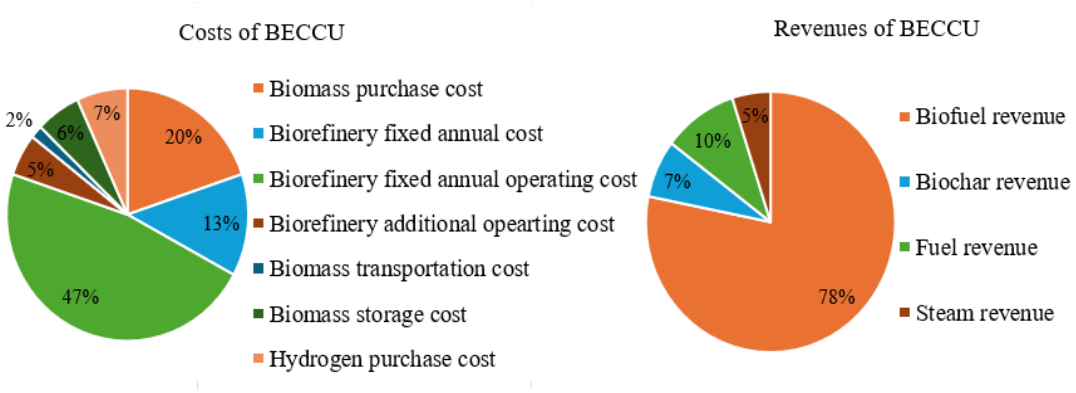


Figure 4-4 Percentage of the Optimal costs of BECCS, and Revenues of Bioproducts under Mature-Market Medium Scenario

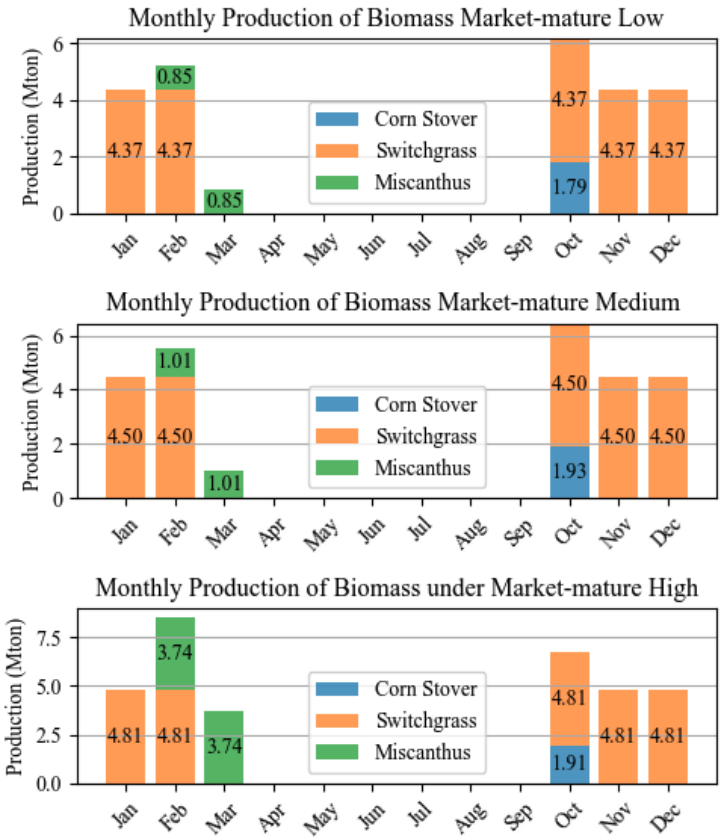


Figure 4-5 Monthly Production of Corn Stover, Switchgrass, and Miscanthus under Low, Medium, and High Market-Mature Scenarios in Southeast Area of United States

variability in biomass supply. However, during September no production occurs, which could lead to the loss of money to maintain the operating of biorefineries. A breakdown by biomass type in Error! Reference source not found. **(b)** offers further insights into the dynamics of feedstock distribution. Switchgrass, for instance, constitutes the largest portion of the supply chain, with extended seasonal availability, especially through spring and summer. In contrast, corn stover and miscanthus have more constrained seasonal windows, concentrated in specific months, requiring biorefineries to rely heavily on stored biomass to maintain production continuity. These patterns underscore the logistical challenges inherent in a medium market maturity scenario. The dispersed distribution of biomass feedstock and the resulting storage demands lead to increased operational costs, highlighting the need for flexible biorefinery operations capable of adapting to seasonal variations and the uneven spatial distribution of biomass resources.

The flow of biomass feedstock through the BECCS supply chain illustrates the transformation of switchgrass and corn stover into biofuel, with various byproducts contributing to a diverse output mix as shown in **Figure 4-6**. Switchgrass as the primary feedstock, with corn stover playing a supplementary role. This allocation reflects the availability and processing efficiency of each biomass type within the BECCS framework. Biofuel, the main product, emerges with a substantial output volume, highlighting its role as a key component of the supply chain's bioenergy objectives. Additionally, byproducts such as biochar and steam are produced in smaller amounts. Converting CO_2 emissions to diesel during production offers potential for further utilization or sequestration, aligning with the broader goals of emission reduction and sustainable resource management within the BECCS framework.

The distribution of biorefineries and biomass resources across the southeastern United States reveals strategic decisions in locating facilities to maximize supply chain efficiency and minimize transportation costs. **Figure 4-7** highlights the spatial layout of both new and existing biorefineries, along with biomass-rich areas and selected elevator locations, under a medium market maturity scenario where biorefineries are equipped to handle multiple biomass types. The figure shows that new biorefineries, indicated by blue circles, are positioned close to areas with abundant biomass resources, particularly in the

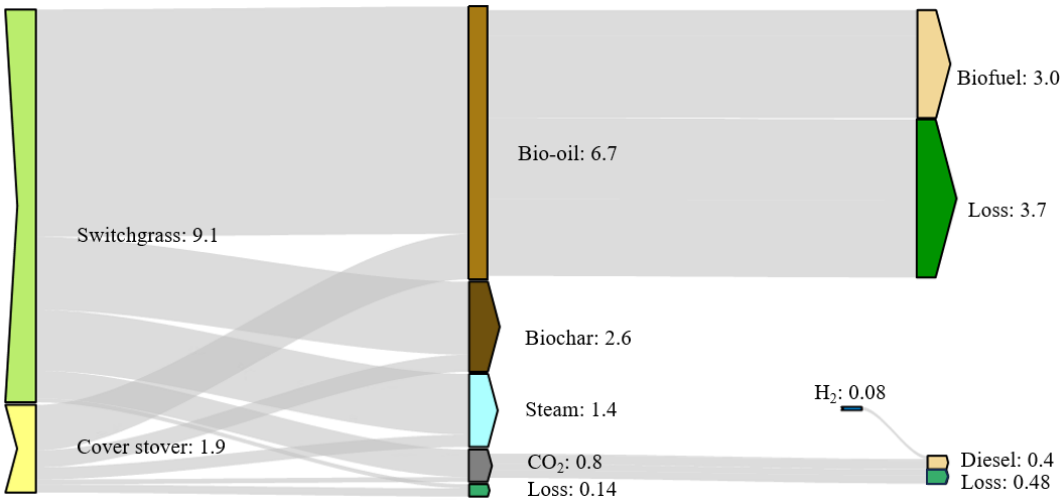


Figure 4-5 Biomass Feedstock Feed in and Biofuel and Bio-products Feed out under Market-mature Medium and Biorefinery Handles Multiple Types of Biomass Scenario

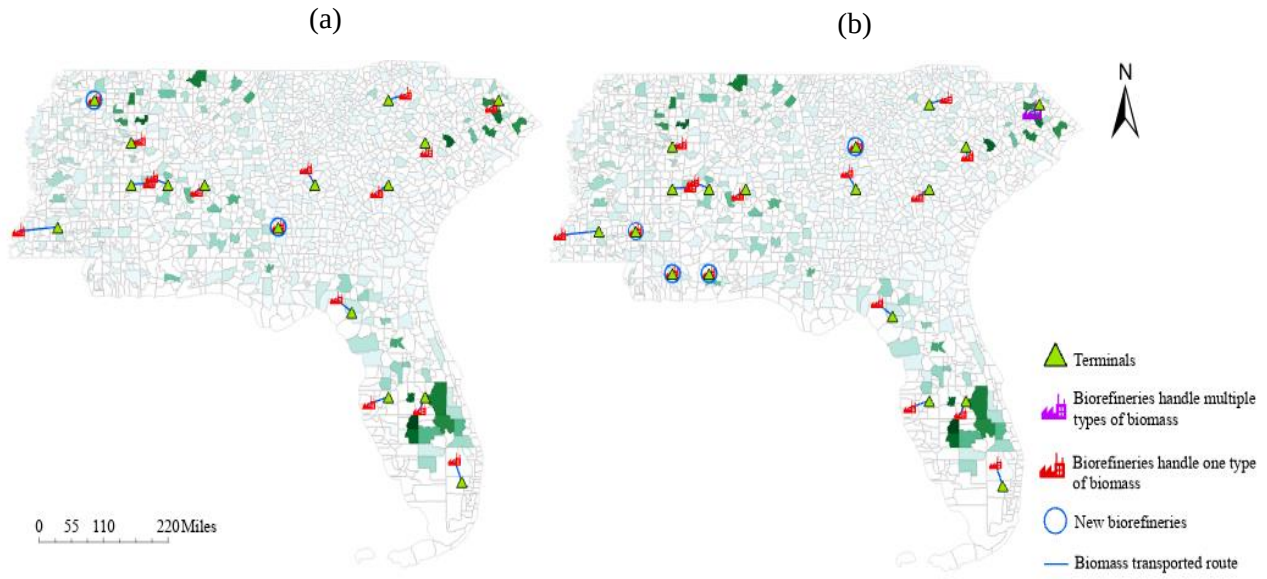


Figure 4-6 The comparison of distribution map of elevators, selected biorefineries and biomass resources under market-mature medium scenario. Figure 7(a) is biorefinery can only handle one type of biomass. Figure 7(b) is biorefinery can handle multiple types of biomass under low variable

western and southern regions. This strategic placement allows for efficient resource access and reduces transportation distance, thus lowering logistical costs. Existing biorefineries are also distributed near biomass-dense zones, reflecting an established network that leverages proximity to feedstock sources. When we reduce the unit variable operating cost to 10% of the current level, biorefineries process multiple types of biomass will be considered and offer significant operational flexibility, adapting to seasonal fluctuations in biomass availability. By diversifying the feedstock types available for processing, these facilities maintain a steady supply throughout the year, optimizing resource utilization and enhancing the resilience of the bioenergy supply chain. This diversified approach reduces reliance on any single biomass type, ensuring that production levels remain stable even if certain feedstocks experience seasonal or regional shortages.

4.5.3 Sensitivity and Uncertainty Analysis

The major contributors of the total profit of circular BECCS system include the costs for biomass feedstock purchase, transportation, and storage, the capital and operating expenditure of biorefineries, and the biofuel price. A sensitivity analysis was conducted on these key components, varying each from 20% to 200% of baseline values to assess their impact on total profit, as illustrated in **Figure 4-8**. The results reveal that fixed operating costs for biorefineries have the most significant effect on profitability. As these costs increase, total profit shows a significant decline. When the unit fixed operating cost increases to 200% of the baseline value, the system becomes economically infeasible, demonstrating no profitability. Additionally, changes in biofuel prices exhibit a notable influence on total profit as well. Higher biofuel prices directly enhance revenue, supporting a more robust profit margin even as other costs fluctuate. The minimum selling price of biofuel produced from the circular BECCS system is $2.62/gallon. This sensitivity analysis underscores the importance of cost management across all operational areas in the BECCS supply chain. The investment in cost-stabilizing measures, particularly for biorefinery operations, could improve resilience to economic shifts.
We further investegated the impact of variations in the biorefinery unit fixed operating cost and biofuel price on total costs, revenues, and profit, as well as the quantities of

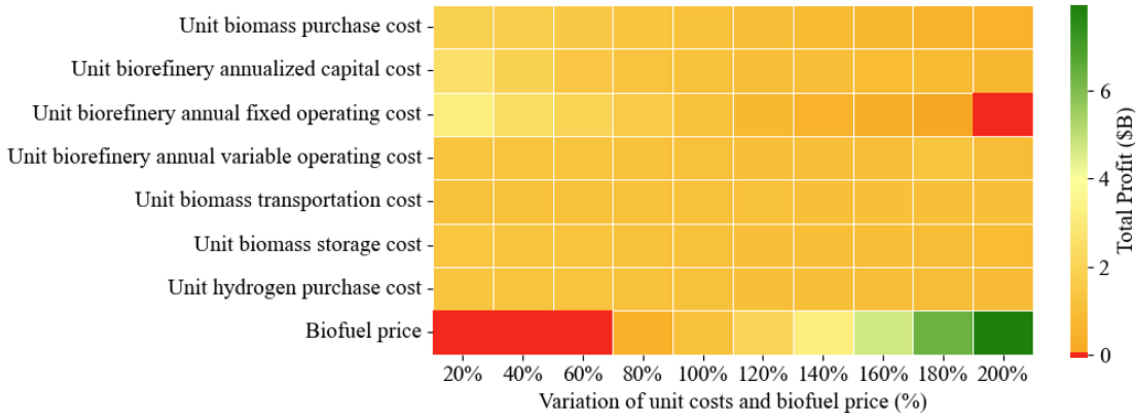


Figure 4-7 Sensitivity Analysis: The Impact of Unit Costs and Biofuel Price Vary from 20% to 200% on the Total Profit

harvested biomass, produced biofuels, and captured CO_2 within the BECCS system as shwon in **Figure 4-9**. As fixed operating costs increase, the system demonstrates a clear downward trend in biomass utilization, biofuel production, and byproduct outputs, such as biochar, steam, and diesel. At lower cost levels (20% to 80% of the baseline), the system maintains robust biomass flows from farms to elevators, reaching 25 million tons at 20% cost. However, as costs rise to 180%, biomass processing falls significantly, dropping to around 5 million tons, and completely halts at 200%, indicating the system's economic infeasibility at excessive cost levels. Biofuel production mirrors this trend, with higher production observed at lower operating costs (approximately 6 million tons at 20%) and diminishing steadily as costs increase, reaching zero production at 200%. Biochar and diesel outputs also follow a similar pattern, highlighting the cascading impact of fixed cost increases on various production outputs and byproducts. This drop in outputs directly correlates with reductions in biomass purchases, biorefinery operational expenses, and transportation costs, underscoring the direct relationship between operational costs and production levels in the BECCS supply chain. In contrast, the impact of biofuel price on the BECCS system indicates that higher prices stimulate biomass processing and biofuel production. However, when the biofuel price exceeds a 140% increase, the growth in total costs, bioproduct production, and CO_2 emissions shows only marginal increases. This suggests that it is unnecessary to raise the biofuel price beyond this threshold to achieve significant economic or environmental impact.

The biorefinery production capacity and the biomass to biofuel conversion rates could also impact on the performance and economic viability of the BECCS system as well. As shown in **Figure 4-10**, under conditions where production capacity is increased to 120% of the base level, we observe a dramatic impact across several metrics, with biofuel, biochar, diesel, steam, and CO_2 capture all rising by approximately 22% to 40%. This increase demonstrates that scaling up production enhances biomass processing and improves output levels, directly contributing to greater profit margins. Conversely, reducing production capacity to 80% leads to sharp declines, with bio-product output falling by 5% to 7%, and profit decreasing by around 18%. This trend highlights the importance of maintaining adequate production capacity for optimal BECCS system

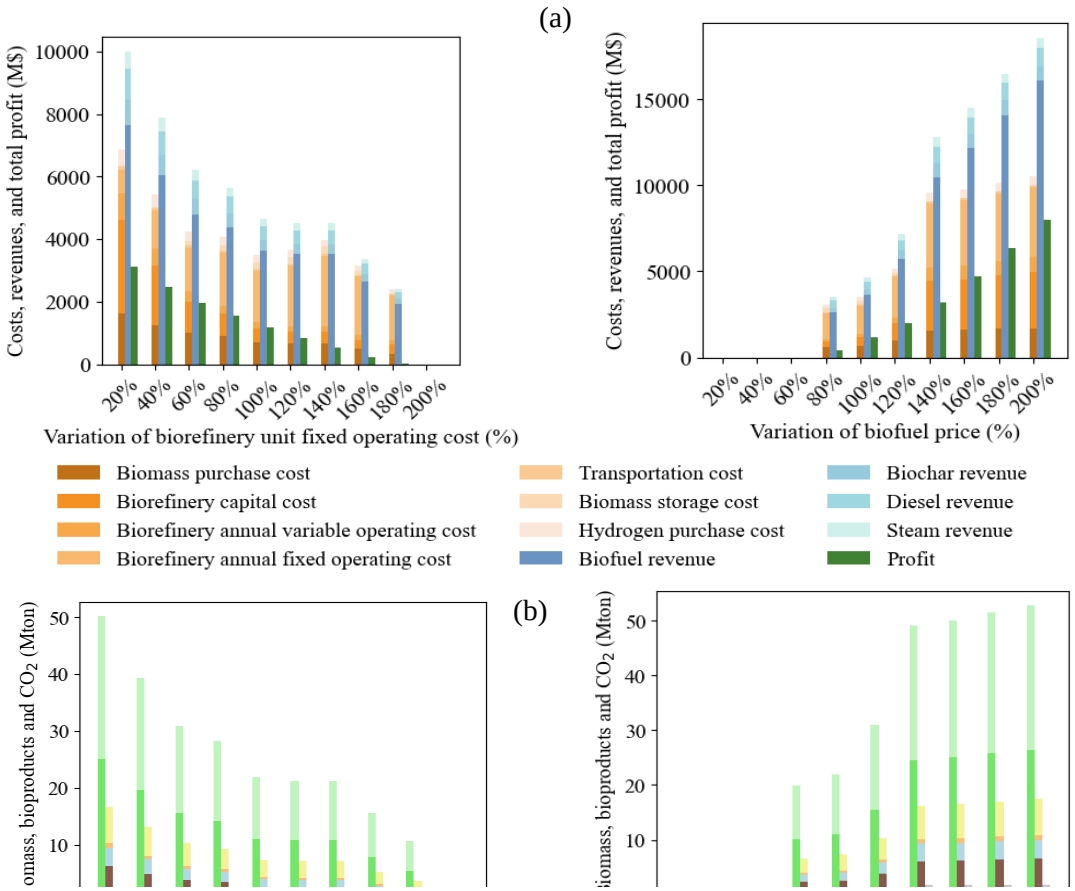


Figure 4-8 Sensitivity Analysis: The Impact of Unit Biorefinery Fixed Operating Cost and Biofuel Price Vary from 20% to 180%. Figure 9(a) is the impact on all other costs, revenues, and total profit. Figure 9(b) is the impact on harvest biomass, produced products, and captured CO_2

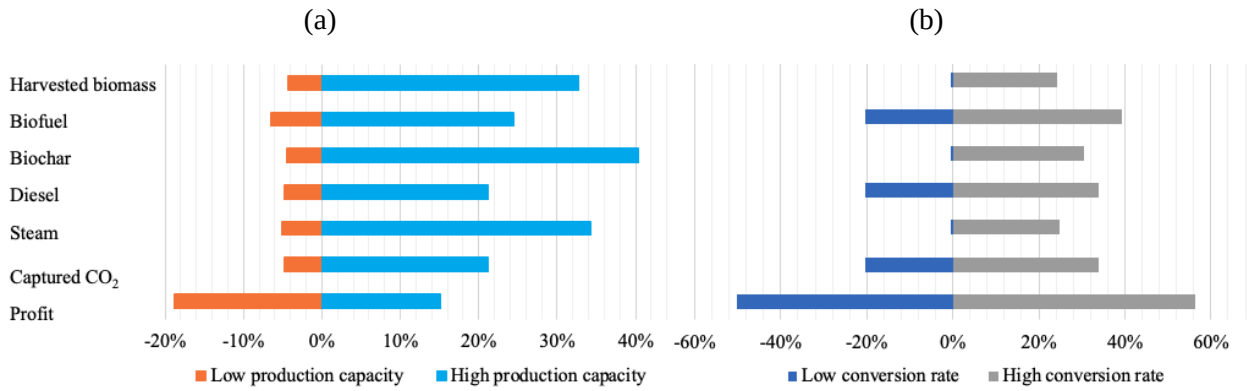


Figure 4-9 Sensitivity Analysis: The Impact of Biorefinery Production Capacity and Bio-oil to Biofuel Conversion Rate Vary from 80% to 120% on Harvested Biomass, Produced Biofuel, Biochar, Diesel, Steam, Captured CO_2, and Profit. Figure 10(a) is under both low and high production capacities. Figure 10 (b) is under low and high biofuel conversion rates

4.6 Policy and Regulatory Recommendations

In the policy and regulatory recommendations section, we provided supportive policies and regulatory frameworks that incentivize BECCS deployment and address potential barriers. These frameworks must address current gaps, promote technological advancements, and provide economic and environmental incentives. In the United States, several significant policies and regulators are established for BECCS as shown in **Table 4-4**. These initiatives aim to incentivize low-carbon biofuels, expand financial support for carbon capture projects, and promote the infrastructure necessary for large-scale deployment of BECCS technologies. Although these policies establish a foundation for advancing bioenergy and carbon capture technologies, significant gaps persist in ensuring a reliable and consistent biomass supply, fostering public acceptance, and optimizing the logistics of carbon transportation and storage within the circular BECCS framework. Based on the results of this study, several key policy areas emerge as critical for long-term viability of the circular BECCS.

Biomass Supply and Logistics Planning

To address the biomass feedstore supply risk, the policies should incentivize the development of biomass supply chains that account for seasonal variability and regional climate conditions. For instance, in the southeast regions, where corn stover is available performance conversion rates, the system's sensitivity to conversion efficiency becomes even more evident. When the conversion rates rise to 120% of the base scenario, total profit experiences a substantial increase of roughly 55%, underscoring the economic benefits of enhanced conversion technologies. Conversely, a reduction in conversion rates to 80% yields significant declines in bio-products and CO_2 capture, with reductions ranging from 1% to 20%. These results suggest that improving conversion efficiency is a powerful lever for boosting both economic and environmental outcomes within the BECCS system. The findings align with prior analyses, emphasizing that investments in advanced biorefinery technology and conversion efficiency are critical to realizing the full potential of bioenergy systems.

This study conducted uncertainty analyses by disturbing each parameter as well. For each parameter, a normal distribution was assumed, a Monte Carlo simulation yields the 95%

Table 4-4 The Timeline of Significant Policy Developments of EBCCU in the United States

Year	Policy/Regulation	Description	Source
2005 (expanded 2007)	U.S. Renewable Fuel Standard (RFS)	Mandated renewable fuel blending in transportation fuels. RFS2 (2007) expanded the inclusion of advanced biofuels derived from biomass.	(*Alternative Fuels Data Center: Renewable Fuel Standard*, 2007)
2009	California Low Carbon Fuel Standard (LCFS)	Established carbon intensity targets for transportation fuels, incentivizing low-carbon biofuels and incorporating lifecycle carbon analysis.	(California Air Resources Board, 2011)
2018	U.S. 45Q Carbon Capture Tax Credit (Expanded)	Expanded tax credits for carbon capture and storage, benefiting bioenergy plants implementing carbon capture technologies.	(The Section 45Q Tax Credit for Carbon Sequestration, 2023)
2020	California Carbon Capture and Sequestration Protocol	Allowing carbon capture projects to generate credits under California's LCFS, supporting BECCS as a GHG reduction strategy.	(California Air Resources Board, 2018)
2022	International Energy Agency (IEA) Net Zero by 2050 Roadmap	Emphasized BECCS as a key technology to achieve net-zero emissions globally by 2050, with large-scale deployment needed by the 2030s.	(*An Updated Roadmap to Net Zero Emissions by 2050 – World Energy Outlook 2022 – Analysis - IEA*, 2022)
2022	U.S. Inflation Reduction Act	Significantly increased 45Q tax credits, promoting carbon capture projects and supporting the expansion of BECCS technologies.	(Enel North America, 2022)
2021-2022	U.S. Clean Energy Incentives in Bipartisan Infrastructure Law	Included investments in carbon capture and storage, promoting infrastructure development for BECCS in the U.S.	(Enel North America, 2021)

in October and miscanthus in February, storage policies need to be strengthened. A national biomass supply monitoring system could help predict supply fluctuations and confidence intervals, and a standard deviation set to 20% of the mean to introduce variability. The distribution of total profit, total costs, revenue, biofuel production, and CO_2 capture provides valuable insights into the performance of the BECCS system under various uncertainty scenarios. As uncertainty levels increase, we observe fluctuations across these metrics, highlighting the sensitivity of the supply chain to variations in economic and operational factors as shown in Error! Reference source not found.. In terms of total profit, the model demonstrates resilience within a certain range but reveals a notable decrease as operational uncertainties intensify. This decline underscores the critical role of stable cost

and revenue conditions in maintaining profitability. Revenue distribution mirrors this trend, showing a steady decline when uncertainty factors lead to increased costs or reduced production efficiency. The system's ability to generate revenue is closely tied to biofuel output, which serves as the primary revenue driver within the BECCS framework. Biofuel production also experiences a reduction under heightened uncertainty, indicating that disruptions in feedstock availability or processing costs directly impact the volume of biofuels generated. This reduction in biofuel output consequently affects CO_2 capture, as carbon capture efficiency is intrinsically linked to the amount of biomass processed. With lower biomass conversion, the volume of CO_2 captured decreases proportionally, reducing the system's environmental benefits.

ensure that sufficient biomass is available to maintain continuous biorefinery operations. To improve biomass collection, storage facilities, and transportation networks, regional governments should implement regulations that incentivize the development of infrastructure, such as dedicated biomass transport routes, centralized storage facilities, and pretreatment depots. This would reduce costs and inefficiencies associated with transporting bulky, low-density biomass feedstocks. Collaboration between policymakers and the agricultural and forestry sectors is essential to optimize logistics. Policies could promote partnerships between bioenergy producers, farmers, and foresters to establish sustainable biomass harvesting, collection, and transportation practices that do not

conflict with food production or ecosystem conservation.

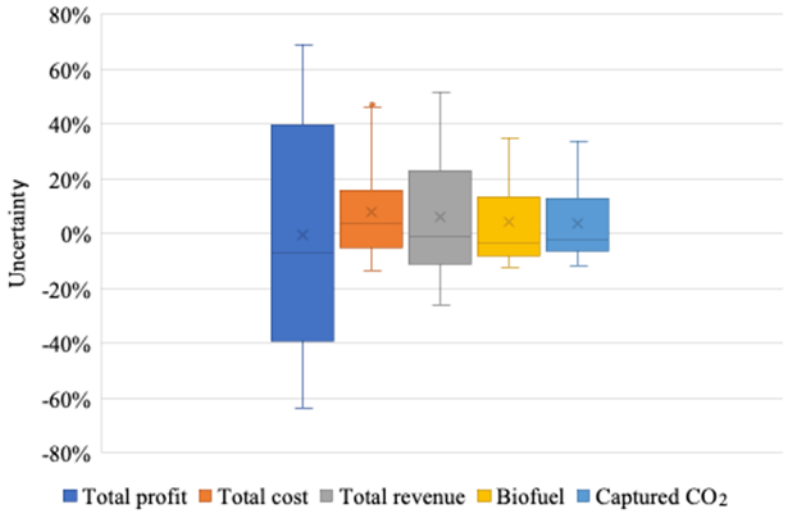


Figure 4-10 The Distribution of Total Profit, Total Cost, Total Revenue, Produced Biofuel, and Captured CO_2

Incentives for BECCS Technology

The existing studies only discuss biomass to bioenergy and biofuel with carbon capture and storage. This study utilizes captured carbon emissions during production to valuable biodiesel while recycling side products such as biochar and steam. Governments should establish incentives, such as tax credits or direct subsidies, for companies that integrate carbon capture with bio-diesel production. These incentives could be modeled after the existing 45Q tax credit but should be expanded to cover carbon utilization for biofuel production. This would encourage industries to invest in technologies that transform CO_2 into commercially viable products like biodiesel, creating a circular economy around carbon emissions. Policies should also provide support for integrating biochar into agricultural and industrial applications, such as soil amendment for carbon sequestration or in industrial processes to replace fossil fuels. Additionally, incentives should be offered for using recycled steam for energy recovery within the production process. As seen in numerical experiments, refineries capable of handling multiple feedstocks are more efficient and flexible. The 45Q tax credit should also be expanded to include smaller-scale bioenergy plants and offer increased financial support for BECCS projects using multiple types of biomasses. A tiered subsidy system based on the scale of biofuel production could incentivize the construction of multi-biomass refineries.

Public Awareness and Acceptance

To enhance social acceptance of BECCS, public awareness campaigns should inform citizens about the benefits of biomass-biofuel technologies while recycling biochar and steam and the role of carbon capture and utilization in achieving climate targets. Governments should introduce regulations that require developers of BECCS projects to hold public consultations and community meetings before the project approval stage. This will ensure that local communities are informed about the project and its potential benefits, addressing concerns and misconceptions early on. Governments could establish a voluntary or mandatory certification program for BECCS facilities that demonstrate sustainable practices in biomass sourcing, carbon utilization, and by-product recycling. Certified projects would be recognized for their contributions to reducing emissions and

creating a circular economy.

Monitoring and Evaluation

A national framework should be established to monitor the performance of BECCS projects, ensuring that biofuel production meets sustainability and carbon reduction targets. Governments could introduce carbon accounting standards that track both the biofuel yields and the net CO_2 sequestered in geological formations.

Develop metrics to monitor the effectiveness of policies and regulations. Conduct regular evaluations and adjust policies as necessary to ensure continuous improvement and effectiveness. Policies supporting BECCS should be subject to regular evaluation and adaptation based on technological advancements and market conditions. A flexible regulatory framework will allow for adjustments in response to new data and emerging best practices in bioenergy production.

4.7 Conclusion

This study demonstrates the significant potential of the circular biomass-bioenergy and biofuel with carbon capture and utilization (BECCS) to address both renewable energy demands and environmental concerns. Through a comprehensive techno-economic analysis, we have shown that the circular BECCS system not only provides renewable energy alternatives but also contributes to carbon mitigation efforts through the capture and utilization of CO_2 emissions during production. The numerical experiments highlight the viability of this system under different market maturity scenarios. Under each scenario, the results reveal critical insights into the biomass supply chain, conversion processes, and the production of biofuel, biochar, and steam, as well as the associated costs and revenues. In the high market maturity scenario, the system reaches its full potential, with 11.4 million tons of biomass processed, resulting in 3.0 million tons of biofuel, 2.6 million tons of biochar, and 1.4 million tons of steam. Notably, the overall profit climbs to nearly $1.2 billion, underscoring the economic viability of the BECCS system in a well-developed market. The revenue generated from biofuel production alone increases substantially, while biochar and steam offer significant additional streams of income. Across all scenarios, the production of biochar and steam offers important secondary benefits, not only in terms of additional revenue but also as contributors to the

circular economy. Biochar, with its potential applications in soil improvement and carbon sequestration, and steam, which can be used for energy recovery, provide opportunities to enhance the sustainability and economic resilience of the system. Sensitivity and uncertainty analyses reveal the system's performance under various economic and operational conditions, highlighting the importance of biofuel pricing and biorefinery fixed operating costs. Increased operating costs constrain production capacity and limit economic viability. The minimal selling price of biofuel produced from the circular BECCS system is $2.62/gallon. Favorable biofuel prices significantly boost biomass processing, biofuel output, and CO_2 capture, but it is unnecessary to raise the biofuel price beyond 140% of the current level. Under uncertainty scenarios, fluctuations in total profit underscore the need for stable operational conditions and cost-effective strategies of the biorefinery to support system resilience.

The implementation of well-designed policy measures is essential for addressing key challenges hindering large-scale BECCS deployment. Incentives for biomass supply chain infrastructure, such as subsidies for storage facilities, dedicated transportation networks, and pretreatment depots, can reduce logistical costs and stabilize biomass feedstock supply year-round, mitigating seasonal variability. Similarly, financial mechanisms like expanded carbon capture tax credits and subsidies for integrating CO_2 capture with biofuel production will encourage investment in BECCS projects, making the system more economically viable while fostering a circular economy by converting carbon emissions into valuable resources. Moreover, the flexibility offered by biorefineries capable of handling multiple biomass types provide a critical pathway to improving operational efficiency and reducing supply chain disruptions. These biorefineries can adapt to seasonal availability, ensuring a steady flow of feedstock throughout the year, minimizing downtime, and enhancing resilience against regional shortages. By leveraging diverse biomass sources, multi-feedstock facilities also reduce dependence on any single resource, further strengthening the BECCS supply chain's adaptability and long-term sustainability.

In conclusion, while BECCS represents a promising technology for achieving climate goals and developing a sustainable bioenergy sector, its successful deployment requires a

coordinated effort across technological, economic, and policy domains. With appropriate investments in infrastructure, research, and public awareness, the BECCS system can become a cornerstone of future energy strategies aimed at reducing greenhouse gas emissions and promoting circular economic practices. However, there are still some limitations of this study. While the numerical model accounts for different biomass types and seasons, real-world uncertainties related to climate, agricultural practices, and unexpected disruptions in the supply chain could significantly impact the consistency of biomass feedstock supply. The need for storage and pre-treatment systems is critical but requires further exploration of scalability and cost-effectiveness. The study assumes certain technological efficiencies, such as the availability of biorefineries capable of handling multiple biomass types and effective carbon capture technologies. However, the real-world deployment of such technologies is still in its early stages, with several technical, financial, and operational barriers.

CHAPTER FIVE
CONCLUSIONS AND RECOMMENDATIONS

This study presents a comprehensive analysis of the sustainable supply chain network design for renewable energy, focusing on carbon dioxide conversion to fuels, hydrogen logistics, and circular biomass-bioenergy with carbon capture and storage systems. The research integrates techno-economic analysis, supply chain network modeling, and life cycle assessment (LCA) to address challenges and optimize solutions for renewable energy systems.

In Chapter Two, we investigated the techno-economic feasibility of CO_2-to-fuels conversion pathways, specifically Fischer-Tropsch synthesis (FTS) and methanol (MeOH). A mixed-integer linear programming model optimized the supply chain network, considering spatial distribution, pathway selection, and production capacity. Results revealed that the FTS pathway offers superior economic performance and environmental benefits under reduced hydrogen and electricity costs. Sensitivity analysis highlighted the critical role of hydrogen pricing, electricity costs, and CO_2 recycling efficiency. The findings demonstrate the potential for significant carbon emission reductions while meeting fuel demand, emphasizing the importance of infrastructure investment and cost-effective renewable electricity integration.

Chapter Three explored hydrogen logistics for fuel cell electric long-haul trucks, comparing gaseous hydrogen, liquid hydrogen, and ammonia as delivery pathways. A mixed-integer programming model evaluated these pathways under different market penetration rates. Liquid hydrogen emerged as the most cost-effective solution, with a levelized cost of $4.6/kg for 10% market penetration. However, the study identified critical challenges, including reducing operating costs for gaseous hydrogen stations, optimizing energy losses for ammonia cracking, and scaling refueling capacities. These findings underscore the need for targeted investment in infrastructure and technology to support hydrogen's role in decarbonizing transportation.

In Chapter Four, we assessed the techno-economic feasibility of biomass-bioenergy and biofuel systems incorporating biochar recycling and carbon capture and storage. Using a two-stage mixed-integer programming model, we optimized the supply chain for seasonal and spatial biomass availability. Results demonstrated that biofuel production is economically viable across market conditions, with switchgrass as the dominant

feedstock. Sensitivity analyses revealed that fixed operating costs and biofuel prices are pivotal to profitability. Multi-feedstock biorefineries showed potential for higher profitability and stability, emphasizing the importance of flexible infrastructure and supply chain planning.

Several recommendations in policy, infrastructure, technology and collaboration are involved in several aspects. Policies promoting renewable energy adoption, such as subsidies for hydrogen infrastructure, carbon credits for CO_2 conversion, and incentives for biomass-bioenergy systems, are essential to enhance economic feasibility and environmental benefits. Strategic investments in hydrogen refueling networks, CO_2 conversion facilities, and multi-feedstock biorefineries are critical for scaling up renewable energy technologies. Continued innovation in CO_2 conversion efficiency, hydrogen storage and delivery, and biomass conversion processes will address current technical limitations and reduce costs. Cross-sector collaboration between governments, industries, and academia is vital to align objectives, optimize resource allocation, and develop integrated renewable energy systems. Raising awareness about the benefits of renewable energy and engaging stakeholders in decision-making processes will build support for sustainable energy transitions.

This research provides a foundation for optimizing renewable energy supply chains and highlights areas for future exploration, including alternative CO_2 conversion technologies, advancements in hydrogen carriers, and long-term sustainability assessments for biomass systems. By addressing these recommendations, policymakers and stakeholders can accelerate the transition to a more sustainable energy future.

However, the models do not fully account for long-term policy changes, subsidies, or market dynamics that could significantly influence renewable energy adoption. Building on this research, future efforts should focus on incorporating stochastic optimization and real-time data to address uncertainties in supply chain variables such as demand fluctuations, energy prices, and policy shifts.

LIST OF REFERENCES

Abdmouleh, Z., Alammari, R. A. M., & Gastli, A. (2015). Review of policies encouraging renewable energy integration & best practices. In *Renewable and Sustainable Energy Reviews* (Vol. 45, pp. 249–262). Elsevier Ltd. https://doi.org/10.1016/j.rser.2015.01.035

Ahmed, G., Raziq, F., Hanif, M., Khan, J., Munawar, K. S., Wu, M., Cao, X., & Liu, Z. (2019). Oxygen-Cluster-Modified Anatase with Graphene Leads to Efficient and Recyclable Photo-Catalytic Conversion of CO_2 to CH4 Supported by the Positron Annihilation Study. *Scientific Reports*, *9*(1), 1–8. https://doi.org/10.1038/s41598-019-49694-w

Al Ghafri, S. Z., Munro, S., Cardella, U., Funke, T., Notardonato, W., Trusler, J. P. M., Leachman, J., Span, R., Kamiya, S., Pearce, G., Swanger, A., Rodriguez, E. D., Bajada, P., Jiao, F., Peng, K., Siahvashi, A., Johns, M. L., & May, E. F. (2022). Hydrogen liquefaction: a review of the fundamental physics, engineering practice and future opportunities. In *Energy and Environmental Science* (Vol. 15, Issue 7, pp. 2690–2731). Royal Society of Chemistry. https://doi.org/10.1039/d2ee00099g

Alper, E., & Yuksel Orhan, O. (2017). CO_2 utilization: Developments in conversion processes. *Petroleum*, *3*(1), 109–126. https://doi.org/10.1016/j.petlm.2016.11.003

Alper, K., Tekin, K., Karagöz, S., & Ragauskas, A. J. (2020). Sustainable energy and fuels from biomass: a review focusing on hydrothermal biomass processing. *Sustainable Energy & Fuels*, *4*(9), 4390–4414. https://doi.org/10.1039/D0SE00784F

Alternative Fuels Data Center: Alternative Fueling Station Locator. (2024). https://afdc.energy.gov/stations#/analyze?tab=station&country=US&maximum_vehicle_class=HD&show_map=true

Alternative Fuels Data Center: Renewable Fuel Standard. (2007). https://afdc.energy.gov/laws/RFS.html

AMMONIA TRANSPORT & STORAGE. (2023). www.ptx-hub.org

Amos, W. A. (2023). *Costs of Storing and Transporting Hydrogen*. http://www.doe.gov/bridge/home.html

Amponsah, N. Y., Troldborg, M., Kington, B., Aalders, I., & Hough, R. L. (2014). Greenhouse gas emissions from renewable energy sources: A review of lifecycle considerations. *Renewable and Sustainable Energy Reviews*, *39*, 461–475. https://doi.org/10.1016/J.RSER.2014.07.087

An updated roadmap to Net Zero Emissions by 2050 – World Energy Outlook 2022 – Analysis - IEA. (2022). https://www.iea.org/reports/world-energy-outlook-2022/an-updated-roadmap-to-net-zero-emissions-by-2050

Andersson, J., & Grönkvist, S. (2019). Large-scale storage of hydrogen. In *International Journal of Hydrogen Energy* (Vol. 44, Issue 23, pp. 11901–11919). Elsevier Ltd. https://doi.org/10.1016/j.ijhydene.2019.03.063

Arent, D., Pless, J., Mai, T., Wiser, R., Hand, M., Baldwin, S., Heath, G., Macknick, J., Bazilian, M., Schlosser, A., & Denholm, P. (2014). Implications of high renewable electricity penetration in the U.S. for water use, greenhouse gas emissions, land-use, and materials supply. *Applied Energy*, *123*, 368–377. https://doi.org/10.1016/J.APENERGY.2013.12.022

Arutyunov, V. S., & Lisichkin, G. V. (2017). Energy resources of the 21st century: problems and forecasts. Can renewable energy sources replace fossil fuels? *Russian Chemical Reviews*, *86*(8), 777–804. https://doi.org/10.1070/RCR4723/XML

Baliban, R. C., Elia, J. A., Floudas, C. A., Gurau, B., Weingarten, M. B., & Klotz, S. D. (2013). Hardwood biomass to gasoline, diesel, and jet fuel: 1. Process synthesis and global optimization of a thermochemical refinery. *Energy and Fuels*, *27*(8), 4302–4324. https://doi.org/10.1021/ef302003f

Balta-Ozkan, N., & Baldwin, E. (2013). Spatial development of hydrogen economy in a low-carbon UK energy system. *International Journal of Hydrogen Energy*, *38*(3), 1209–1224. https://doi.org/10.1016/J.IJHYDENE.2012.11.049

BETO Biofuels Techno-Economic Analyses (TEA) Database | BioEnergy KDF. (2023). Retrieved September 7, 2024, from https://bioenergykdf.ornl.gov/content/beto-biofuels-tea-database

Blanco, H. (2022). *What's best for Hydrogen transport: ammonia, liquid hydrogen, LOHC or pipelines? energypost.eu/whats-best-for-hydrogen-transport-ammonia-liquid-hydrogen-lohc-or-pipelines*.

Blanco, H., Jinks, B., Bianco, E., & Sezer, U. (2022). *INNOVATION OUTLOOK RENEWABLE AMMONIA in partnership with About IRENA Valuable review and feedback was also provided by IRENA colleagues RENEWABLE AMMONIA 3 CONTENTS*. www.irena.org

Bosu, S., & Rajamohan, N. (2024). Recent advancements in hydrogen storage - Comparative review on methods, operating conditions and challenges. *International Journal of Hydrogen Energy*, *52*, 352–370. https://doi.org/10.1016/J.IJHYDENE.2023.01.344

Buttler, A., & Spliethoff, H. (2018). Current status of water electrolysis for energy storage, grid balancing and sector coupling via power-to-gas and power-to-liquids: A review. In *Renewable and Sustainable Energy Reviews* (Vol. 82, pp. 2440–2454). Elsevier Ltd. https://doi.org/10.1016/j.rser.2017.09.003

Carbon Capture and Sequestration Protocol Under the Low Carbon Fuel Standard | California Air Resources Board. (2018). https://ww2.arb.ca.gov/resources/documents/carbon-capture-and-sequestration-protocol-under-low-carbon-fuel-standard

Carbon Dioxide Utilization | netl.doe.gov. (2023).

Centi, G., Perathoner, S., Salladini, A., & Iaquaniello, G. (2020). Economics of CO_2 Utilization: A Critical Analysis. *Frontiers in Energy Research*, *8*(September), 1–16. https://doi.org/10.3389/fenrg.2020.567986

CO_2 *Stationary Sources | netl.doe.gov*. Retrieved January 10, 2022, from https://netl.doe.gov/node/6096

Connor McDonald, L. B. and B. H. (2013). *Factsheet Biofuel Decision Support System*. http://bdss.tennessee.edu/Home/GetFact?cropType=Switchgrass

Corbeau, A.-S. (2022). *HYDROGEN: A HOT COMMODITY LACKING SUFFICIENT STATISTICS*.

Critical Review on Carbon based Materials. (2023).

Danso-Boateng, E., & Achaw, O. W. (2022). Bioenergy and biofuel production from biomass using thermochemical conversions technologies—a review. In *AIMS Energy* (Vol. 10, Issue 4). https://doi.org/10.3934/energy.2022030

David, J., & Herzog, H. (2023). *The Cost of carbon capture*.

Demir, M. E., & Dincer, I. (2018). Cost assessment and evaluation of various hydrogen delivery scenarios. *International Journal of Hydrogen Energy*, *43*(22), 10420–10430. https://doi.org/10.1016/j.ijhydene.2017.08.002

Department of Transportation. Bureau of Transportation Statistics. (2017). *Freight Analysis Framework (FAF5)* . https://doi.org/10.21949/1529116

Diesel and Jet Fuel Prices | Bureau of Transportation Statistics. Retrieved January 4, 2024, from https://www.bts.gov/browse-statistical-products-and-data/freight-facts-and-figures/diesel-and-jet-fuel-prices

Dijkman, T. J., & Benders, R. M. J. (2010). Comparison of renewable fuels based on their land use using energy densities. *Renewable and Sustainable Energy Reviews*, *14*(9), 3148–3155. https://doi.org/10.1016/J.RSER.2010.07.029

DOE/EERE. (2023). *U.S. Billion-Ton Update: Biomass Supply for a Bioenergy and Bioproducts Industry*.

Doliente, S. S., Narayan, A., Tapia, J. F. D., Samsatli, N. J., Zhao, Y., & Samsatli, S. (2020). Bio-aviation Fuel: A Comprehensive Review and Analysis of the Supply Chain Components. *Frontiers in Energy Research*, *8*, 499009. https://doi.org/10.3389/FENRG.2020.00110/BIBTEX

Elia, J. A., Baliban, R. C., & Floudas, C. A. (2012). Nationwide energy supply chain analysis for hybrid feedstock processes with significant CO_2 emissions reduction. *AIChE Journal*, *58*(7), 2142–2154. https://doi.org/10.1002/aic.13842

Elia, J. A., Baliban, R. C., & Floudas, C. A. (2014). Nationwide, regional, and statewide energy supply chain optimization for natural gas to liquid transportation fuel (GTL) systems. *Industrial and Engineering Chemistry Research*, *53*(13), 5366–5397. https://doi.org/10.1021/ie401378r

Elia, J. A., Baliban, R. C., Floudas, C. A., Gurau, B., Weingarten, M. B., & Klotz, S. D. (2013). Hardwood biomass to gasoline, diesel, and jet fuel: 2. Supply chain optimization framework for a network of thermochemical refineries. *Energy and Fuels*, *27*(8), 4325–4352. https://doi.org/10.1021/EF400430X/SUPPL_FILE/EF400430X_SI_001.PDF

Forsberg, C. W., Dale, B. E., Jones, D. S., Hossain, T., Morais, A. R. C., & Wendt, L. M. (2021). Replacing liquid fossil fuels and hydrocarbon chemical feedstocks with liquid biofuels from large-scale nuclear biorefineries. *Applied Energy*, *298*(March), 117225. https://doi.org/10.1016/j.apenergy.2021.117225

Freer, M., Gough, C., Welfle, A., & Lea-Langton, A. (2021a). Carbon optimal bioenergy with carbon capture and storage supply chain modelling: How far is too far? *Sustainable Energy Technologies and Assessments*, *47*. https://doi.org/10.1016/j.seta.2021.101406

Freer, M., Gough, C., Welfle, A., & Lea-Langton, A. (2021b). Carbon optimal bioenergy with carbon capture and storage supply chain modelling: How far is too far? *Sustainable Energy Technologies and Assessments*, *47*, 101406. https://doi.org/10.1016/j.seta.2021.101406

Freer, M., Gough, C., Welfle, A., & Lea-Langton, A. (2022a). Putting Bioenergy With Carbon Capture and Storage in a Spatial Context: What Should Go Where? *Frontiers in Climate*, *4*(March), 1–21. https://doi.org/10.3389/fclim.2022.826982

Freer, M., Gough, C., Welfle, A., & Lea-Langton, A. (2022b). Putting Bioenergy With Carbon Capture and Storage in a Spatial Context: What Should Go Where? *Frontiers in Climate*, *4*, 1055–1065. https://doi.org/10.3389/fclim.2022.826982

Gareiou, Z., Drimili, E., & Zervas, E. (2021). Public acceptance of renewable energy sources. *Low Carbon Energy Technologies in Sustainable Energy Systems*, 309–327. https://doi.org/10.1016/B978-0-12-822897-5.00012-2

Genovese, M., & Fragiacomo, P. (2023). Hydrogen refueling station: Overview of the technological status and research enhancement. *Journal of Energy Storage*, *61*, 106758. https://doi.org/10.1016/J.EST.2023.106758

Global hydrogen demand by sector in the Sustainable Development Scenario, 2019-2070. (2020, September 10). IEA.

GLOBAL HYDROGEN TRADE TO MEET THE 1.5°C CLIMATE GOAL PART II TECHNOLOGY REVIEW OF HYDROGEN CARRIERS. (2022). www.irena.org/publications

Gold, S., & Seuring, S. (2011). Supply chain and logistics issues of bio-energy production. *Journal of Cleaner Production*, *19*(1), 32–42. https://doi.org/10.1016/J.JCLEPRO.2010.08.009

Gonzalez-Garay, A., Heuberger-Austin, C., Fu, X., Klokkenburg, M., Zhang, D., van der Made, A., & Shah, N. (2022). Unravelling the potential of sustainable aviation fuels to decarbonise the aviation sector. *Energy and Environmental Science*, *15*(8), 3291–3309. https://doi.org/10.1039/d1ee03437e

Green Power Pricing | US EPA. Retrieved February 5, 2024, from https://www.epa.gov/green-power-markets/green-power-pricing

Ham Radio - US Detail Grid. Retrieved May 6, 2022, from https://www.coilgun.info/rover/grid-map-us-4digit.htm

Han, Y., Kamkeng, A. D. N., Otitoju, O., Ding, Y., & Wang, M. (2023). *Techno-economic assessment of modified Fischer-Tropsch to synthesis process for direct* CO_2 *conversion into jet fuel*. https://ssrn.com/abstract=4631853

Happs, R. M., Hanes, R. J., Bartling, A. W., Field, J. L., Harman-Ware, A. E., Clark, R. J., Pendergast, T. H., Devos, K. M., Webb, E. G., Missaoui, A., Xu, Y., Makaju, S., Shrestha, V., Mazarei, M., Stewart, C. N., Millwood, R. J., & Davison, B. H. (2024a). Economic and Sustainability Impacts of Yield and Composition Variation in Bioenergy Crops: Switchgrass (Panicum virgatum L.). *ACS Sustainable Chemistry and Engineering*, *12*(5), 1897–1910. https://doi.org/10.1021/acssuschemeng.3c05770

Happs, R. M., Hanes, R. J., Bartling, A. W., Field, J. L., Harman-Ware, A. E., Clark, R. J., Pendergast, T. H., Devos, K. M., Webb, E. G., Missaoui, A., Xu, Y., Makaju, S., Shrestha, V., Mazarei, M., Stewart, C. N., Millwood, R. J., & Davison, B. H. (2024b). Economic and Sustainability Impacts of Yield and Composition Variation in Bioenergy Crops: Switchgrass (Panicum virgatum L.). *ACS Sustainable Chemistry and Engineering*, *12*(5), 1897–1910. https://doi.org/10.1021/ACSSUSCHEMENG.3C05770

Hasan, M. R. ; R. C. (2009). Use of algae and aquatic macrophytes as feed in small-scale aquaculture. In *Aquaculture* (Vol. 531).

Haszeldine, R. S., Flude, S., Johnson, G., & Scott, V. (2018). Negative emissions technologies and carbon capture and storage to achieve the Paris Agreement commitments. *Philosophical Transactions of the Royal Society A: Mathematical, Physical and Engineering Sciences*, *376*(2119). https://doi.org/10.1098/RSTA.2016.0447

Hepburn, C., Adlen, E., Beddington, J., Carter, E. A., Fuss, S., Mac Dowell, N., Minx, J. C., Smith, P., & Williams, C. K. (2019). The technological and

economic prospects for CO_2 utilization and removal. *Nature*, *575*(7781), 87–97. https://doi.org/10.1038/s41586-019-1681-6

Holmatov, B., Hoekstra, A. Y., & Krol, M. S. (2019). Land, water and carbon footprints of circular bioenergy production systems. *Renewable and Sustainable Energy Reviews*, *111*, 224–235. https://doi.org/10.1016/J.RSER.2019.04.085

Houchins, C., & James, B. D. (2020). *2020 DOE Hydrogen and Fuel Cells Program Review Hydrogen Storage Cost Analysis (ST100)*.

Huang, E., Zhang, X., Rodriguez, L., Khanna, M., de Jong, S., Ting, K. C., Ying, Y., & Lin, T. (2019). Multi-objective optimization for sustainable renewable jet fuel production: A case study of corn stover based supply chain system in Midwestern U.S. *Renewable and Sustainable Energy Reviews*, *115*(September), 109403. https://doi.org/10.1016/j.rser.2019.109403

Hydrogen Delivery Scenario Analysis Model. (2022). https://hdsam.es.anl.gov/index.php?content=hdsam

Hydrogen Production | Department of Energy. Retrieved February 5, 2024, from https://www.energy.gov/eere/fuelcells/hydrogen-production

Hydrogen Shot | Department of Energy. Retrieved October 1, 2023, from https://www.energy.gov/eere/fuelcells/hydrogen-shot

Hydrogen's Role in Transportation. (2022, February 25). Office of Energy Efficiency and Renewable Energy.

Iakovou, E., Karagiannidis, A., Vlachos, D., Toka, A., & Malamakis, A. (2010). Waste biomass-to-energy supply chain management: A critical synthesis. *Waste Management*, *30*(10), 1860–1870. https://doi.org/10.1016/J.WASMAN.2010.02.030

IRENA and AEA. (2022). Innovation Outlook: Renewable Ammonia. *International Renewable Energy Agency*, 144.

Jouny, M., Luc, W., & Jiao, F. (2018). General Techno-Economic Analysis of CO_2 Electrolysis Systems. *Industrial and Engineering Chemistry Research*, *57*(6), 2165–2177. https://doi.org/10.1021/acs.iecr.7b03514

Jürgens, S., Oßwald, P., Selinsek, M., Piermartini, P., Schwab, J., Pfeifer, P., Bauder, U., Ruoff, S., Rauch, B., & Köhler, M. (2019). Assessment of combustion properties of non-hydroprocessed Fischer-Tropsch fuels for aviation. *Fuel Processing Technology*, *193*, 232–243. https://doi.org/10.1016/J.FUPROC.2019.05.015

Kapelewski, M. T., Runčevski, T., Tarver, J. D., Jiang, H. Z. H., Hurst, K. E., Parilla, P. A., Ayala, A., Gennett, T., Fitzgerald, S. A., Brown, C. M., & Long, J. R. (2018). Record High Hydrogen Storage Capacity in the Metal-Organic Framework Ni2(m-dobdc) at Near-Ambient Temperatures. *Chemistry of Materials*, *30*(22), 8179–8189. https://doi.org/10.1021/ACS.CHEMMATER.8B03276/SUPPL_FILE/CM8B03276_SI_002.ZIP

Kast, J., Morrison, G., Gangloff, J. J., Vijayagopal, R., & Marcinkoski, J. (2018). Designing hydrogen fuel cell electric trucks in a diverse medium and heavy duty market. *Research in Transportation Economics*, *70*, 139–147. https://doi.org/10.1016/J.RETREC.2017.07.006

Kevin Gould, D. P. and P. K. (2015). *Corn stover baling logistics - Agriculture*. https://www.canr.msu.edu/news/corn_stover_baling_logistics

Kibria, M. G., Edwards, J. P., Gabardo, C. M., Dinh, C. T., Seifitokaldani, A., Sinton, D., & Sargent, E. H. (2019). Electrochemical CO_2 Reduction into Chemical Feedstocks: From Mechanistic Electrocatalysis Models to System Design. *Advanced Materials*, *31*(31). https://doi.org/10.1002/adma.201807166

Kim, S., Zhang, X., Reddy, A. D., Dale, B. E., Thelen, K. D., Jones, C. D., Izaurralde, R. C., Runge, T., & Maravelias, C. (2020). Carbon-Negative

Biofuel Production. *Environmental Science & Technology*, *54*(17), 10797–10807. https://doi.org/10.1021/acs.est.0c01097

Kumaravel, V., Bartlett, J., & Pillai, S. C. (2020). Photoelectrochemical Conversion of Carbon Dioxide (CO_2) into Fuels and Value-Added Products. *ACS Energy Letters*, 486–519. https://doi.org/10.1021/acsenergylett.9b02585

Kwon, E., Yi, H., & Jeon, Y. J. (2013). Synergetic sustainability enhancement via current biofuel infrastructure: Waste-to-energy concept for biodiesel production. *Environmental Science and Technology*, *47*(6), 2817–2822. https://doi.org/10.1021/ES304001Y/ASSET/IMAGES/LARGE/ES-2012-04001Y_0005.JPEG

Lahnaoui, A., Wulf, C., Heinrichs, H., & Dalmazzone, D. (2019). Optimizing hydrogen transportation system for mobility via compressed hydrogen trucks. *International Journal of Hydrogen Energy*, *44*(35), 19302–19312. https://doi.org/10.1016/J.IJHYDENE.2018.10.234

Le, P.-A., Trung, V. D., Nguyen, P. L., Bac Phung, T. V., Natsuki, J., & Natsuki, T. (2023). The current status of hydrogen energy: an overview. *RSC Advances*, *13*(40), 28262–28287. https://doi.org/10.1039/D3RA05158G

Lee, M. Y., Park, K. T., Lee, W., Lim, H., Kwon, Y., & Kang, S. (2020). Current achievements and the future direction of electrochemical CO_2 reduction: A short review. *Critical Reviews in Environmental Science and Technology*, *50*(8), 769–815. https://doi.org/10.1080/10643389.2019.1631991

Leila, M., Whalen, J., & Bergthorson, J. (2018). Strategic spatial and temporal design of renewable diesel and biojet fuel supply chains: Case study of California, USA. *Energy*, *156*(2018), 181–195. https://doi.org/10.1016/j.energy.2018.04.196

Leslie, A. (2023). *An Analysis of the Operational Costs of Trucking: 2023 Update*.

Li, F., Huang, Y., Gao, C., & Wu, X. (2021). The enhanced photo-catalytic CO_2 reduction performance of g-C3N4 with high selectivity by coupling CoNiSx.

Materials Research Bulletin, *144*(April), 111488. https://doi.org/10.1016/j.materresbull.2021.111488

Li, L., Xu, C., Chen, C., Wang, Y., Jiao, L., & Yuan, H. (2013). Sodium alanate system for efficient hydrogen storage. In *International Journal of Hydrogen Energy* (Vol. 38, Issue 21, pp. 8798–8812). https://doi.org/10.1016/j.ijhydene.2013.04.109

Li, X., Anderson, P., Jhong, H. R. M., Paster, M., Stubbins, J. F., & Kenis, P. J. A. (2016). Greenhouse Gas Emissions, Energy Efficiency, and Cost of Synthetic Fuel Production Using Electrochemical CO_2 Conversion and the Fischer-Tropsch Process. *Energy and Fuels*, *30*(7), 5980–5989. https://doi.org/10.1021/acs.energyfuels.6b00665

Li, Z., Li, K., Du, P., Mehmandoust, M., Karimi, F., & Erk, N. (2022). Carbon-based photocatalysts for hydrogen production: A review. *Chemosphere*, *308*, 135998. https://doi.org/10.1016/J.CHEMOSPHERE.2022.135998

Liu, N., Xie, F., Lin, Z., & Jin, M. (2020). Evaluating national hydrogen refueling infrastructure requirement and economic competitiveness of fuel cell electric long-haul trucks. In *Mitigation and Adaptation Strategies for Global Change* (Vol. 25, Issue 3, pp. 477–493). Springer. https://doi.org/10.1007/s11027-019-09896-z

Low Carbon Fuel Standard | California Air Resources Board. (2011). https://ww2.arb.ca.gov/our-work/programs/low-carbon-fuel-standard/about

Ma, Y., Tian, H., Cheng, H., Xuan, Y., Shang, L., & Yang, Y. (2024a). The economic and environmental sustainability of converting Miscanthus to hydrocarbon biofuel by pyrolysis and catalytic hydrotreatment. *Biomass and Bioenergy*, *181*. https://doi.org/10.1016/j.biombioe.2023.107041

Ma, Y., Tian, H., Cheng, H., Xuan, Y., Shang, L., & Yang, Y. (2024b). The economic and environmental sustainability of converting Miscanthus to

hydrocarbon biofuel by pyrolysis and catalytic hydrotreatment. *Biomass and Bioenergy*, *181*. https://doi.org/10.1016/j.biombioe.2023.107041

Malladi, K. T., & Sowlati, T. (2018). Biomass logistics: A review of important features, optimization modeling and the new trends. *Renewable and Sustainable Energy Reviews*, *94*, 587–599. https://doi.org/10.1016/J.RSER.2018.06.052

Matos-Ríos, D. M., Martínez-Guido, S. I., Ortega, J. M. P., Gómez-Castro, F. I., García-Trejo, J. F., & Gutiérrez-Antonio, C. (2022). Optimal Supply Chain Design for Renewable Aviation Fuel Production in México Considering the Full Use of Nonedible Biomass. *ACS Sustainable Chemistry and Engineering*, *10*(30), 9770–9786. https://doi.org/10.1021/ACSSUSCHEMENG.2C01176/ASSET/IMAGES/LARGE/SC2C01176_0007.JPEG

Megia, P. J., Vizcaino, A. J., Calles, J. A., & Carrero, A. (2021). Hydrogen Production Technologies: From Fossil Fuels toward Renewable Sources. A Mini Review. *Energy and Fuels*, *35*(20), 16403–16415. https://doi.org/10.1021/ACS.ENERGYFUELS.1C02501/ASSET/IMAGES/LARGE/EF1C02501_0004.JPEG

Mehmeti, A., Angelis-Dimakis, A., Arampatzis, G., McPhail, S. J., & Ulgiati, S. (2018). Life Cycle Assessment and Water Footprint of Hydrogen Production Methods: From Conventional to Emerging Technologies. *Environments 2018, Vol. 5, Page 24*, *5*(2), 24. https://doi.org/10.3390/ENVIRONMENTS5020024

Mike Jacobson, L. B. B. H. and C. M. (2012). *Factsheet Biofuel Decision Support System*. http://bdss.tennessee.edu/Home/GetFact?cropType=Miscanthus

Moghadasi, S., Long, Y., Jiang, L., Munshi, S., McTaggart-Cowan, G., & Shahbakhti, M. (2024). Design and performance analysis of hybrid electric class 8 heavy-duty regional-haul trucks with a micro-pilot natural gas engine in

real-world highway driving conditions. *Energy Conversion and Management*, *309*, 118451. https://doi.org/10.1016/J.ENCONMAN.2024.118451

Mulky, L., Srivastava, S., Lakshmi, T., Sandadi, E. R., Gour, S., Thomas, N. A., Shanmuga Priya, S., & Sudhakar, K. (2024). An overview of hydrogen storage technologies – Key challenges and opportunities. *Materials Chemistry and Physics*, *325*, 129710. https://doi.org/10.1016/J.MATCHEMPHYS.2024.129710

Mullen, C. A., Boateng, A. A., Goldberg, N. M., Lima, I. M., Laird, D. A., & Hicks, K. B. (2010). Bio-oil and bio-char production from corn cobs and stover by fast pyrolysis. *Biomass and Bioenergy*, *34*(1), 67–74. https://doi.org/10.1016/J.BIOMBIOE.2009.09.012

Na, J., Seo, B., Kim, J., Lee, C. W., Lee, H., Hwang, Y. J., Min, B. K., Lee, D. K., Oh, H. S., & Lee, U. (2019). General technoeconomic analysis for electrochemical coproduction coupling carbon dioxide reduction with organic oxidation. *Nature Communications*, *10*(1). https://doi.org/10.1038/s41467-019-12744-y

Niermann, M., Timmerberg, S., Drünert, S., & Kaltschmitt, M. (2021). Liquid Organic Hydrogen Carriers and alternatives for international transport of renewable hydrogen. *Renewable and Sustainable Energy Reviews*, *135*. https://doi.org/10.1016/j.rser.2020.110171

Nolan, A., MC Donnell, K., MC Siurtain, M., Carroll, J. P., Finnan, J., & Rice, B. (2009). Conservation of miscanthus in bale form. *Biosystems Engineering*, *104*(3), 345–352. https://doi.org/10.1016/J.BIOSYSTEMSENG.2009.06.025

Notton, G., Nivet, M. L., Voyant, C., Paoli, C., Darras, C., Motte, F., & Fouilloy, A. (2018). Intermittent and stochastic character of renewable energy sources: Consequences, cost of intermittence and benefit of forecasting. *Renewable and Sustainable Energy Reviews*, *87*, 96–105. https://doi.org/10.1016/J.RSER.2018.02.007

openLCA Nexus: The source for LCA data sets. Retrieved October 25, 2022, from https://nexus.openlca.org/downloads

Parks, G., Boyd, R., Cornish, J., Remick, R., & Review Panel, I. (2020). *Hydrogen Station Compression, Storage, and Dispensing Technical Status and Costs: Systems Integration*. http://www.osti.gov/bridge

Preuster, P., Papp, C., & Wasserscheid, P. (2017). Liquid organic hydrogen carriers (LOHCs): Toward a hydrogen-free hydrogen economy. *Accounts of Chemical Research*, *50*(1), 74–85. https://doi.org/10.1021/ACS.ACCOUNTS.6B00474/ASSET/IMAGES/LARGE/AR-2016-00474U_0005.JPEG

Qin, Y., Niu, G., Wang, X., Luo, D., & Duan, Y. (2020). Conversion of CO_2 in a low-powered atmospheric microwave plasma: In-depth study on the trade-off between CO_2 conversion and energy efficiency. *Chemical Physics*, *538*(March), 110913. https://doi.org/10.1016/j.chemphys.2020.110913

Rafiee, A., Rajab Khalilpour, K., Milani, D., & Panahi, M. (2018). Trends in CO_2 conversion and utilization: A review from process systems perspective. *Journal of Environmental Chemical Engineering*, *6*(5), 5771–5794. https://doi.org/10.1016/j.jece.2018.08.065

Reinhart, T. E. (2015). *Commercial Medium- and Heavy-Duty Truck Fuel Efficiency Technology Study - Report #1*.

Renewable Energy Agency, I. (2012). *RENEWABLE ENERGY TECHNOLOGIES: COST ANALYSIS SERIES Biomass for Power Generation Acknowledgement*. www.irena.org/Publications

Riera, J. A., Lima, R. M., & Knio, O. M. (2023). A review of hydrogen production and supply chain modeling and optimization. *International Journal of Hydrogen Energy*, *48*(37), 13731–13755. https://doi.org/10.1016/J.IJHYDENE.2022.12.242

Sayer, M., Ajanovic, A., & Haas, R. (2024). Economic and environmental assessment of different hydrogen production and transportation modes. *International Journal of Hydrogen Energy*, *65*, 626–638. https://doi.org/10.1016/J.IJHYDENE.2024.04.073

Schmidt, P., Batteiger, V., Roth, A., Weindorf, W., & Raksha, T. (2018). Power-to-Liquids as Renewable Fuel Option for Aviation: A Review. *Chemie-Ingenieur-Technik*, *90*(1), 127–140. https://doi.org/10.1002/cite.201700129

Seo, S. K., Yun, D. Y., & Lee, C. J. (2020). Design and optimization of a hydrogen supply chain using a centralized storage model. *Applied Energy*, *262*, 114452. https://doi.org/10.1016/J.APENERGY.2019.114452

Shi, R., Chen, X., Qin, J., Wu, P., & Jia, L. (2022). The State-of-the-Art Progress on the Forms and Modes of Hydrogen and Ammonia Energy Utilization in Road Transportation. *Sustainability (Switzerland)*, *14*(19), 1–25. https://doi.org/10.3390/su141911904

Singh, A., Olsen, S. I., & Pant, D. (2013). Importance of Life Cycle Assessment of Renewable Energy Sources. *Green Energy and Technology*, *0*(9781447153634), 1–11. https://doi.org/10.1007/978-1-4471-5364-1_1

Sinsel, S. R., Riemke, R. L., & Hoffmann, V. H. (2020). Challenges and solution technologies for the integration of variable renewable energy sources—a review. *Renewable Energy*, *145*, 2271–2285. https://doi.org/10.1016/J.RENENE.2019.06.147

Smith, W. A., Wendt, L. M., Bonner, I. J., & Murphy, J. A. (2020). Effects of Storage Moisture Content on Corn Stover Biomass Stability, Composition, and Conversion Efficacy. *Frontiers in Bioengineering and Biotechnology*, *8*, 529086. https://doi.org/10.3389/FBIOE.2020.00716/BIBTEX

Spurgeon, J. M., & Kumar, B. (2018). A comparative technoeconomic analysis of pathways for commercial electrochemical CO_2 reduction to liquid products.

Energy and Environmental Science, *11*(6), 1536–1551. https://doi.org/10.1039/c8ee00097b

Stavrakas, V., Spyridaki, N. A., & Flamos, A. (2018). Striving towards the Deployment of Bio-Energy with Carbon Capture and Storage (BECCS): A Review of Research Priorities and Assessment Needs. *Sustainability 2018, Vol. 10, Page 2206*, *10*(7), 2206. https://doi.org/10.3390/SU10072206

Tagomori, I., Daioglou, V., Rochedo, P., Angelkorte, G., Schaeffer, R., van Vuuren, D., & Szklo, A. (2023). BLOEM: A spatially explicit model of bioenergy and carbon capture and storage, applied to Brazil. *GCB Bioenergy*, *15*(2), 116–127. https://doi.org/10.1111/GCBB.13008

The Bipartisan Infrastructure Law | Enel North America. (2021). https://www.enelnorthamerica.com/insights/resource-centers/the-bipartisan-infrastructure-law

The Busiest & Biggest Airports in the US. Retrieved November 24, 2024, from https://www.stratosjets.com/blog/busiest-us-airports/

The Haber Process. (2023). https://chem.libretexts.org/@go/page/1344

The Haber Process - Chemistry LibreTexts. (2023). Retrieved October 23, 2024, from https://chem.libretexts.org/Bookshelves/Physical_and_Theoretical_Chemistry_Textbook_Maps/Supplemental_Modules_(Physical_and_Theoretical_Chemistry)/Equilibria/Le_Chateliers_Principle/The_Haber_Process

The role of hydrogen and ammonia in meeting the net zero challenge. (2023).

The Section 45Q Tax Credit for Carbon Sequestration. (2023). https://crsreports.congress.gov

Tian, X., & Pei, J. (2023). Study progress on the pipeline transportation safety of hydrogen-blended natural gas. *Heliyon*, *9*(11), e21454. https://doi.org/10.1016/J.HELIYON.2023.E21454

Tsagkari, M., Couturier, J. L., Kokossis, A., & Dubois, J. L. (2016). Early-Stage Capital Cost Estimation of Biorefinery Processes: A Comparative Study of Heuristic Techniques. *Chemsuschem*, *9*(17), 2284. https://doi.org/10.1002/CSSC.201600309

USDrive. (2013). *Hydrogen Storage Technologies Roadmap Hydrogen Delivery Technical Team Roadmap*. www.uscar.org.

Verma, S., Kim, B., Jhong, H. R. M., Ma, S., & Kenis, P. J. A. (2016). A gross-margin model for defining technoeconomic benchmarks in the electroreduction of CO_2. *ChemSusChem*, *9*(15), 1972–1979. https://doi.org/10.1002/cssc.201600394

Villalba-Herreros, A., d'Amore-Domenech, R., Crucelaegui, A., & Leo, T. J. (2023a). Techno-Economic Assessment of Large-Scale Green Hydrogen Logistics Using Ammonia As Hydrogen Carrier: Comparison to Liquified Hydrogen Distribution and In Situ Production. *ACS Sustainable Chemistry and Engineering*, *11*(12), 4716–4726. https://doi.org/10.1021/ACSSUSCHEMENG.2C07136/ASSET/IMAGES/LARGE/SC2C07136_0003.JPEG

Villalba-Herreros, A., d'Amore-Domenech, R., Crucelaegui, A., & Leo, T. J. (2023b). Techno-Economic Assessment of Large-Scale Green Hydrogen Logistics Using Ammonia As Hydrogen Carrier: Comparison to Liquified Hydrogen Distribution and In Situ Production. *ACS Sustainable Chemistry and Engineering*, *11*(12), 4716–4726. https://doi.org/10.1021/ACSSUSCHEMENG.2C07136/ASSET/IMAGES/LARGE/SC2C07136_0003.JPEG

Wang, W. C., Liu, Y. C., & Nugroho, R. A. A. (2022). Techno-economic analysis of renewable jet fuel production: The comparison between Fischer-Tropsch synthesis and pyrolysis. *Energy*, *239*, 121970. https://doi.org/10.1016/j.energy.2021.121970

Wassermann, T., Muehlenbrock, H., Kenkel, P., & Zondervan, E. (2022). Supply chain optimization for electricity-based jet fuel: The case study Germany. *Applied Energy*, *307*(August 2021), 117683. https://doi.org/10.1016/j.apenergy.2021.117683

Wassermann, T., Schnuelle, C., Kenkel, P., & Zondervan, E. (2020). Power-to-Methanol at Refineries as a Precursor to Green Jet Fuel Production: a Simulation and Assessment Study. *Computer Aided Chemical Engineering*, *48*, 1453–1458. https://doi.org/10.1016/B978-0-12-823377-1.50243-3

Wietschel, M., Hasenauer, U., & de Groot, A. (2006). Development of European hydrogen infrastructure scenarios—CO_2 reduction potential and infrastructure investment. *Energy Policy*, *34*(11), 1284–1298. https://doi.org/10.1016/J.ENPOL.2005.12.019

Xu, L., Xiu, Y., Liu, F., Liang, Y., & Wang, S. (2020). Research Progress in Conversion of CO_2 to Valuable Fuels. *Molecules 2020, Vol. 25, Page 3653*, *25*(16), 3653. https://doi.org/10.3390/MOLECULES25163653

Yao, B., Xiao, T., Makgae, O. A., Jie, X., Gonzalez-Cortes, S., Guan, S., Kirkland, A. I., Dilworth, J. R., Al-Megren, H. A., Alshihri, S. M., Dobson, P. J., Owen, G. P., Thomas, J. M., & Edwards, P. P. (2020). Transforming carbon dioxide into jet fuel using an organic combustion-synthesized Fe-Mn-K catalyst. *Nature Communications*, *11*(1). https://doi.org/10.1038/s41467-020-20214-z

Yilmaz, C., & Kaska, O. (2018). Performance analysis and optimization of a hydrogen liquefaction system assisted by geothermal absorption precooling refrigeration cycle. *International Journal of Hydrogen Energy*, *43*(44), 20203–20213. https://doi.org/10.1016/J.IJHYDENE.2018.08.019

Yoder, A. M., Murphy, D. J., & Dehart, A. F. (2013). A Technical Review on Safety in On-Farm Biomass Production and Storage Systems: Status and Industry Needs. *American Society of Agricultural and Biological Engineers Annual*

International Meeting 2013, ASABE 2013, *6*, 1-. https://doi.org/10.13031/AIM.20131620568

You, F., & Wang, B. (2011). Life Cycle Optimization of Biomass-to-Liquid Supply Chains with Distributed–Centralized Processing Networks. *Industrial & Engineering Chemistry Research*, *50*(17), 10102–10127. https://doi.org/10.1021/ie200850t

Zang, G., Sun, P., Elgowainy, A., Bafana, A., & Wang, M. (2021). Life Cycle Analysis of Electrofuels: Fischer-Tropsch Fuel Production from Hydrogen and Corn Ethanol Byproduct CO_2. *Environmental Science and Technology*, 2–11. https://doi.org/10.1021/acs.est.0c05893

Zhang, T., Uratani, J., Huang, Y., Xu, L., Griffiths, S., & Ding, Y. (2023). Hydrogen liquefaction and storage: Recent progress and perspectives. *Renewable and Sustainable Energy Reviews*, *176*, 113204. https://doi.org/10.1016/J.RSER.2023.113204

Zhao, D., Tian, Q., Li, Z., & Zhu, Q. (2016). A new stepwise and piecewise optimization approach for CO_2 pipeline. *International Journal of Greenhouse Gas Control*, *49*, 192–200. https://doi.org/10.1016/j.ijggc.2016.03.005

VITA

Rui Zhou was born in Chengdu, China. She graduated in 2018 with a bachelor's degree in industrial & systems engineering in Nanchang Hangkong University, China. In the fall of 2018, she joined the Department of Industrial and Systems Engineering of the University of Tennessee, Knoxville (UTK), and started to work on the coffee supply planning under climate change with Dr. Mingzhou Jin for a master's degree. In the spring of 2021, she continued to pursue a doctor's degree in ISE with Dr. Mingzhou Jin at UTK and started to work on sustainable supply chain network design for renewable energy. She is expected to complete his Doctor of Philosophy degree in 2024. Her research interests include mixed integer programming, stochastic programming, network flow problem, sustainability, techno-economic analysis, and life cycle assessment.